Friction Enhancements to Asphalt Pavement Surfaces

August 2024
Final Report

Project number TR202206
MoDOT Research Report number cmr 24-015

PREPARED BY:

Alireza Roshan

Magdy Abdelrahman

Missouri University of Science and Technology

PREPARED FOR:

Missouri Department of Transportation

Construction and Materials Division, Research Section

1. Report No. cmr 24-015	**2. Government Accession No.**	**3. Recipient's Catalog No.**
4. Title and Subtitle Friction Enhancements to Asphalt Pavement Surfaces		**5. Report Date** June 2024 Published: August 2024
		6. Performing Organization Code
7. Author(s) Alireza Roshan, https://orcid.org/0000-0002-9399-3501 Magdy Abdelrahman, https://orcid.org/0000-0002-8722-0203		**8. Performing Organization Report No.**
9. Performing Organization Name and Address Department of Civil, Architectural and Environmental Engineering Missouri University of Science and Technology 1401 N. Pine St. Rolla, MO 65409		**10. Work Unit No. (TRAIS)**
		11. Contract or Grant No. MoDOT project # TR202206
12. Sponsoring Agency Name and Address Missouri Department of Transportation (SPR-B) Construction and Materials Division P.O. Box 270 Jefferson City, MO 65102		**13. Type of Report and Period Covered** Final Report (February 2022-August 2024)
		14. Sponsoring Agency Code

15. Supplementary Notes
Conducted in cooperation with the U.S. Department of Transportation, Federal Highway Administration. MoDOT research reports are available in the Innovation Library at https://www.modot.org/research-publications.

16. Abstract
Maintaining the appropriate amount of pavement friction is critical for safe driving. Missouri Department of Transportation (MoDOT) has used high friction surface treatment (HFST) since 2013 to restore pavement surface friction where traffic has worn down pavement surface aggregates and to improve wet crash locations. Conventional HFST application consists of a polymer resin layer, which is used to bond the pavement with high abrasion, high angularity and texture, and polish resistant aggregates (e.g., Calcined Bauxite (CB) / (chat, slag)). Construction routines and pre-existing pavement conditions affect the performance of HFST made with polymer resin. Highway agencies examine existing pavement surface conditions before determining whether HFST can be used, as it is not intended as a repair for surface distress conditions, such as rutting. The relatively high cost of constructing, and removing, HFST with polymer resins along with the durability concerns due to existing pavement conditions, has led state agencies to consider high friction surface treatment with asphalt-based binders as an alternative. This research evaluates alternative asphalt binders for use in surface friction treatments. The research program evaluated the friction performance of HFST applications made with asphalt-based binders including newly developed modified asphalt binders. An updated Life-Cycle-Cost (LCC) EXCEL program was developed to conduct cost analysis based on the performance of the tested binder-aggregate combinations. The study showed acceptable asphalt-based binders for HFST applications and recommended continuing the development of asphalt-based binders to enhance the performance of HFST applications.

17. Key Words High Friction Asphalt Treatment; HFST; Epoxy binder; Asphalt-based binder for HFST; Dynamic friction tester; DFT; C-T meter	**18. Distribution Statement** No restrictions. This document is available through the National Technical Information Service, Springfield, VA 22161.

19. Security Classification (of this report) Unclassified	**20. Security Classification (of this page)** Unclassified	**21. No. of Pages** 157	**22. Price**

Friction Enhancements to Asphalt Pavement Surfaces

By

Alireza Roshan

Ph.D. Student

And

Magdy Abdelrahman, Ph.D.

Missouri Asphalt Pavement Association (MAPA) Endowed Professor

Missouri University of Science and Technology

Missouri Department of Transportation

Project # TR202206

June 2024

Copyright Permissions

Disclaimer

Acknowledgments

The authors would like to express their great appreciation to the Missouri Department of Transportation for supporting them with the funds, instruments, and information.

Table of Contents

List of Figures

List of Tables

List of Abbreviations

AADT	Average Annual Daily Traffic
AIMS	Aggregate Image Measurement System
AMD 15	After 15-minutes of Micro-Deval polishing time
AMD 30	After 30-minutes of Micro-Deval polishing time
AMD 105	After 105-minutes of Micro-Deval polishing time
AMD 180	After 180-minutes Micro-Deval polishing time
AMD 240	After 240-minutes Micro-Deval polishing time
BMD	Before Micro-Deval polishing
BP	British Pendulum
BPN	British Pendulum Number
CB	Calcined Bauxite
COF	Coefficient of Friction
CTM	Circular Texture Meter
DFT	Dynamic Friction Tester
DFT20	COF value measured by DFT at 20 km/hr
DFT40	COF value measured by DFT at 40 km/hr
DFT50	COF value measured by DFT at 50 km/hr
EFST	Enhanced Friction Surface Treatment
FN	Friction Number
GA	Gradient Angularity
HFST	High Friction Surface Treatment
HMA	Hot Mix Asphalt
IFI	International Friction Index
LAA	Los Angeles Abrasion
LCCA	Life Cycle Cost Analysis
MAS	Maximum Aggregate Size
MD	Micro-Deval
MPD	Mean Profile Depth
MTD	Mean Texture Depth

NMAS	Nominal Maximum Aggregate Size
NPV	Net Present Value
PSV	Polished Stone Value
SN	Skid Number
SN40R	Skid Number measured at 40 mi/hr by a skid trailer with Ribbed tires
SN(50)	Skid Number measured at 50 mi/hr by a skid trailer with smooth tires
TWPD	Three-Wheel Polishing Device
TX	Texture
UVC	Uncompacted Void Content

EXECUTIVE SUMMARY

High Friction Surface Treatment (HFST) is an effective and economical solution that has demonstrated its ability to increase pavement friction and reduce crash rates worldwide. The adoption of HFST in the United States has experienced significant growth over the past 15 years. Initially, in 2005, only a few demonstration installations existed; however, by 2021, 44 states had implemented at least one HFST installation with the primary objective of improving road safety. The Missouri Department of Transportation (MoDOT) has used HFST since 2013 to restore pavement surface friction where traffic has worn down pavement surface aggregates and to improve wet crash locations. Conventional HFST application consists of a polymer resin layer, which is used to bond the pavement with high abrasion, high angularity and texture, and polish resistant aggregates (e.g., Calcined Bauxite (CB)).

The relatively high cost of constructing, and removing, HFST with polymer resins along with the durability concerns due to existing pavement conditions, has led state agencies to consider high friction surface treatment alternatives. Agencies examine existing pavement surface conditions before determining whether HFST can be used, because HFST is not intended to be a repair for surface distress, such as rutting. The relatively high cost of constructing, and removing, HFSTs with polymer resins along with the durability concerns due to existing pavement conditions, has led state agencies to consider high friction surface treatments with asphalt-based binders as an alternative. A recent study investigated the feasibility of applying resin-epoxy HFST on normally deteriorated pavement surfaces and examined a potential alternative using an asphalt-based binder instead. The asphalt-based application used the same hard, highly angular, fine aggregate, as the polymer-based application and is referenced as high friction chip seal (HFCS), or high friction seal coating (HFSC). The asphalt-based application was recommended for pavement areas where HFST is not suitable because of surface deterioration.

This research is focused on evaluating the performance of HFST applications made with asphalt-based binders as alternatives to polymer resins (epoxy) binders. The presented research is an extension of the completed research #TR202005 “Evaluation of Alternatives to Calcined Bauxite for Use in HFST” with asphalt-based binders. This study provides additional testing data and performance information on the selected aggregates and asphalt-based binders to assist MoDOT in future HFST applicability. More consistent experiments with additional aggregate gradations were included in the testing program of this study. Polymer-modified asphalt binders were developed and tested in HFST applications, as outlined in this report.

The aggregate testing contained three categories: the first was physical properties testing, the second durability testing, and the third was performance testing. Physical testing included aggregate gradation, specific gravity and absorption, and uncompacted void content (UVC) of fine aggregates testing. Durability testing included Los Angeles Abrasion (LAA), sodium sulfate soundness, water-alcohol freeze thaw, and acid-insoluble residue testing. Physical properties and durability tests were run to classify the aggregates and identify the routine tests that investigate the performance of the proposed aggregates as HFST materials. Performance testing included Micro-Deval (MD) polishing, also considered a durability test, and Aggregate Image Measurement System (AIMS). The MD results reflected the aggregates’ resistances to polishing and abrasion. The AIMS explored the changes that occurred to the Texture (TX) indices and Gradient Angularity (GA) indices, using the gradient method, for the coarse aggregates before

polishing and after 105, 180, and 240 minutes of MD polishing. Asphalt binder testing involved binder characterization for performance grade (PG) binders and emulsion binders and pull-off testing for all tested binders. Friction testing involved using the Dynamic Friction Tester (DFT) to examine the Coefficient of Friction (COF) values before and after polishing using the Three-Wheel Polishing Device (TWPD) and the circular track texture meter (CT-Meter) to determine the Mean Profile Depth (MPD). Finally, the British Pendulum (BP) test evaluated the aggregates' surface frictional properties before and after a 10-hr polishing time using the British Wheel.

The analysis of testing data revealed variations in binder performance based on aggregate size and type, directly impacting both frictional properties and economic feasibility. The study highlighted the critical role of binder selection in maximizing frictional performance and economic efficiency. The findings suggest that while epoxy resin offers excellent performance for certain aggregates and conditions, modified PG binders, particularly in specific ratios, provide a balanced solution for both friction and cost across varying aggregate sizes and types. This insight is valuable for infrastructure planning and maintenance, ensuring long-term durability and safety of road surfaces.

The researchers developed a simple Life-Cycle-Cost (LCC) process using Excel to calculate the Net Present Value (NPV) for HFST applications based on BP, DFT, or CTM results. The major input data for the LCC program were categorized into material and project specifics. Performance prediction models were used to convert the input data into Skid Number (SN) values. The predicted terminal SN was compared with the recommended terminal SN using rehabilitation matrix. This matrix was proposed based on the predicted and recommended terminal SN values. Finally, the output data were calculated; these data presented the NPVs for the HFST applications. Based on the lowest NPV, the best HFST application was selected.

The presented data and conclusions of this study will assist MoDOT in enhancing road safety by using the appropriate HFST at a reduced cost. The outcomes of this study shall assist MoDOT in identifying possible alternative asphalt binder-aggregate combinations that provide comparable frictional characteristics to those of the current HFST practices with Calcined Bauxite and epoxy resin and provide comparable performance.

CHAPTER 1: INTRODUCTION

High Friction Surface Treatment (HFST) is an effective and economical solution that has demonstrated its ability to increase pavement friction and reduce crash rates worldwide. The adoption of HFST in the United States has experienced significant growth over the past 15 years. Initially, in 2005, only a few demonstration installations existed; however, by 2021, 44 states had implemented at least one HFST installation with the primary objective of improving road safety (FHWA-SA-21-093). The Missouri Department of Transportation (MoDOT) has used HFST since 2013 to restore pavement surface friction where traffic has worn down pavement surface aggregates and to improve wet crash locations. Conventional HFST applications consist of a polymer resin layer, which is used to bond the pavement with high abrasion, high angularity and texture, and polish resistant aggregates (e.g., Calcined Bauxite (CB)). The relatively high cost of constructing, and removing, HFST with polymer resins along with the durability concerns due to existing pavement conditions, has led state agencies to consider high friction surface treatment with asphalt-based binders as an alternative. This research is focused on testing HFST applications with asphalt-based binders as alternatives to polymer resins (epoxy) binders.

1.1 Research Objectives

This project will evaluate alternative binders for use in surface friction treatments. The main objective of this research study is to evaluate, assess, and identify the use of high friction aggregate sources in asphalt-based surface treatment applications. The frictional characteristics of HFST will be measured using state-of-the-art methods that prove to correlate well with field performance. The outcomes of this study shall assist MoDOT in evaluating the suitability of available asphalt-based binders to be used with the selected aggregate sources as HFST combinations.

The presented research is an extension of the completed research #TR202005 “Evaluation of Alternatives to Calcined Bauxite for Use in HFST” with asphalt-based binders. This study provides additional testing data and performance information on the selected aggregates and asphalt-based binders to assist MoDOT in future HFST applicability. More consistent experiments with additional aggregate gradations were included in the testing program of this study. Additional asphalt binders were developed and tested in HFST, as outlined in this report.

1.2 Research Management

The presented research has been conducted at the facilities of Missouri University of Science and Technology (Missouri S&T). Dr. Magdy Abdelrahman serves as the principal investigator of this contract, and Dr. John Myers serves as co-investigator. Mr. Alireza Roshan, Ph.D. student at Missouri S&T, led the team of students who conducted the testing and led the report writing and data analysis effort.

1.3 Report Organization

In addition to HFST performance testing, the presented research includes physical testing, durability testing, and aggregate performance testing. Adopted asphalt binders were tested and evaluated. Literature review on the HFST practice, materials, constructions, and testing is

presented in Chapter 2. Experimental considerations including material selection, testing matrices, and standards is presented in Chapter 3. Physical properties testing and durability testing of aggregate sources are presented in Chapter 4. The aggregate performance testing includes the Aggregate Image Measurement System (AIMS), the Micro-Deval (MD) test, the British Wheel test, the British Pendulum (BP) test, and the Dynamic Friction test. The aggregate performance testing results are discussed in Chapter 5. Binder performance testing is presented in Chapter 6. High friction performance testing is presented in Chapter 7. Testing results were analyzed and used to predict and compare the friction performance of the asphalt-based aggregate combinations; results and discussions are presented in both Chapter 5 and Chapter 7. Cost analysis is presented in Chapter 8; a Life-Cycle-Cost (LCC) simple program has been developed based on the performance of the tested asphalt based-aggregate combinations. Conclusions and recommendations are presented in Chapter 9. This research provides recommendations for future screening and testing of potential HFST with asphalt-based binders and future specifications.

Appendix A presents lists of the state HFST application and performance specifications and testing standards. Appendix B presents physical properties, durability, and performance testing and sample preparation procedures. Appendix C presents image examples of the tested HFST coupons and slabs of different asphalt based-aggregate combinations. Appendix D provides details on the LCC analysis and calculations as used in this study.

CHAPTER 2: LITERATURE REVIEW

2.1 Introduction

High friction surface treatment (HFST) is a specialized safety and pavement surface treatment that can significantly and rapidly increase the friction of pavement surfaces. This increased friction helps to reduce crashes, injuries, and fatalities that are associated with insufficient pavement friction. HFST can help compensate for deficiencies in road design, such as sharp curves or inadequate superelevation, by providing the necessary friction for vehicles to maintain traction and stay on the intended path. Additionally, HFST can restore pavement surface friction in areas where existing pavement aggregates have become polished and worn down by traffic over time (FHWA-SA-21-093).

A considerable number of highway crashes happen on specific road sections with certain surface conditions, like horizontal curves and intersections, which are more prone to accidents. Ensuring sufficient friction is essential, as reduced traction can lead to accidents. Heavy traffic can cause pavement surfaces to become polished prematurely, lowering friction and raising the risk of vehicles losing control, skidding, or crashing during high speeds, sharp turns, or sudden braking. HFST can effectively restore friction levels to these polished pavements. Numerous studies have highlighted pavement friction as a crucial factor influencing the likelihood of traffic crashes; as pavement friction decreases, roadway crashes tend to increase significantly (Mayora and Pina, 2009; McGovern et al., 2011; Musey and Park, 2016; Najafi et al., 2017). Wallman and Astrom (2001) discovered that improving the pavement friction coefficient from below 0.15 to the range of 0.35 to 0.44 can lead to a 75% reduction in car accident rates.

According to the Federal Highway Administration (FHWA) Everyday Counts program, High Friction Surface Treatment (HFST) is frequently employed to improve the surface friction of asphalt pavement in areas with high crash rates, including horizontal curves, deceleration ramps, and intersection approaches. As of now, HFSTs have been deployed in 44 states across the United States, with 24 states having established their own implementation programs for this technology (Bosin et al.,2018).

Numerous studies have demonstrated that the use of HFST has had a significant impact on reducing crash rates at curves, at intersections, and with wet surface conditions (Milstead et al. 2011; Heitzman, Michael; Moore 2017; Harkey et al. 2008). In particular, FHWA has investigated the use of HFST as a means to reduce crash fatalities and injuries near or at horizontal curves through the Surface Enhancements at Horizontal Curves (SEAHC) project conducted across the United States (FHWA, 2019).

Harkey et al. (2008) conducted a study on New York's Skid Accident Reduction Program, comparing crash rates before and after friction treatments. They found that HFST resulted in a 24% reduction in all crashes and a 57% reduction in wet-weather crashes. Additionally, FHWA evaluated 60 HFST sections in Kentucky and observed a 78% reduction in total crashes and an 85% reduction in wet-weather crashes due to HFST implementation (FHWA-CAI-14-019). Several projects have demonstrated the effectiveness of HFST in reducing roadway departure crashes. For instance, Li Q. et al. (2016) utilized 3D laser imaging technology to gather pavement surface data at 21 HFST demonstration sites across 10 states, observing various

environmental and traffic conditions. Musey. et al. (2017) reviewed 122 HFST sites in Pennsylvania and found that HFST provided significant safety benefits, particularly on horizontal curves with a radius of less than 300 feet.

HFST is considered a non-conventional pavement surface treatment because it utilizes materials not typically used in traditional paving practices. The surface aggregate is responsible for providing the actual skid resistance, while the resin binder plays a crucial role in bonding the aggregate to the underlying pavement surface, ensuring the durability and effectiveness of the treatment. Calcined Bauxite has a well-established history of offering excellent polish and abrasion resistance properties, which are essential for High Friction Surface Treatment (HFST) applications. Notably, Calcined Bauxite is the sole aggregate permitted for HFST under the current American Association of State Highway and Transportation Officials (AASHTO) specification, as well as in nearly all state specifications. Its acceptance extends to other countries with substantial HFST utilization, including the United Kingdom and New Zealand (Highways England 2019, NZTA 2011).

Performance is the key consideration when evaluating the friction of HFST application and HFST is known for its ability to maintain good long-term friction performance. However, it's important to note that the friction performance can decline significantly toward the end of its lifespan. This deterioration is often attributed to end-of-life aggregate loss, which occurs due to a reduction in the resin binder's binding capacity as it ages, compounded by vehicle shear forces acting on the HFST surface. As the aggregate loss progresses, especially on wheel paths, it exposes the smooth epoxy or resin binder layer, leading to a substantial reduction in friction (Pranav, et al.,2021).

HFST aggregate achieves its friction-enhancing properties through the interplay of microtexture and macrotexture. Microtexture, the finer surface roughness of aggregate particles, aids in creating friction by means of adhesion, which is a small-scale interaction and bonding between the aggregate particles and the rubber of vehicle tires. Conversely, macrotexture, the more apparent texture formed by the aggregate particles and the spaces among them, is vital for preventing skid at higher speeds and in moist conditions by allowing water to be channeled away from under the tire, ensuring the tire maintains contact with the aggregate surface. Furthermore, macrotexture is essential for the hysteresis aspect of friction, affecting tire and aggregate particle interaction in both wet and dry conditions. In scenarios where macrotexture is lacking, microtexture alone is insufficient for ensuring tire grip on wet surfaces at high speeds, leading to a decrease in frictional effectiveness (FHWA-SA-21-093). Given the critical role that both micro- and macrotexture play in preserving pavement friction, it is essential for the aggregate used in HFST to exhibit resistance to polishing and abrasion. This ensures that such textural properties are maintained despite the wear induced by vehicular traffic over the treatment's lifespan.

Under the current specifications set forth by the American Association of State Highway and Transportation Officials (AASHTO:MP 41-22), Calcined Bauxite is the exclusive aggregate approved for use as HFST aggregate. The leading producers of bauxite, the raw material for CB, include Australia, China, Brazil, India, Guinea, and Jamaica, as reported by Wilson et al. (2016). Refractory-grade Calcined Bauxite is produced by heating raw bauxite to temperatures ranging from 2,900 to 3,000°F. This process yields a dense, highly pure, and stable aggregate. Characterized by a high alumina content of at least 87 percent and a very low alkali content of no

more than 0.4 percent, refractory-grade bauxite stands out for its minimal impurities and a bulk density of 3.1 or greater.

Due to concerns regarding the expense and the necessity of importing calcined bauxite from abroad, extensive research has been conducted to explore alternative aggregates that can be sourced domestically. This research includes numerous laboratory analyses and small-scale field tests as reported by Heitzman et al. (2015), Wilson and Mukhopadhyay (2016), Heitzman and Moore (2017), Pratt (2018b), Li et al. (2017, 2019) and Deef-Allah and Abdelrahman (2021). These comprehensive evaluations have consistently demonstrated that no other material matches the superior long-term friction performance provided by calcined bauxite. However, it is important to acknowledge that these alternative aggregates, which encompass materials like flint, steel slag, basalt, granite, emery, taconite, rhyolite and Meramec can still offer adequate frictional properties for specific applications that require less intense friction, such as bridge deck overlays.

The application of a resin binder, such as epoxy resin, polyester resin, polyurethane resin, acrylic resin, or methyl methacrylate (MMA), is integral to bonding the aggregate layer with the pavement surface (FHWA 2021; Merritt, Moravec, and Heitzman 2014; Wilson and Mukhopadhyay 2016). In the United States, epoxy resin and polyester resin are the most commonly used resin binder materials for HFST, although methyl methacrylate (MMA) has been used to a limited extent by agencies. These resin binders are typically multi-component, thermosetting, exothermic materials known for their high strength and low modulus properties. They exhibit resistance to chemicals, ultraviolet light, and are sensitive to moisture during the curing process.

Epoxy resins are two-part systems with a 1:1 volume mixing ratio, comprising a resin and a curing agent that hardens the epoxy through a heat-releasing reaction. Application requires temperatures above 50°F (10°C) (FHWA-RC-20-0009, 2019), and curing times vary with temperature per manufacturer guidelines. Key properties of the resin binder that affect HFST performance include viscosity, which influences flow and penetration, gel time, which determines the window for spreading and aggregate placement, cure rate, which dictates hardening speed and traffic reopening time, adhesion strength to the pavement (ASTM C1583), and thermal compatibility, which reflects bond stability under temperature changes.

2.2 High Friction Surface Treatment (HFST) Applications

This section outlines the necessary precautions to consider both prior to and throughout the application of HFST. Additionally, it provides a summary and demonstration of HFST application techniques, categorized by the specific method of binder mixing, the process of applying binder and aggregate, and the advantages, disadvantages, and rates of application.

2.2.1 Pre-Application Inspection and Surface Preparation

A successful HFST application depends on a thorough pre-application inspection and surface preparation process. This step ensures a clean, sound substrate for optimal performance and longevity of the treatment.

By following these pre-application measures, a suitable foundation is established for successful HFST installation and long-lasting performance.

- **Pavement Condition Assessment:** The pavement surface must be inspected for existing distresses such as fatigue cracking, rutting, raveling, delamination, or bleeding (FHWA, 2022; Wilson & Mukhopadhyay, 2016). Areas with severe distress are not suitable candidates for HFST and require repair or replacement before proceeding. For extensively fractured concrete slabs, removal and replacement is necessary (Wilson & Mukhopadhyay, 2016).

- **Crack Sealing:** Cracks exceeding 0.25 inches in width and depth require sealing with rubberized asphalt at least 30 days before HFST application (FHWA-SA-22-016, MoDOT, 2015). Polymer resin crack sealants can expedite the process by allowing HFST installation after gelation (FHWA-SA-22-016).

- **Surface Cleaning:** Asphalt surfaces must be meticulously cleaned using mechanical sweepers and high-pressure air with proper oil capture systems to remove dirt and debris (Heitzman & Moore, 2017; MoDOT, 2015). Rigid pavements may require shot blasting to eliminate contaminants like debris, dust, and laitance (a weak mortar layer).

- **Protection Measures:** Utilities, curbs, and drainage structures in the vicinity of the application zone need protection to prevent inadvertent coating with HFST. Existing pavement markings near the application area must be covered or removed entirely, as HFST may not adhere well to thermoplastic markings (FHWA-SA-22-016).

- **Age Restriction:** HFST application on newly placed asphalt pavements less than 30 days old is not recommended (MoDOT, 2015).

2.2.2 Material Mixing Precautions and Conditions for HFST

Improper mixing of resin binders can lead to premature aggregate loss and increased wear in the wheel path (FHWA-SA-22-016). Resin binders typically set in 2-4 hours (Wilson & Mukhopadhyay, 2016). The recommended thickness is 50% of the nominal maximum aggregate size (50-65 mils) to ensure proper embedding (FHWA, 2020; Wilson & Mukhopadhyay, 2016; FHWA-SA-22-016). Too thin a layer will not retain aggregates effectively, while too thick a layer can reduce friction by encapsulating the aggregates (FHWA-SA-22-016). Aggregates should be applied before the resin reaches its gel time to ensure proper embedding (FHWA, 2020; Wilson & Mukhopadhyay, 2016). Automated methods can broadcast aggregates immediately after resin placement, addressing timing issues (FHWA-SA-22-016). HFST should be applied to new asphalt pavements 30 days after construction and to new rigid pavements after 28 days ("High Friction Surface Treatments in Pennsylvania", n.d.; FHWA-CAI-14-019, n.d.). Double-layer HFST may be necessary for coarse and open-graded asphalt surfaces to prevent resin percolation, offering increased durability in harsh environments and high-traffic zones, though it is less flexible than single-layer HFST (Wilson & Mukhopadhyay, 2016; FHWA-SA-22-016).

2.3 Service Life of HFST

The longevity of HFST is influenced by a complex interplay of factors, making it difficult to provide a single, definitive lifespan estimate. Here is a breakdown of the key considerations.

Impactful Factors:

- Pavement condition: The underlying pavement's structural integrity significantly impacts HFST life expectancy. A properly installed HFST on a sound pavement will exhibit greater longevity (FHWA-SA-22-016).
- Installation quality: Proper application techniques, including uniform resin binder thickness and timely aggregate embedment, are crucial for optimal service life (RSTA ADEPT, 2017).
- Climate: Environmental factors like weather severity play a role. Harsh climates can accelerate wear (NCAT, 2015).
- Traffic characteristics:
    - Volume: Higher traffic volume translates to increased wear and tear, reducing lifespan. Studies suggest a potential 5-year service life for roads with 50,000 vehicles daily and 5-8 years for 15,000 vehicles (FHWA-SA-22-016).
    - Traffic mix: The presence of heavy trucks with studded tires or chains can lead to faster wear within wheel paths (RSTA ADEPT, 2017).
    - Traffic patterns: The nature of traffic movement (e.g., frequent braking or turning) can influence wear patterns.

Service Life Estimates:

- Reported Range: Studies and industry reports suggest a service life range of 7 to 12 years for properly installed HFST (FHWA-SA-22-016; RSTA ADEPT, 2017).
- Limited Long-Term Data: As a relatively new technology in the U.S., there are few HFST installations exceeding 10 years. However, some installations remain functional and effective in reducing crashes after 8-10 years (NCAT, 2018).
- Test Track Results: Accelerated wear testing on test tracks indicates some HFST sections lasting over 30 million equivalent single-axle loads (ESALs) while maintaining friction properties (NCAT, 2015).
- International Experience: The Road Surface Treatment Association (RSTA) from the UK reports an average service life of 12 years for cold-applied HFST (RSTA ADEPT, 2017).

Monitoring and Evaluation:

- Friction Testing: As the primary purpose of HFST is to enhance friction, remaining life should be assessed based on friction performance, not just visual appearance. A seemingly worn HFST may still provide sufficient friction and safety benefits (RSTA ADEPT, 2017).

- Regular inspections are crucial to identify potential issues and ensure continued effectiveness.

2.4 Cost of High Friction Surface Treatment (HFST)

The cost of HFST encompasses materials, labor, equipment, and traffic control. Here is a breakdown of the cost considerations:

Cost Range:

- Reported Range (2017): $21 - $26 per square yard ($yd^2$) (FHWA-SA-18-004). Costs decrease for larger projects.

- Real-world Example: A 2017 project for the Georgia Department of Transportation treating 1,200,000 yd^2 across 16 counties averaged $21.00/$yd^2$. This aligns with the reported national range. Similar pricing was observed in projects from California, New York, Pennsylvania, South Carolina, and New Jersey (FHWA-SA-18-004). It is important to note that some of these projects may have included additional services in their unit pricing, such as mobilization, traffic control, striping, remedial crack sealing, and patching.

Cost Drivers:

- Epoxy Resin Binder: The primary cost driver is the epoxy resin binder, along with equipment and labor (FHWA-SA-18-004).

- Contracting Method: Agency contracting mechanisms significantly impact overall installed costs.

Project Scope:

- Stand-alone Projects: It is recommended to keep HFST projects separate from paving or other related work through prime contracts. This avoids additional markups from general contractors on the HFST unit price (FHWA-SA-18-004).

Cost Reduction Strategies:

- Turnkey Contracts: Soliciting projects as turnkey, encompassing all aspects (mobilization, materials, labor, equipment, and traffic control), can be cost-effective.

- Project Size: Larger projects and those bundled with other safety-related items typically experience lower costs per square yard.
- Direct Contracting: Specifying only HFST-related work increases the likelihood of contracting directly with specialized installers, potentially reducing costs.

There are three primary methods for applying HFST, each with its own advantages and limitations, Table 2-1 depicts the construction methods of the HFST (FHWA-CAI-14-019 n.d.; Wilson and Mukhopadhyay 2016).

Table 2-1 Construction methods of the HFST

Feature	Manual Method	Machine-Aided Manual (Semi-Automated) Method	Fully Automated Method
Applicability	Small areas (up to 200 sq. yd.)	Medium-sized applications (not explicitly defined)	Large-scale, systemic installations
Binder Mixing	Manual mixing in buckets on-site (Jiffy mixer recommended)	Mixing machine on trucks	Metered, mixed, and applied by truck-mounted system
Binder Application	Poured and spread by hand using squeegees	Pumped from trucks and spread by workers using squeegees	Automatic application across the pavement surface
Aggregate Application	Broadcast by hand or blower	Broadcast by hand or blower	Dropped uniformly on the binder layer
Application Rate	200-300 sq. yd./hr	300 sq. yd./hr	1,500-2,300 sq. yd./hr
Benefits	Low cost for small areas	Faster application, reduced lane closure time	High-quality application, lower overall project cost (large projects)
Drawbacks	Safety concerns for workers, human error, slow application	Potential human error in binder application, lower efficiency than fully automated	Expensive equipment, less adaptable to highly textured surfaces

2.5 High Friction Surface Treatment (HFST): Potential Issues and Considerations

While High Friction Surface Treatment (HFST) offers many benefits, it is not without its challenges. Construction practices and the condition of the existing pavement significantly impact HFST performance.

2.5.1 Distresses Caused by Construction and Existing Pavement Defects

Research by the Texas Transportation Institute (TTI) identified that construction issues and pre-existing pavement defects can significantly shorten HFST lifespan. Selecting suitable pavements for HFST based on visual assessments is challenging and subjective, potentially missing signs of future problems like raveling or cracking (Anderson et al., 2011). Premature HFST failure often results from poor site conditions, unsuitable materials, or inadequate installation, while terminal failure is due to aggregate loss from traffic wear over time. Delamination, caused by inadequate macrotexture, improper surface preparation, or underlying pavement failure, is a critical premature failure mechanism, reducing skid resistance and safety. Addressing these issues during installation is essential for HFST longevity and effectiveness.

2.5.1.1 Delamination

The bond between the resin binder and pavement surface in HFST is partially mechanical, which involves the interlocking of the resin binder with the pavement surface through macrotexture. If the pavement surface has insufficient macrotexture, the mechanical bond can be weakened. Additionally, poor bond strength can result from improper surface preparation, such as inadequate cleaning that leaves behind dust and debris, hindering the bond between the resin binder and pavement surface. These conditions can lead to delamination of the HFST from the pavement surface. Inadequate surface preparation is the potential factor that can cause this failure in HFST. Proper surface preparation is critical to ensure effective and long-lasting HFST application (FHWA-SA-21-093).

2.5.2 Asphalt Incompatibility

Another concern is the incompatibility between the epoxy resin binder used in HFST and asphalt surfaces. This incompatibility can lead to high thermal and tensile stresses in the asphalt layer.

The main reason for these stresses is that the coefficient of expansion and contraction of epoxy resin is two to three times greater than that of asphalt mixtures (Bennert et al., 2021). This mismatch, combined with weakened asphalt and temperature variations (thermal cycling), often leads to substrate failure due to shallow horizontal cracks and delamination.

Potential causes of underlying pavement failure when HFST is applied include excessive moisture, which weakens the pavement, and thermal incompatibility, where differing thermal expansion rates cause cracking. Additionally, pre-existing pavement conditions can contribute to failure, as distressed pavements may not support the added weight and traffic loads from the HFST layer.

2.6 High Friction Chip Seal (HFCS)

While the current epoxy-resin-based High Friction Surface Treatment (HFST) offers benefits, it also has limitations, particularly regarding compatibility with existing asphalt pavements. The New Jersey Department of Transportation (NJDOT) addressed compatibility concerns between traditional epoxy-resin HFST and existing asphalt pavements by developing a High Friction Chip Seal (HFCS) application (NJDOT, DIVISION 420).

HFCS mimics the application process of traditional epoxy-resin HFST. However, it utilizes asphalt materials that are more compatible with existing asphalt pavements.

2.6.1 Key Feature of HFCS

A hot asphalt binder is used as the primary adhesive mechanism in HFCS applications, replacing the epoxy resin. The chosen asphalt binder needs a balance of properties; high-temperature stiffness to ensure that the aggregates stay bonded during hot weather and resist loosening or movement and regional low-temperature performance, because the binder must also be suitable for the specific region's low-temperature cracking resistance requirements.

This approach by NJDOT offers a potential solution for applying high-friction surface treatments on asphalt pavements while mitigating compatibility issues associated with traditional epoxy-resin binders.

2.6.1.1 Asphalt Binder Selection

To address compatibility issues, a PG88-22 asphalt binder was chosen. This binder adheres to AASHTO M320 standards and fulfills the Federal Aviation Administration's (FAA) P404 Fuel Resistant (FR) Asphalt Mixture requirements. The PG88-22 designation indicates its suitability for high-performance pavements and resistance to permanent deformation at elevated temperatures (88). The FR properties provide an additional benefit for SR68, which likely experiences some level of fuel exposure.

2.6.1.2 Aggregate Selection and Pre-coating

The selected aggregate for the HFCS resembled the typical gradation of Calcined Bauxite used in conventional HFST. However, for potentially improved durability, these aggregates were precoated with 0.4% to 0.8% asphalt (by dry weight) before application. This pre-coating likely enhances the bonding between the aggregate and the asphalt binder.

2.6.1.3 HFCS Application Process by NJDOT

1. A layer of hot FR asphalt binder is applied to the pavement surface.
2. Precoated aggregate is spread evenly onto the hot asphalt binder.
3. Rubber-tired rollers are used to firmly seat the aggregate chips into the hot asphalt binder, ensuring proper embedment.

4. Once the aggregates are seated, the pavement surface is swept and vacuumed to remove any loose materials.

This specific example of HFCS implementation by NJDOT showcases a practical approach for applying high-friction surfaces on asphalt pavements. It combines improved compatibility with potentially better durability through the using pre-coated aggregates.

2.7 High Friction Surface Treatment (HFST) and High Friction Chip Seal (HFCS) Standards

While various states have established their own standards for HFST applications, the Federal Highway Administration (FHWA) provides general guidelines (FHWA-SA-21-093). These state standards served as the primary basis for most tests conducted in this project. Specifications related to HFST for some other states are provided in Appendix A.

2.7.1 MoDOT High Friction Surface Treatment (HFST) Standard

The Missouri Department of Transportation (MoDOT) currently utilizes NJSP-15-13B as the standard specification for High Friction Surface Treatment (HFST) applications. The tests of resin binder (polymeric and MMA) systems are summarized in Table 2-2. MoDOT's current standard, NJSP-15-13B, also specifies requirements for the aggregate used in High Friction Surface Treatment (HFST) applications. NJSP-15-13B mandates the use of Calcined Bauxite (CB) as the aggregate for HFST. Table 2-3 (shown below) summarizes the specific requirements for CB according to MoDOT specifications.

2.7.2 AASHTO MP 41-22

AASHTO MP 41-22 supersedes the provisional standard AASHTO PP 79-14, which was previously referenced in MoDOT's NJSP-15-13B document. This update signifies a shift towards a more comprehensive and up-to-date standard for HFST materials. In the appendix A, a summary of the necessary tests and corresponding specifications as per AASHTO MP 41-22, is provided.

2.7.3 High Friction Chip Seal (HFCS) standard

NJDOT currently utilizes Division 420 – Pavement Preservation Treatments (Section 424 Chip Seal) as the standard specification for HFCS applications.

Asphalt Binder Application:

Apply the asphalt binder at the manufacturer's recommended temperature. Use an application rate of 0.30 to 0.38 gallons per square yard, determined during the test strip.

HFCS Aggregate:

The fine aggregate must be clean, dry, and pure manufactured Calcined Bauxite stone sand, free of contaminants, and meet the specifications listed in Appendix A.

Table 2-2 Required testing for resin binder systems (Missouri DOT 2015)

Test	Standard
Adhesive Strength at 24h	ASTM D4541
Compressive Strength	ASTM C579
Cure Time (Dry Through Time)	ASTM D1640
Durometer Hardness (Shore D)	ASTM D2240
Elongation at Breakpoint	AASHTO M 235
Gel Time (Class C)	AASHTO M 235
Ultimate Tensile Strength	AASHTO M 235
Viscosity (Class C)	ASTM D2556
Water Absorption	AASHTO M 235

Table 2-3 MoDOT's requirements for CB

Test	Threshold Value	Specification
Degradation Resistance (LAA)[a]	20% Loss Max	AASHTO T 96
Moisture Content	0.2% Max	AASHTO T 255
Aluminum Oxide Content	87% Min	ASTM C25
Gradation (% passing)		AASHTO T 27
#4 Sieve	100% Min	
#6 Sieve	95% Min	
#16 Sieve	5% Max	

a= LAA: Los Angeles Abrasion.

CHAPTER 3: EXPERIMENTAL CONSIDERATIONS

3.1 Introduction

A preliminary testing program, aimed at narrowing down the material selection process and focusing the subsequent testing program on specific binder sources and aggregates will be an essential step in the research project. The objective is to streamline the research efforts and ensure that the most promising materials are chosen for further investigation. The preliminary testing phase will encompass all the selected materials under consideration. This comprehensive assessment will allow for an initial evaluation of their characteristics, properties, and performance.

3.2 Aggregate Selection

Calcined Bauxite, Rhyolite, Meramec, and Flint were selected as test aggregates. New and numerous samples of these aggregates, each type from the same source, were received for testing. The selection process considered the information shown in Table 3-1, which provides information on received sizes, Maximum Aggregate Size (MAS), Nominal Maximum Aggregate Size (NMAS), sources, and additional notes. These aggregates underwent testing to assess their compliance with the MoDOT requirements for High Friction Surface Treatment (HFST) outlined in NJSP-15-13B, as well as to anticipate any forthcoming modifications to the HFST standard.

Table 3-1 Received aggregate sizes and sources information [2]

Aggregate Type	Commercial Names and Received Sizes	Source	Notes
Calcined Bauxite (CB)	3/8″ × #3: Maximum Aggregate Size (MAS) (3/8″), #3 × 0: MAS (#3), and GRIP Grain: MAS (#4).	Great Lakes Minerals, LLC in Wurtland, Kentucky, U.S. A	The GRIP grain CB is exclusively manufactured for HFST, CB's aluminum oxide content, typically at 87.5%, specified in the majority of HFST specifications.
Rhyolite (Trap Rock)	1/2″ × 0: MAS (1/2″), and #6 × #16: MAS (#6).	New Frontier Materials in Maryland Heights Missouri, U.S.A.	The common utilization of this aggregate includes road and railroad construction, as well as its application as a chip seal material.
Meramec River	C Gravel: MAS (1 1/2″), 5/16″ Crushed Gravel: MAS (5/16″), Torpedo Gravel: MAS (1/2″), and Coarse Manufactured Sand: MAS (3/8″)	Winter Brothers Material Company in Saint Louis, Missouri, U.S.A.	Meramec River Aggregate is sourced directly from the Meramec River and serves a dual purpose in both road and concrete.

Flint Chat	#6 × #16: NMAS (#6)	Williams Diversified Materials in Baxter Springs, Kansas, U.S. A	The Flint Chat is exclusively manufactured to enhance friction in surface treatments.

In addition to the standard HFST gradation specified by MoDOT, the following aggregate gradations are being considered for initial trials in the asphalt binder applications:

1. HFST gradation specified by MoDOT

Table 3-2 MoDOT standard HFST gradation

Sieve Size	(% Passing)	Specification
No. 4	100 Min	AASHTO T27
No. 6	90 Min	
No. 16	5 Max	

2. Aggregates for Surface Treatment: The gradation specified in Section 413, titled "Aggregates for Surface Treatment" of the "Missouri Standard Specifications, 2023" on page 208, under Use Type II. Referred to medium size for this specific category of aggregates.

Table 3-3 Aggregates for surface treatment

Sieve Size	Type II Grades A, B, or C (% Passing)	Type III/IIIR Grades A, B, or C (%Passing)	Stockpile Tolerance
3/8 inch	100	100 (98*)	+/- N/A
No. 4	90 - 100	70 - 90	+/- 5%
No. 8	65 - 90	45 – 70	+/- 5%
No. 16	45 - 70	28 – 50	+/- 5%
No. 30	30 - 50	19 – 34	+/- 5%

No. 50	18 - 30	12 – 25	+/- 4%
No. 100	10 - 21	7 – 18	+/- 3%
No. 200	5 - 15	5 - 15	+/- 2%

3. Aggregates for Seal Coats: The gradation outlined in Section 1003, titled "Aggregates for Seal Coats" of the "Missouri Standard Specifications, 2023" on page 536, under Grade A2. This gradation is being considered for the trials. Referred to coarse size for this specific category of aggregates.

Table 3-4 Aggregates for seal coats

Sieve Size	Grade A1 (%Passing)	Grade A2 (%Passing)	Grade B1 (%Passing)	Grade B2 (% Passing)	Grade C (% Passing)
1/2 inch	100	100	100	100	100
3/8 inch	97-100	100	95-100	100	95-100
1/4 inch	-	97-100	-	95-100	-
No. 4	0-25	-	0-30	-	0-35
No. 8	-	-	0-30	-	0-30
No. 200	0-1.0	0-1.5	0-2	0-2.5	0-2

4. Additional Larger Aggregate Size(s): An extra-large aggregate size (1/2"~ 3/8") was obtained to ensure that the aggregates remain intact and well-distributed during hot summertime conditions.

3.2 Binder Selection

A range of binders suitable for high friction surface treatments were considered as potential replacements for epoxy. These binders included both traditional and specialized options known for their compatibility with the selected aggregates and their ability to enhance frictional characteristics. Given the incompatibility of epoxy with the substrate asphalt pavement, the objective of this project was to identify a suitable binder that could effectively replace epoxy in the high friction surface treatment application.

Asphalt binders considered as potential replacements for epoxy include:

PG Binders:

1- PG76-22, supplied by Pure Asphalt Co., Chicago Illinois

2- PG94-10, supplied by Pure Asphalt Co., Chicago Illinois

3- PG64-22, supplied by APAC Southern Missouri

4- Blended PG94-10/PG76-22 with various percentage

Based on some performance test results, it was observed that PG76-22 exhibited unfavorable softness characteristics to explore potential alternatives to epoxy resin. Consequently, in light of these findings, the decision was made to utilize a mixture of PG94-10 and PG76-22 binders in the subsequent steps of the research. Two different proportions were considered for the binder mixing: The first mixture consisted of equal parts (50%) of PG94-10 and PG76-22 (50/50 PG94-10/PG76-22), while the second mixture comprised 60% PG94-10 and 40% PG76-22(60/40 PG94-10/PG76-22). Subsequently, these two newly formulated binders were used to prepare samples for further analysis and testing.

Emulsion Binders:

CRS-2P

CRS-2PSC

Polymer-modified, cationic, water-based emulsified asphalt intended for use as a bituminous binder in chip seals.

Modified Binders:

In addition to the blended binders, the experimental approach included the preparation of two laboratory-modified binders. These modified binders were specifically formulated to overcome the limitations associated with conventional PG binders and blended binders. The formulation process involved incorporating various additives and modifiers to enhance their properties and functionalities. These additives were selected based on their potential to address the specific issues observed in the PG binders and blended binders. The two developed modified binders are based on PG64-22 and PG76-22 unmodified binders and were modified with 8% and 6% of Kraton D0243KT polymer modifier, respectively. The modified binders are listed as PG82-22 (PM) for the 8% modifier and PG88-16 (PM) for the 6% modifier. Please note that the modified binder PG88-16 (PM) is different from the regular PG88-16 binder; both binders were used in the testing program. The binders selected for this study are listed in Figure 3-1. Details about the aggregate-binder combinations are listed in Tables 3-6 and 3-7.

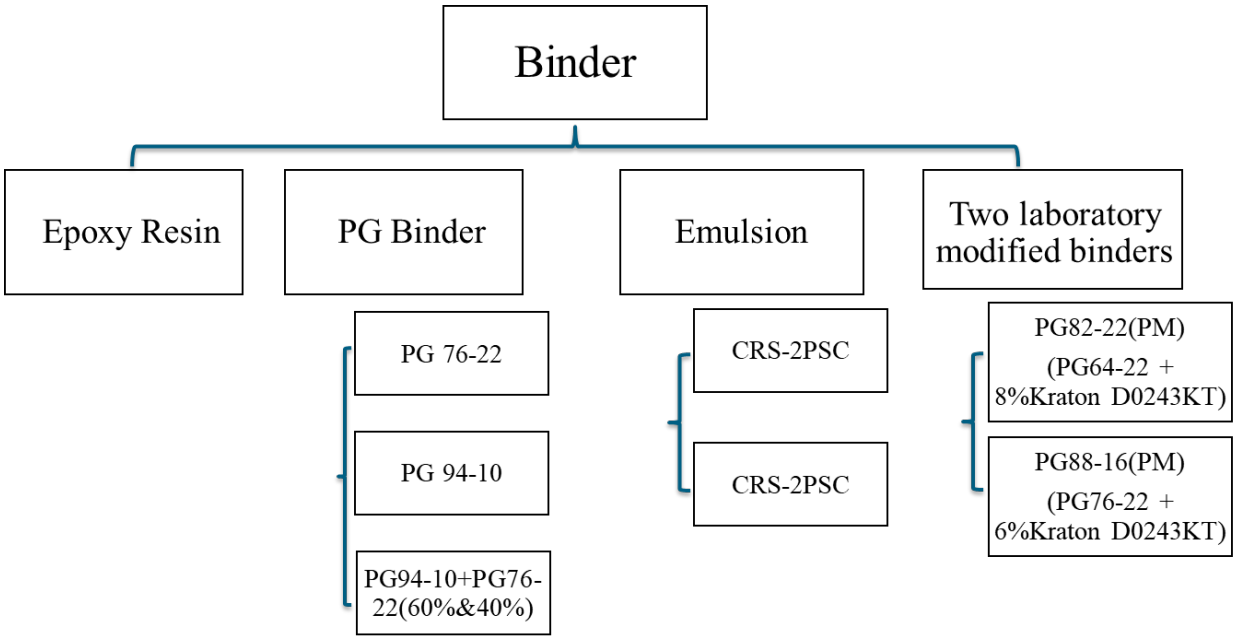

Figure 3.1 Binder selection

3.3 Experimental Design

The experimental design for aggregates, as illustrated in Figure 3.2, is organized into three main categories of testing. The initial category concentrates on testing the physical properties, aiming to evaluate the basic characteristics of the aggregates. The second category is focused on durability testing, which investigates the aggregates' ability to withstand various environmental conditions. The third category is devoted to performance testing, assessing the functionality of the aggregates, and their suitability for specific uses. For the binders, as shown in Figure 3-3, the physical and rheological properties were analyzed using a rotational viscometer (RV), dynamic shear rheometer (DSR), and bending beam rheometer (BBR). Additionally, the binder bond strength (BBS) test was performed to determine the pull-off tensile strength of various binders under dry and wet conditions.

3.3.1 Aggregate Testing Matrix

The aggregate testing matrix outlined in Table 3-5 encompassed three distinct testing categories: physical properties testing, durability testing, and performance testing. Each category delved into specific aspects of aggregate characteristics, focusing on different size gradations as per the applicable standards. In physical properties testing, the focus was on aggregate gradation, specific gravity, absorption, and Uncompacted Void Content (UVC) of fine aggregates. This encompassed a range of aggregate sizes to assess their physical attributes comprehensively. Durability testing, on the other hand, delved into aspects like Los Angeles Abrasion (LAA) resistance, sodium sulfate soundness, water-alcohol freeze-thaw durability, and acid-insoluble residue analysis. These tests were conducted across various aggregate sizes to evaluate their resistance to different forms of environmental stress.

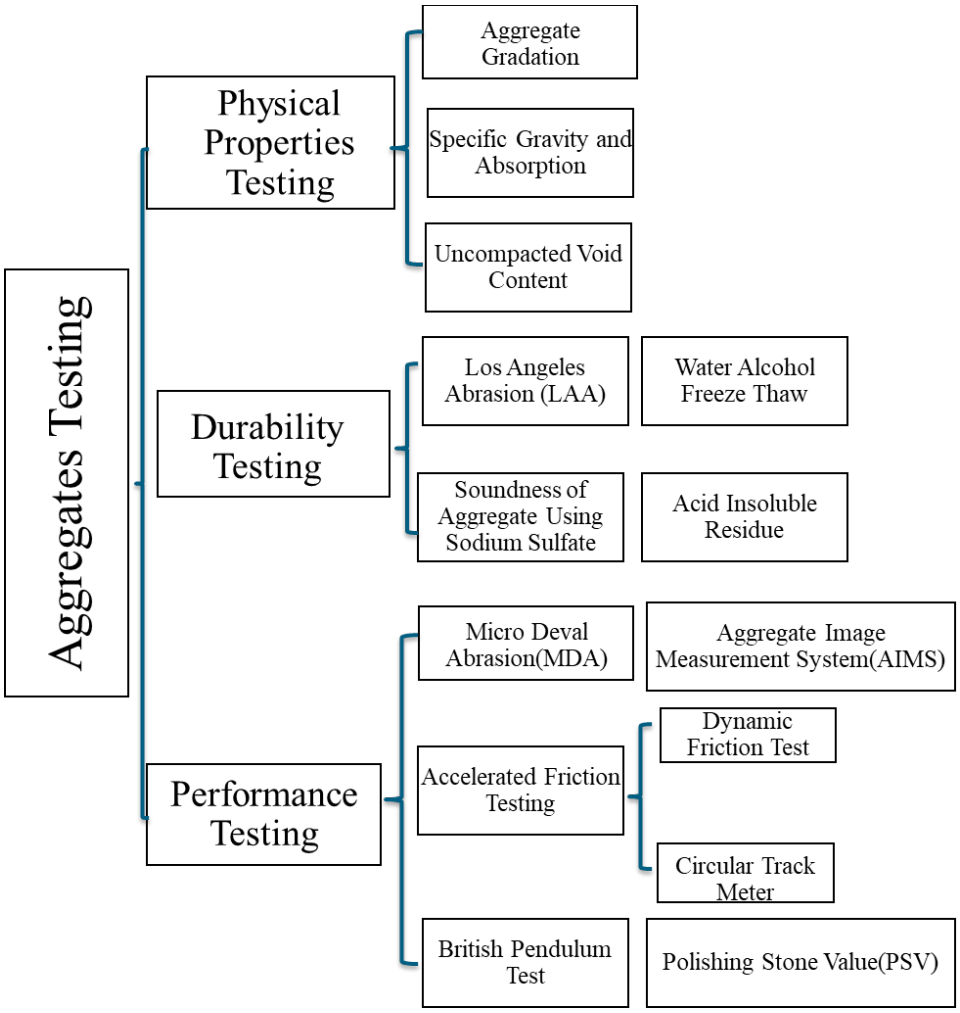

Figure 3.2 Experimental design of aggregates

Performance testing, crucial for assessing the suitability of aggregates, binders, and their combinations for practical applications, included Micro-Deval (MD) polishing to gauge abrasion resistance, Aggregate Image Measurement System (AIMS) analysis for shape and texture evaluation, and accelerated friction testing using methods like the British Pendulum (BP) test, Dynamic Friction Test (DFT), and Circular Track Meter (CTM). Each of these tests was conducted across a spectrum of aggregate types and sizes, as well as with different binders, to comprehensively capture their performance characteristics. Table 3-6 shows the British Pendulum test matrix, and Table 3-7 shows the Dynamic Friction and CT meter tests matrix. The specific aggregate percentages and weights used in MD and UVC tests are detailed in Table 3-8, highlighting the diversity of aggregates evaluated and the rigorous testing protocols employed to assess their properties thoroughly. Performance testing was conducted in two main stages starting with all aggregate sources for the first stage as shown in Table 3-6. Finalized performance testing was focused on two aggregate sources, Calcine Bauxite and Rhyolite, as shown in Table 3-7.

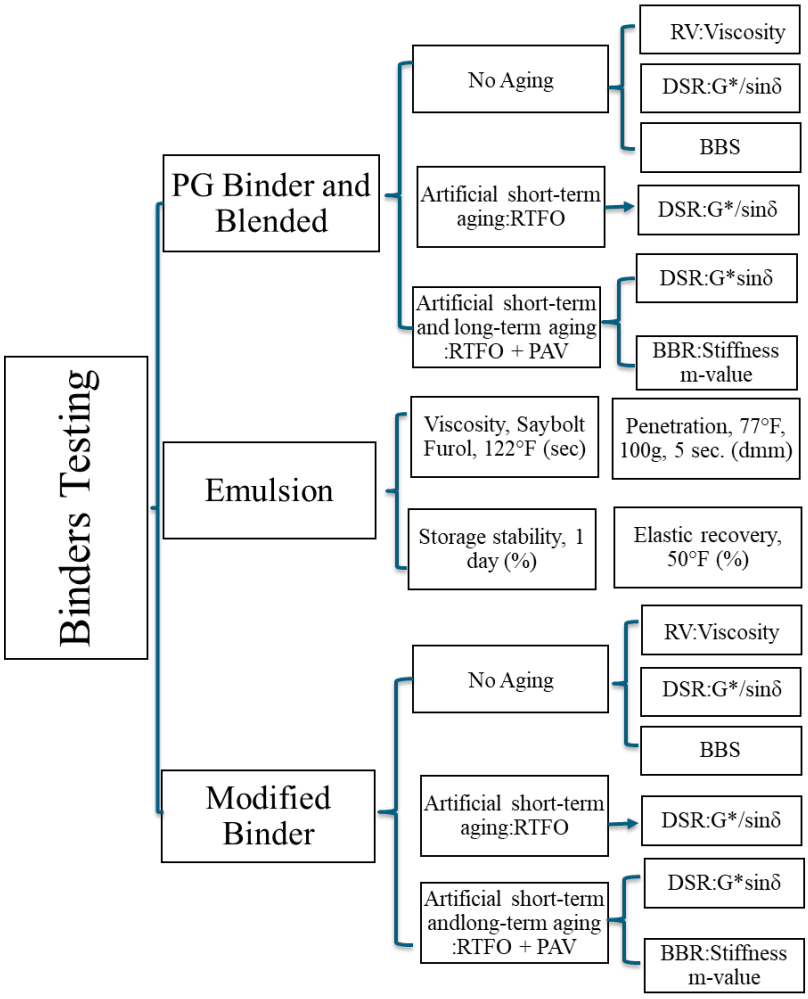

Figure 3.3 Experimental design of binders

3.3.2 Aggregate Physical Properties Testing

To categorize the aggregates, the research team examined the physical properties of each aggregate source. These tests, typically rapid and straightforward, are standard procedures routinely applied to aggregates used across diverse applications.

3.3.2.1 Aggregate Gradation

The assessment followed the guidelines of ASTM C136/C136M-and AASHTO T 27 (as-delivered gradation). Determining the as-delivered gradations of these aggregates was crucial to ascertain if they fell within the size range specified in the MoDOT requirements file (NJSP-15-13B) for High Friction Surface Treatment (HFST). Refer to Table 3-5 for details on the sieves utilized for aggregate gradation.

Table 3-5 Aggregate testing matrix

Aggregate Testing		Calcined Bauxite	CB	CB	Meramec	MR	MR	Flint Chat	FC	FC	Rhyolite	Rh	Rh	Rh
		#3/8*3	#3*8	#6*16	Torpedo	Coarse man sand	WB 5*16	BA	75	CME	#3/8*1/4	#3/4*3/8	#1/2*1/4	HFST
Physical Properties Tests	Aggregate Gradation	3/4"-#200	3/4"-#200	3/4"-#200	3/4"-#8	3/4"-#100	3/4"-#100	3/4"-#200	3/4"-#30	3/4"-#30	3/4"-#8	3/4"-#8	3/4"-#8	
	Specific Gravity & Absorption	1/4"-#4	1/4"-#4	#6-16	1/4"-#4	1/4"-#4	#6-16	#6-16	1/4"-#4	1/4"-#4	#6-16	1/4"-#4	1/4"-#4	#6-16
	Uncompacted Void Content	1/4"-#4	1/4"-#4	#6-16	1/4"-#4	1/4"-#4	#6-16	#6-16	1/4"-#4	1/4"-#4	#6-16	1/4"-#4	1/4"-#4	#6-16
Durability Testing	Los Angeles Abrasion	C	D	D	B	D	D	D	D	C	C	B	B	D
	Sodium sulfate soundness	#6-16	#4-6	#4-6	#4-6	#4-6	1/4"-#4	#4-6	#4-6	#4-6	#4-6	#4-6	1/4"-#4	
	Water Alcohol Freeze-Thaw	1/4"-#4	#6-8	#6-8	1/4"-#4	#6-8	#6-8	#6-8	#6-8	1/4"-#4	1/4"-#4	1/4"-#4	1/4"-#4	#6-8
	Acid Insoluble Residue			#6-8			#6-8	#6-8						#6-8
Performance Testing	Micro-Deval (MD)	105/120/180/240 min		15, 30 min	105/120/180/240 min	15,30 min			15, 30 min	105/120/180/240 min	105/120/180/240 min			15, 30 min
		3/8"-#4		#6-16	3/8"-#4	#6-16			#6-16	3/8"-#4	3/8"-#4			#6-16
	AIMS	(3/8-#4)			(3/8-#4)					(3/8-#4)	(3/8-#4)			
	CTM													
	DFT													
	BPT													

Table 3-6 British Pendulum test matrix

		Aggregate Type	Calcined Bauxite			Rhyolite				Meramec			Flint		
		Aggregate Size	HFST	M	C	HFST	M	C	EL	HFST	M	C	HFST	M	C
Binder Type	Epoxy Resin	Pre-polish													
		Post-polish													
	PG94-10	Pre-polish													
		Post-polish													
	PG88-16	Pre-polish													
		Post-polish													
	PG82-16	Pre-polish													
		Post-polish													
	Emulsion CRS-2P	Pre-polish													
		Post-polish													
	Emulsion CRS-2PSC	Pre-polish													
		Post-polish													
	PG82-22 (PM)	Pre-polish													
		Post-polish													
	PG88-16 (PM)	Pre-polish													
		Post-polish													

M= Medium, C=Coarse, EL= Extra-Large, Test Completed

Table 3-7 Dynamic Friction and CT meter tests matrix

			Binder Type							
Conditioning	Aggregate Type	Aggregate Size	Epoxy	PG88-16	CRS-2P	CRS-2P	CRS-2PSC	CRS-2PSC	PG82-22(PM)	PG88-16(PM)
30K	Calcined Bauxite	HFST								
	Calcined Bauxite	M				**(50%M +50%C)**		**(50%M +50%C)**		
	Calcined Bauxite	C								
	Rhyolite	HFST								
	Rhyolite	M				**(50%M +50%C)**		**(50%M +50%C)**		
	Rhyolite	C								
70K	Calcined Bauxite	HFST								
	Calcined Bauxite	M								
	Calcined Bauxite	C								
	Rhyolite	HFST								
	Rhyolite	M								
	Rhyolite	C								
140K	Calcined Bauxite	HFST								
	Calcined Bauxite	M								
	Calcined Bauxite	C								
	Rhyolite	HFST								
	Rhyolite	M								
	Rhyolite	C								

M= Medium, C=Coarse, EL= Extra-Large, Test Completed

Table 3-8 Specific aggregates' percentages/weights used in Micro-Deval and Uncompacted Void Content testing

Gradation Testing	Weight for UVC Test (g) Sample (8 - #100)	Weight for MD Test (g) Sample (3/8″ - #4)	Weight for MD and UVC Tests (g) Sample (#6-#16)
3/8″ - 1/4″	-	750	-
1/4″ - #4	-	750	-
#4 - #6	-	-	-
#6 - #8	-	-	53%
#8 - #10	44	-	21.1%
#10 - #12	-	-	13.7%
#12 - #16	-	-	11.19%
#16 - #30	57	-	-
#30 - #50	72	-	-
#50 - #100	17	-	-
#8 - #100	53	-	-

3.3.2.2 Specific Gravity and Absorption of Aggregates

This evaluation adhered to ASTM C128 for fine aggregates' gradations and AASHTO T 85 for coarse aggregates' gradations. The aggregate sizes employed in this assessment are listed in Table 3-5. Specific gravity was denoted as bulk specific gravity (G_{sb}), bulk specific gravity saturated surface dry ($G_{sb\text{-}SSD}$), or apparent specific gravity (G_{sa}). According to AASHTO T 85, aggregates smaller than #4 were excluded; however, if coarse aggregates contained a significant proportion of materials finer than #4, it was advised to include materials retained up to #8. For further specifics on the aggregate sizes used in this test, refer to Table 3-5. Table 3-9 outlines the minimum weights of aggregates used in the specific gravity and absorption tests according to the Nominal Maximum Aggregate Size (NMAS).

Table 3-9 Minimum weights of aggregates used in specific gravity and absorption tests

NMAS (inch)	Minimum Mass of Test Sample (g)
½	2000
¾	3000
1	4000
1 ½	5000
2	8000
2 ½	12000
3	18000

3.3.2.3 Uncompacted Void Content of Fine Aggregate

The Uncompacted Void Content (UVC) test was carried out according to ASTM C1252 − 17. This test serves as an indirect measure of fine aggregate angularity. For aggregate (#8 - #100) test method A from ASTM C1252 – 17 was utilized. Testing employed test methods B (#6 - #8) and C (#6 - #16) for the specified aggregate sizes. Refer to Table 3-5 for specific details.

3.3.3 Aggregate Durability Testing

Aggregates employed in High Friction Surface Treatment (HFST) applications endure exposure to external weather conditions, de-icing agents, and snowplowing, making the assessment of aggregate durability crucial.

3.3.3.1 Los Angeles Abrasion Test

This test, conducted according to ASTM C131/C131M − 20 and AASHTO T 96 standards, assesses the quality, hardness, and durability of aggregates by measuring their resistance to impact and abrasion. The results provide insights into aggregate toughness and degradation under heavyweights during compaction and traffic conditions. Gradings B, C, or D were used, as indicated in Table 3-5, with specific parameters determined by ASTM specifications.

3.3.3.2 Soundness of Aggregate Using Sodium Sulfate

The soundness of aggregates using sodium sulfate was assessed following AASHTO T 104-99 (2011) on aggregates sized (#4 - #6) (see Table 3-5). This test involved subjecting aggregate

samples to cycles of immersion, drying, washing, and sieving, followed by mass loss percentage calculations.

3.3.3.3 Water-Alcohol Freeze Thaw

The water-alcohol freeze-thaw resistance of aggregates was evaluated as per MoDOT standard 106.3.2.14 TM-14, aiming to assess aggregate soundness. Tested aggregates (#6 - #8) underwent cycles of freezing, thawing, drying, sieving, and mass loss percentage calculations to gauge their soundness.

3.3.2.4 Acid Insoluble Residue

Aggregates were tested for acid-insoluble residues following ASTM D3042 – 17 on (#6 - #8) sized aggregates (refer to Table 3-5). This test determined the percentage of insoluble residues in carbonate aggregates using hydrochloric acid, aiding in identifying excessively polishing carbonate aggregates.

3.3.4 Aggregate Performance Testing

3.3.4.1 Micro-Deval and Aggregate Image Measurement System

The aggregates underwent testing for their degradation and polish resistance using the Micro-Deval (MD) apparatus. This test aimed to assess aggregates' durability and resistance to polishing, abrasion, and grinding in the presence of water, as indicated in studies by Li et al. (2017) and Roshan et al. (2024). The MD test for coarse aggregates followed ASTM D6928 – 17 on aggregate sizes ranging from 3/8″ to #4, as outlined in Table 3-5. The test was conducted for durations of 105, 180, and 240 minutes with each aggregate undergoing testing at all time intervals. Samples of all aggregates were tested using the Aggregate Image Measurement System (AIMS) alongside pre-MD abrasion samples. AIMS analyzed two sizes (3/8″ – 1/4″ and 1/4″ - #4) for each aggregate to observe changes in Texture (TX) indices and Gradient Angularity (GA) indices post-MD polishing. GA indices were determined based on surface irregularities using black and white images, while TX indices were derived from grayscale images using the wavelet analysis method (Kassem et al., 2013). The fine aggregate MD test followed ASTM D7428 − 15 on Calcined Bauxite (CB) gradation (#6 - #16) for all three aggregates, conducted for 15 and 30 minutes each with two samples per run time and mass loss percentage calculations. All weights in this test were based on oven-dried aggregates.

3.3.4.2 Accelerated Friction Testing

1- Preparing High Friction Surface Treatment Applications on Slabs

Loose asphalt mixtures, which were obtained from MoDOT, and plywood slab sheets were utilized to prepare the slabs for performance tests. The loose mixtures were dense-graded asphalt mixtures with a 12.5-mm Nominal Maximum Aggregate Size (NMAS). These plant mixtures were reheated, and Hot Mix Asphalt (HMA) slabs, measuring 20 inches by 20 inches by 2 inches, were prepared and compacted in the laboratory using a small plate compactor. The preparation of both the HMA and plywood slabs was conducted as outlined in Appendix B.

2- Circular Track meter test (CT meter)

The Circular Texture Meter (CTM) measures the Mean Profile Depth (MPD) at a fixed location according to the standard test procedure ASTM E2157 (2015). The MPD indicates the average depth of the pavement surface texture. It profiles a circle with a circumference of 89.2 cm, dividing it into eight segments. The MPD is calculated for each segment, and the average of these eight values is reported as the MPD for that specific location. Additionally, the speed constant (Sp), as defined in the ASTM E1960 (2015) specification, is calculated using the formula $Sp = 14.2 + 89.7 \times MPD$ for each MPD reading.

3- Dynamic Friction Test

A Three-Wheel Polishing Device (TWPD) was employed to polish the test slabs, as depicted in Figure B-5 and Figure B-6. The TWPD featured three pneumatic rubber wheels mounted on a turntable, equipped with a water spray system designed to simulate wet conditions. This system not only helped reduce wear on the rubber wheels but also washed away surface fines, facilitating further polishing. The researchers measured the Coefficient of Friction (COF) at various stages of the polishing process, including at 0 cycles (initial), 30,000 cycles, 70,000 cycles, and 140,000 cycles (terminal). The COF was assessed using a Dynamic Friction Tester (DFT), as shown in Figure B-5. This measurement was performed at different speeds—20, 40, and 50 km/hr, adhering to the ASTM E1911 - 19 standard. The DFT comprised a circular disk outfitted with three rubber pads, which could rotate up to 100 km/hr. Upon reaching the desired speed, the disk was lowered onto the pavement surface, and the COF was recorded as the speed of the rotating disk gradually decreased. Friction measurements were conducted under wet conditions, and the results presented were based on the average of two replicates.

3.3.5 Measuring Aggregate Coupons' Surface Friction Using the British Pendulum Tester

1- Preparing Aggregate Coupons

The aggregate coupons were prepared according to the procedures outlined in Appendix B. The prepared aggregate coupons can be viewed in Figure B-1. The aggregates used in the preparation of these coupons encompassed all four sizes introduced in this research, as detailed in Section 3-2. The coupons were initially tested for their British Pendulum Number (BPN), then subjected to a polishing process using the British wheel for 10 hours. Following the polishing, the coupons were once again tested to assess their BPN after the 10-hour polishing period.

2- British Pendulum Test

The BPT (British Pendulum Tester) is a highly regarded device utilized in various research fields. Its utilization is governed by established standards set forth by ASTM E303 and AASHTO T 278. The primary function of the BPT is to quantify frictional forces generated when a rubber pad slides across a sample surface. By simulating a velocity equivalent to 10 km/h or 6 mph (Henry, 2000), the BPT enables the measurement of microtexture characteristics (AASHTO T 278). Each coupon underwent a minimum of five initial tests to establish baseline British Pendulum Number (BPN) values. Following these initial assessments, the aggregates on the coupons were subjected to the polishing process using the British wheel. After polishing, the

BPN values were again recorded using the British Pendulum (BP) device to obtain the post-polish BPN values.

3- Accelerated Polishing of Aggregates Using the British Wheel

The aggregates on the coupons were polished using the British wheel, as specified in AASHTO T 279-18, following their initial tests with the British Pendulum (BP) device. For each test run, 14 aggregate coupons were securely clamped around the periphery of the wheel, as shown in Figure B-2. The wheel's speed was maintained at 320 ± 5 rpm. Simultaneously, a pneumatic-tired wheel was lowered to press against the surface of the aggregate coupons. This was done with a total load of 391.44 ± 4.45 N. Through this setup, the aggregates underwent a controlled polishing process, replicating wear patterns similar to those they would encounter under actual road conditions.

3.3.5 Binder Testing

3.3.5.1 PG and Modified Binders

PG binders, including PG64-22 sourced from APAC Southern Missouri, and PG76-22 and PG 94-10 obtained from Pure Asphalt in Chicago, Illinois. Additionally, D0243KT polymer modifier used for developing two modified binders were sourced from Kraton Inc. The method for developing these modified binders is detailed in Appendix B.

A Brookfield rotational viscometer was employed to measure the viscosity of each asphalt binder at 135°C according to AASHTO T 316. This method involves gauging the torque necessary to maintain a cylindrical spindle at a constant rotational speed while it is submerged in the asphalt binder sample, which is kept at a consistent temperature. Additionally, Superpave tests were conducted on the samples to verify their specified grades. To assess the high temperature rheological properties of each binder, a Dynamic Shear Rheometer (DSR) was used as specified in AASHTO T 315. In the DSR tests, the original binders and their corresponding Rolling Thin Film Oven (RTFO) residual binders were tested using a 25 mm spindle at temperatures of 64°C and 76°C with a parallel plate setup. Furthermore, binders that had undergone both RTFO and Pressure Aging Vessel (PAV) treatments (RTFO+PAV residual) were tested using an 8 mm parallel plate at 25°C. All binders (original, RTFO residual, and RTFO+PAV residual) were tested at a frequency of 10 radians per second, equivalent to approximately 1.59 Hz. For the original and short-time aged binders, the DSR was used to determine $G^*/\sin\delta$ to assess the binders' susceptibility to permanent deformation. At intermediate temperatures, the $G^*\sin\delta$ values for RTFO+PAV residual binders were measured to evaluate their fatigue cracking properties. Additionally, a Bending Beam Rheometer (BBR) test, as outlined in AASHTO T 313, was utilized to evaluate the crack properties of the binders at low temperatures.

This test measures the stiffness of the binder samples at temperatures down to -12°C, providing critical data on binder performance in cold environments.

The Binder Bond Strength (BBS) test was conducted using the Positest AT-A apparatus to examine the adhesion strength of the binders. In this test, the loading rate was controlled at 0.7 MPa/s, ensuring a consistent and controlled application of force. Additionally, the thickness of

the asphalt was maintained at 0.2 mm, as recommended by AASHTO TP-91 guidelines. For the BBS test, all specimens were initially cooled to room temperature for 1 hour. Subsequently, some specimens were subjected to ambient conditions (25°C, 30% humidity) for 24 hours to allow for curing. After the curing period, these specimens were tested to determine the pull-off tensile strength under dry conditions. Additionally, other specimens were submerged in a 40°C water bath for durations of 24 hours and 48 hours. Following immersion, these specimens were allowed 1 hour of curing time before testing. The BBS test was then conducted on these immersion specimens to obtain the pull-off tensile strength under wet conditions.

3.3.5.2 Emulsions

CRS-2P and CRS-2PSC asphalt emulsions were utilized in this study. They are used for general asphalt applications and are widely accepted for use by state departments of transportation (DOTs) in this region of the country. CRS-2P is a cationic rapid-setting emulsion with 30% water content. CRS-2PSC is a high-viscosity type emulsion with a 33% water content by weight of the total emulsion. It is noted that 82% of the water breakout for CRS-2P and 80% for CRS-2PSC occurred within the first 6 hours at 95°F, with minimal evaporation observed beyond 24 hours of exposure.

The properties of CRS-2P and CRS-2PSC asphalt emulsions were tested to meet the specific requirements outlined in Missouri's standard specifications for highway construction. These tests included measuring viscosity at 122°F using the Saybolt Furol method (ASTM D-7496), evaluating storage stability after one day (ASTM D-6930), determining penetration at 77°F with a 100g load for 5 seconds (ASTM D-5), and assessing elastic recovery at 50°F (ASTM D-6084).

CHAPTER 4: AGGREGATE PHYSICAL PROPERTIES AND DURABILITY TESTING

4.1 Introduction

This chapter focuses on examining the physical characteristics and durability of aggregates through various tests. These tests aimed to categorize the aggregates and evaluate their suitability as High Friction Surface Treatment (HFST) materials by assessing their performance. Consequently, the physical properties, such as aggregate gradation, specific gravity, absorption, and Uncompacted Void Content (UVC), were analyzed. Additionally, durability tests like the Los Angeles Abrasion (LAA), sodium sulfate soundness, water-alcohol freeze-thaw, and acid-insoluble residue were conducted. By analyzing the results of these physical property and durability tests, comparisons between different aggregates were made to determine their relative merits.

4.2 Physical Properties Testing Results

The aggregates investigated in this study were comprehensively defined, consisting of Calcined Bauxite (CB), Rhyolite (Rhy), Meramec, and Flint chat as a high-friction aggregate material. A series of tests were performed to evaluate and differentiate the performance characteristics among the proposed aggregate types.

4.2.1 Aggregate Gradation

The aggregates proposed for use were initially sieved to various sizes according to Section 3.2. Alongside the standard HFST gradation specified by MoDOT, medium and coarse sizes were also considered. These sizes were then meticulously sorted and remixed in controlled conditions to prepare specimens for subsequent physical, durability, and performance tests, as depicted in Figure 4.1, which shows the different aggregate size gradations. The selection of aggregate sizes was based on available gradations from the manufacturer. The primary objective of the gradation test was to assess whether the aggregates met the current MoDOT requirements for HFST (NJSP-15-13B).

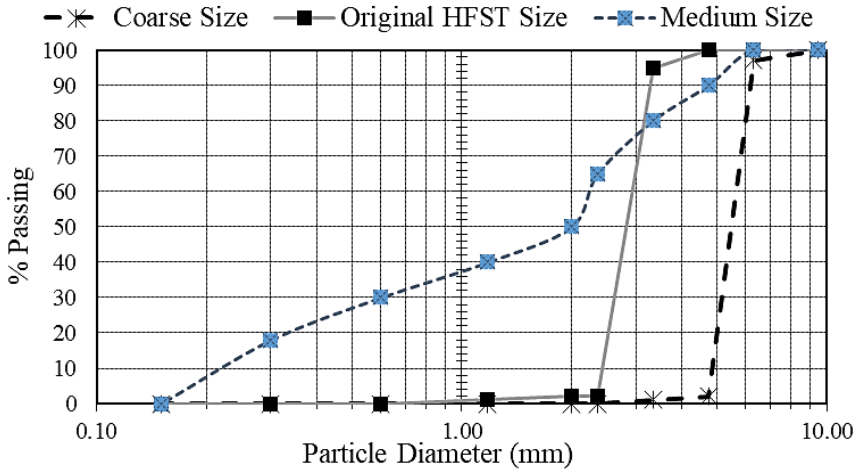

Figure 4.1 Particles size distribution of different sizes

4.2.2 Specific Gravity and Absorption

The specific gravity of the aggregates under investigation was determined for both HFST and coarse sizes, as outlined in Table 3-5 and Section 3.3.2. Among these, Calcined Bauxite (CB) exhibited the highest specific gravity values. This led the researchers to consider specific gravity as a reliable parameter for filtering the investigated aggregates. Additionally, Table 4-1 presents the specific gravity values and water absorption percentages of the materials under study.

Table 4-1 The absorption and specific gravity results

Type	Size	G_{Sb}[a]	$G_{Sb\text{-}SSD}$[b]	G_{sa}[c]	Absorption (%)
Calcined Bauxite	HFST	3.26	3.31	3.42	1.36
	Coarse	3.24	3.32	3.54	2.6
Rhyolite	HFST	2.47	2.53	2.64	2.7
	Coarse	2.56	2.59	2.65	0.86
Meramec	HFST	2.44	2.51	2.62	2.66
	Coarse	2.45	2.52	2.64	2.64
Flint Chat	HFST	2.52	2.56	2.64	1.96
	Coarse	2.51	2.56	2.65	2.18

a: G_{sb}: Bulk specific gravity
b: $G_{sb\ SSD}$: Bulk specific gravity saturated surface dry
c: Gsa: Bulk specific gravity apparent

4.2.3 Uncompacted Void Content

The Uncompacted Void Content (UVC) of fine aggregates was utilized as an indirect measure of their angularity. The UVC percentages for the aggregates listed in Table 3-1 were calculated across two different gradations: (#6 - #16) and the individual fraction size (#6 - #8), to evaluate the impact of aggregate gradation on uncompacted void percentages. These results are displayed in Figure 4.2. No significant difference was noted between the UVC percentages for the #6 - #8 size and the #6 - #16 size. Among these sizes, Calcined Bauxite (CB) exhibited the smallest difference in UVC percentage, while Meramec had the highest UVC difference percentage. Flint Chat recorded the highest uncompacted void percentages (approximately 49%), whereas Meramec had the lowest (approximately 41%).

4.3 Durability Testing Results

The High Friction Surface Treatment (HFST) aggregates are directly exposed to external weather conditions, such as repetitive wetting and drying cycles, de-icing, and snowplowing.

Consequently, it is crucial to investigate the durability of these aggregates. Test specimens were prepared and mixed with different gradations according to the specifications of the tests.

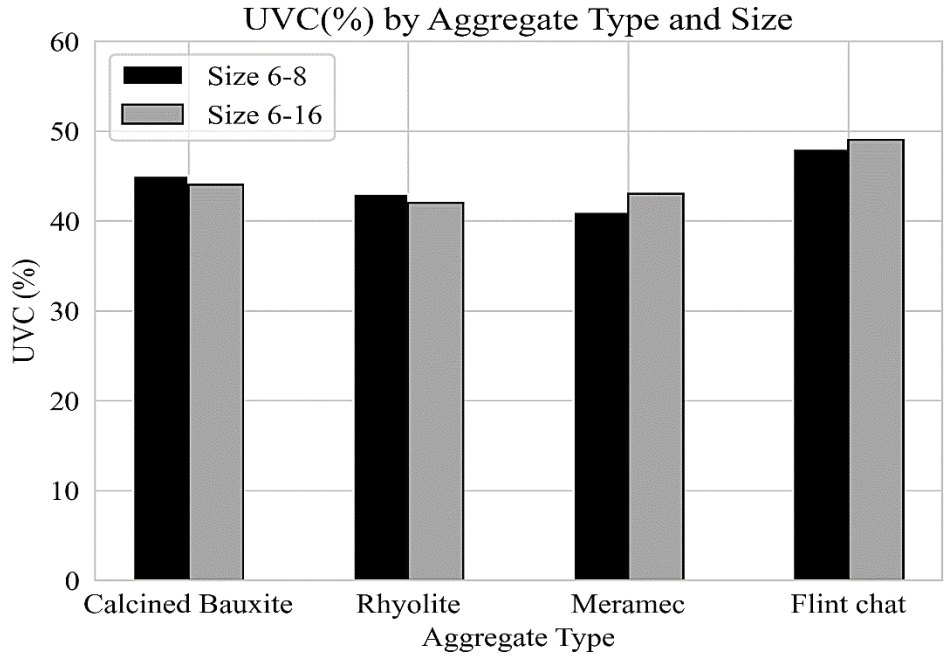

Figure 4.2 Percentages of UVC using two aggregates' sizes

4.3.1 Los Angeles Abrasion

The aggregate samples underwent testing for their resistance to degradation using the Los Angeles Abrasion (LAA) machine. Four aggregates were tested following grading D and C as outlined in Table 3-5. Additionally, based on the aggregate gradations, two aggregates followed grading B (also in Table 3-5). The LAA percentages served as indicators of the quality of the different aggregates. The results of abrasion resistance testing revealed distinct patterns across different grades of aggregates, with percentages indicating the degree of resistance to abrasion. In Grade D, the Meramec aggregate exhibited the highest resistance to abrasion at approximately 15%, followed by Calcined Bauxite, Rhyolite, and Flint. For Grade C aggregates, Calcined Bauxite showed the highest resistance at approximately 17%, followed by Meramec, Flint, and Rhyolite. Moving to Grade B, Rhyolite demonstrated superior abrasion resistance at approximately 17.6%, compared to Meramec at approximately 18%.

As indicated in Section 2.7, the new AASHTO MP 41-22 specification for HFST has transitioned from the traditional Los Angeles Abrasion (LAA) test to the Micro-Deval (MD) test for evaluating fine aggregate abrasion. Moreover, adherence to MoDOT's NJSP-15-13B standard for HFST is crucial, which specifies a maximum allowable LAA percentage of 20%. Notably, all Grade D aggregates in this study met the stringent MoDOT specification. Figure 4.3 presents the results of the Los Angeles test.

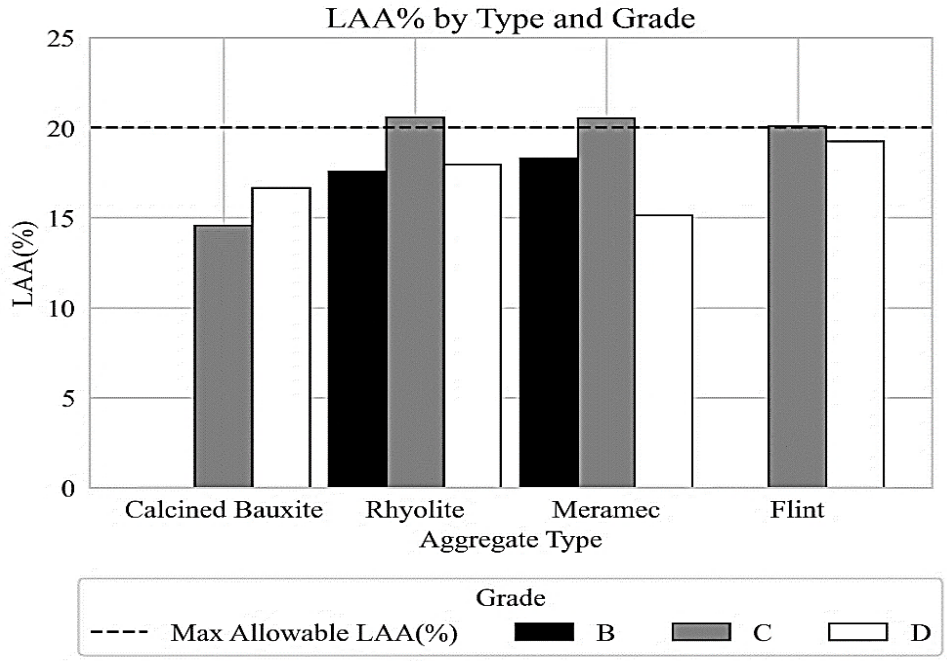

Figure 4.3 Percentages of LAA

4.3.2 Sodium Sulfate Soundness

The sodium sulfate soundness test was carried out to assess the resistance of aggregates to disintegration under repeated immersion in sodium sulfate solutions, followed by oven drying. These tests were specifically conducted on #4 - #6 sized aggregates, as specified in Table 3-5. The results of two replicates are presented in Table 4-2. According to the test results, Calcined Bauxite exhibited the lowest percentage of loss, followed by Meramec, Flint, and Rhyolite. Notably, Rhyolite showed the highest percentage of loss among the tested aggregates, indicating its lower resistance to disintegration under the sodium sulfate soundness test conditions.

4.3.3 Water-Alcohol Freeze Thaw

The water-alcohol freeze-thaw resistances of the aggregates were evaluated specifically on #6 - #8 size, as detailed in Table 3-5. These tests aimed to assess the soundness of coarse aggregates under freeze-thaw conditions. The results depicted in Figure 4.4 revealed that Flint experienced the highest percentage of loss at 19.46%, followed by Calcined Bauxite with 14.74%. In contrast, Rhyolite exhibited the lowest percentage of loss at 10%, indicating its greater resistance to freeze-thaw cycles compared to the other tested aggregates.

Table 4-2 Sodium sulfate soundness test results

Type	Initial Weight (g)	Final Weight (g)	(%) Loss
	200	199.8	0.1

Calcined Bauxite	200	199.74	0.13
Rhyolite	200	192.8	3.6
	200	195.3	2.35
Meramec	200	199.4	0.3
	200	199.55	0.23
Flint Chat	200	198.9	0.55
	200	199	0.5

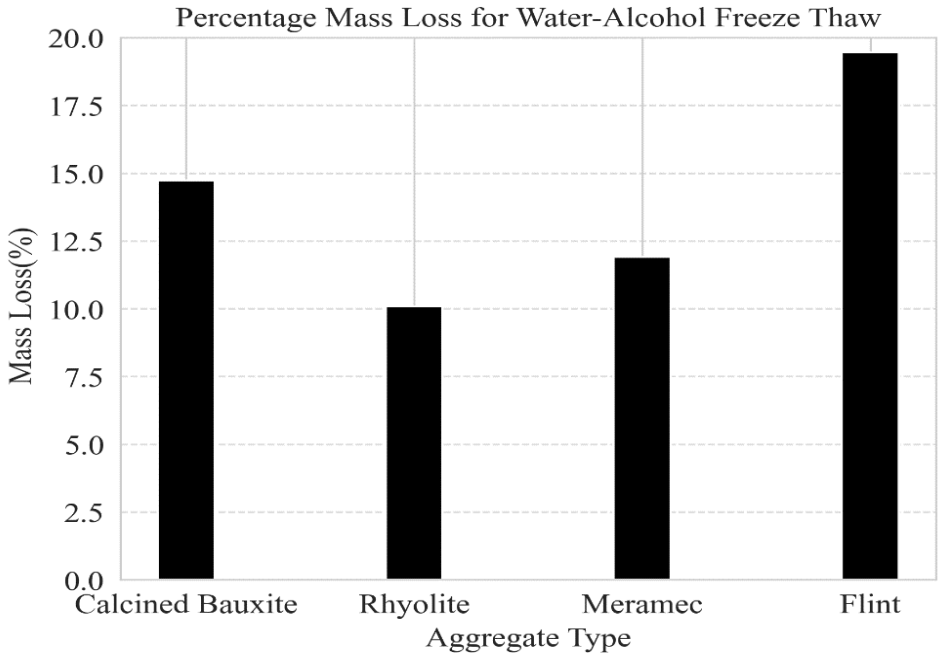

Figure 4.4 Water-alcohol freeze thaw test results

4.3.4 Acid Insoluble Residue

The acid-insoluble residues of Calcined Bauxite and three other aggregates were tested using #6 - #8 size samples. This test involved determining the percentages of noncarbonate (insoluble) residue in carbonate aggregates, which helps assess their susceptibility to polishing. A hydrochloric acid solution was used to trigger reactions with carbonates in the aggregates. The results, shown in Figure 4.5, revealed that Flint had the lowest residue percentage, followed by Rhyolite. Conversely, Calcined Bauxite exhibited the highest residue percentage, followed by Meramec. Notably, all the aggregates tested exceeded the acceptable level of residue.

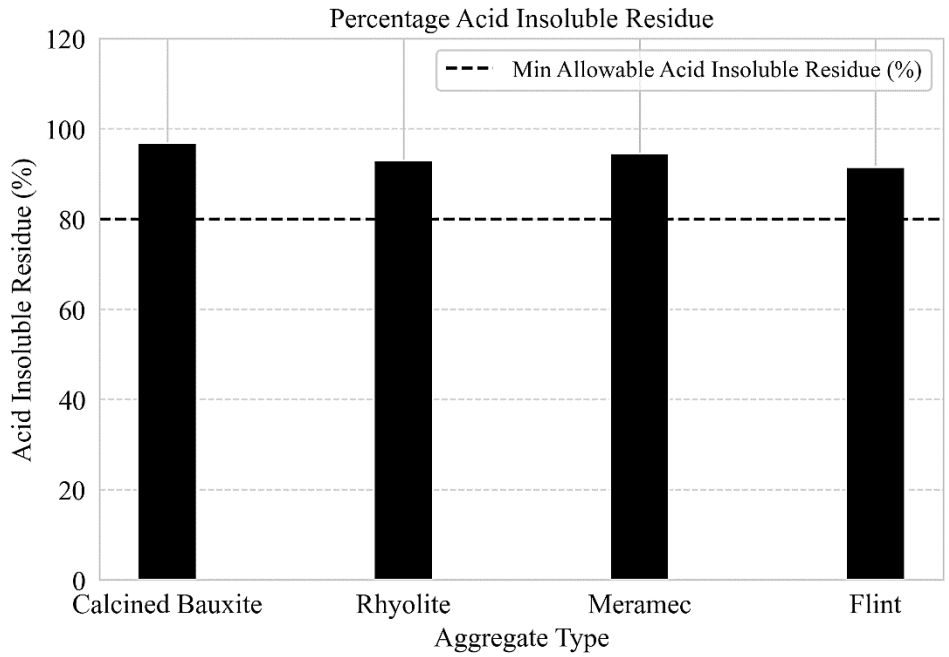

Figure 4.5 Acid insoluble residue percentages

4.4 Summary

This chapter presented the physical properties and durability testing results for the aggregates. The Uncompacted Void Content (UVC) of fine aggregates was measured across two different gradations: #6 - #16 and the individual fraction size #6 - #8. No significant difference was noted between the UVC percentages for the #6 - #8 size and the #6 - #16 size. Among these sizes, Calcined Bauxite (CB) exhibited the smallest difference in UVC percentage, while Meramec had the highest. Flint Chat recorded the highest uncompacted void percentages (approximately 49%), whereas Meramec River Aggregate had the lowest (approximately 41%).

The results of LAA testing revealed that in Grade D, the Meramec exhibited the highest resistance to abrasion at approximately 15%, followed by Calcined Bauxite, Rhyolite, and Flint. For Grade C aggregates, Calcined Bauxite showed the highest resistance at approximately 17%, followed by Meramec, Flint, and Rhyolite. For Grade B, Rhyolite demonstrated superior abrasion resistance at approximately 17.6%, compared to Meramec at approximately 18%. Adherence to MoDOT's NJSP-15-13B standard for HFST, which specifies a maximum allowable LAA percentage of 20%, is crucial. Notably, all Grade D aggregates in this study met the stringent MoDOT specification.

In the soundness tests, Calcined Bauxite exhibited the lowest sodium sulfate soundness test loss at 0.1%, followed by Meramec River Aggregate, Flint, and Rhyolite, with Rhyolite showing the highest loss, indicating lower resistance. For water-alcohol freeze-thaw resistance, Flint had the highest loss (19.46%), followed by Calcined Bauxite (14.74%), and Rhyolite had the lowest (10%). Additionally, the acid-insoluble residues revealed that Flint had the lowest residue percentage, followed by Rhyolite, while Calcined Bauxite exhibited the highest residue percentage, followed by Meramec.

CHAPTER 5: AGGREGATE PERFORMANCE TESTING

5.1 Introduction

This chapter discusses aggregate performance testing results, focusing on comparing different aggregates with various sizes. The performance testing encompassed several tests, such as Micro-Deval (MD) and Aggregate Image Measurement System (AIMS) analysis. Different aggregate sizes were employed for each aggregate type in the MD and AIMS tests to investigate the influence of aggregate size on overall performance.

5.2 Micro-Deval Results

In this section, the Micro-Deval (MD) results are thoroughly discussed for both coarse and fine aggregates. These results act as indicators of the mass losses experienced by different aggregates with varying sizes after undergoing polishing for different durations. Specifically, the coarse aggregates were subjected to polishing times of 105, 180, and 240 minutes, while the fine aggregates were polished for 15 and 30 minutes. Subsections are dedicated to explaining and analyzing the MD results in detail, highlighting the effects of polishing duration on aggregate performance.

5.2.1 Coarse Aggregate

The MD test was conducted on coarse aggregate with 3/8″ - #4 gradation, as specified in Table 3-5. Samples were prepared following ASTM D6928 – 17 (Section 8.4), with a total sample weight of 1500g achieved by combining two portions. The first portion, weighing 750g, had 3/8″ - 1/4″ gradation, while the second portion, also 750g, had 1/4″ - #4 gradation. The percentages of mass loss after 105, 120, 180, and 240 minutes of Micro-Deval polishing (AMD 105, AMD 120, AMD 180, and AMD 240) are depicted in Figure 5.1.

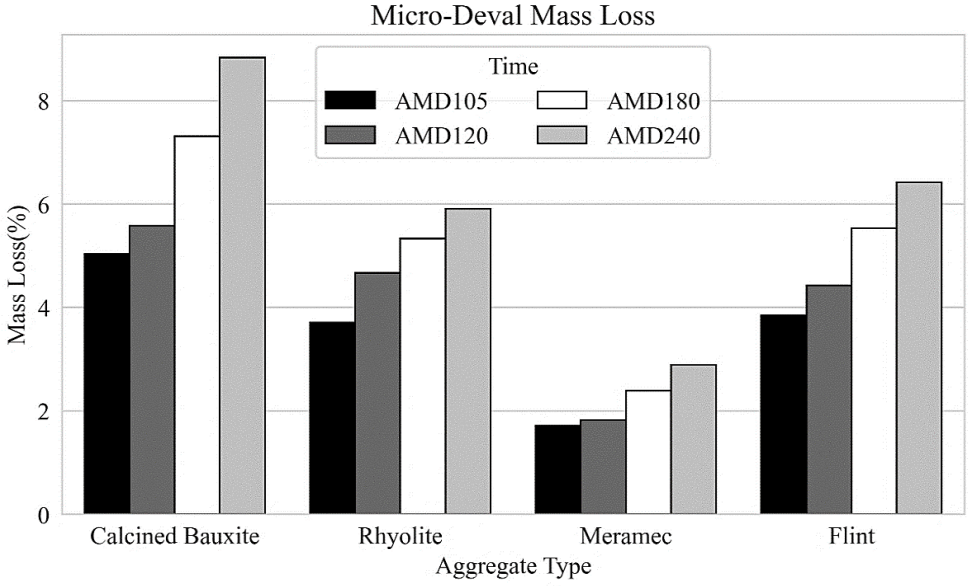

Figure 5.1 Micro-Deval mass losses' percentages with 3/8″ - #4 gradation

Regarding the coarse gradation (3/8″ - #4), Calcined Bauxite exhibited the greatest mass loss percentages, while Meramec River Aggregate, on the contrary, displayed the least mass loss percentages. Rhyolite and Flint demonstrated comparable mass loss percentages for AMD 105, 120, and 180. However, for AMD 240, Rhyolite showcased lower mass loss compared to Flint.

5.2.2 Fine Aggregate

The Micro-Deval (MD) test was conducted for fine aggregates following ASTM D7428 – 15, using a sample weight of 500g. The test was carried out on aggregates with #6 - #16 gradation as outlined in Table 3-5. Figure 5.2 illustrates the percentages of mass losses for aggregates within the #6 - #16 gradation. The MD polishing times included durations of 15 and 30 minutes. Notably, increasing the MD polishing time from 15 to 30 minutes resulted in higher mass loss percentages. Among the aggregates, Meramec exhibited the lowest mass loss percentage after 30 minutes of Micro-Deval polishing time (AMD 30), followed by Calcined Bauxite, Flint, and Rhyolite.

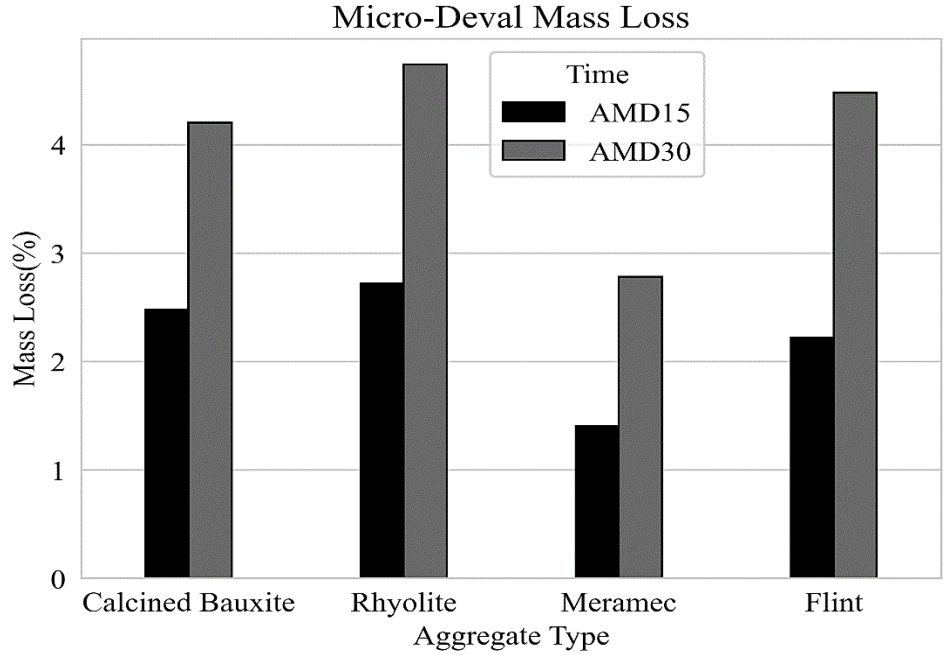

Figure 5.2 Micro-Deval mass losses' percentages with (#6 - #16) gradation

In terms of the fine gradation (#6 - #16), the aggregate with the lowest mass loss percentages was the Meramec. For AMD 15, Calcined Bauxite, Rhyolite, and Flint exhibited comparable mass loss percentages. Nonetheless, Calcined Bauxite displayed lower mass loss compared to Flint and Rhyolite. Overall Rhyolite showed the highest percentage of mass loss for AMD 15 and AMD 30.

5.3 Aggregate Image Measurement System

In this section, the Texture (TX) and Gradient Angularity (GA) indices of aggregates were compared using the Aggregate Image Measurement System (AIMS). The comparisons were

made for different stages: before Micro-Deval polishing (BMD), after 105 minutes of Micro-Deval polishing time (AMD 105), after 180 minutes of Micro-Deval polishing time (AMD 180), and after 240 minutes of Micro-Deval polishing time (AMD 240). These comparisons were conducted for two aggregate sizes: 3/8″ - 1/4″ and 1/4″ - #4 as detailed in Table 3-5.

5.3.1 Effect of Aggregate Size on Texture and Angularity Indices

Figures 5.3 and 5.4 depict the AIMS TX and GA indices concerning aggregates of two different sizes, namely 3/8″ - 1/4″ and 1/4″ - #4, during the polishing stages of BMD, AMD 105, AMD 180, and AMD 240. The reduction in aggregate sizes from 3/8″ - 1/4″ to 1/4″ - #4 led to a decline in TX indices across BMD, AMD 105, AMD 180, and AMD 240 phases. However, Calcined Bauxite exhibited elevated texture for AMD 240 in the 1/4″ - #4 size range compared to 3/8″ - 1/4″.

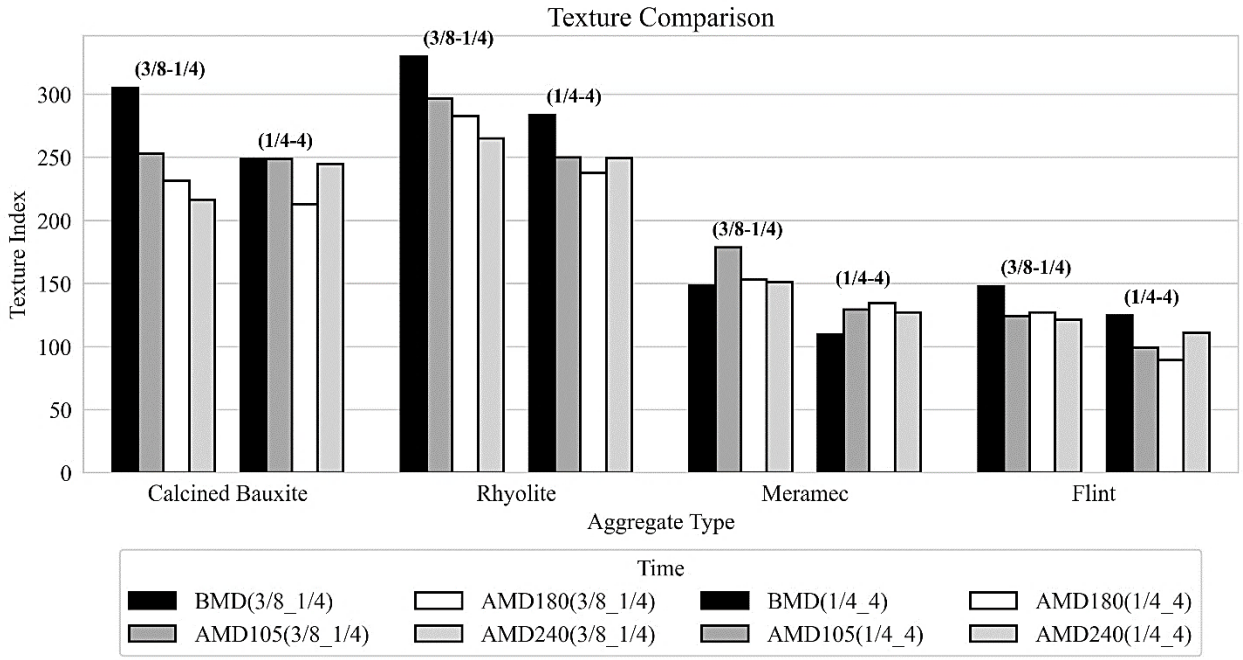

Figure 5.3 Aggregate texture indices

Additionally, Calcined Bauxite, Rhyolite, and Flint displayed diminishing texture trends as the polishing time increased for aggregates of size 3/8″ - 1/4″. Conversely, for size 1/4″ - #4, their texture initially decreased and then experienced an upturn in AMD 240. On the other hand, Meramec demonstrated an increase in texture for both sizes following polishing to AMD 105, followed by a subsequent decrease in texture. Among all the aggregates, Rhyolite displayed the highest TX and GA indices for both sizes. Calcined Bauxite exhibited comparable TX indices, for size 1/4″ - #4. The GA indices for Calcined Bauxite increased over 105, 180, and 240-minute Micro-Deval polishing times as the size of the aggregate was reduced. Figures 5.5 and 5.6 illustrate the percentage changes in the AIMS TX and GA indices for aggregates concerning AMD 105, AMD 180, and AMD 240. The TX indices exhibited a decrease for Calcined Bauxite, Rhyolite, and Flint, while they exhibited an increase for Meramec, in the context of the 3/8″ - 1/4″ size range. Specifically, Calcined Bauxite experienced a texture loss of 29% after 240

minutes of polishing in Micro Deval, Rhyolite lost 20% of its texture, and Flint lost 18% of its texture.

In the context of the 1/4″ - #4 size range, Calcined Bauxite, Rhyolite, and Flint exhibited a lower percentage of texture loss compared to the 3/8″ - 1/4″ size range. Conversely, Meramec demonstrated an increase in texture for this size range. Calcined Bauxite demonstrated that by decreasing the size from 3/8" - 1/4" to 1/4" - #4, the percentage decrease in texture after polishing time was reduced. As depicted in Figure 5.6 the GA indices for the 3/8″ - 1/4″ size range exhibited varying trends with increasing polishing time. Specifically, in the case of Calcined Bauxite and Rhyolite, there was a consistent decrease in angularity as the polishing time increased. In contrast, for Flint, the angularity decreased after 105 minutes, increased after 180 minutes, and then decreased again after 240 minutes of polishing. As for Meramec, its angularity initially decreased after 105 minutes, increased slightly after 180 minutes, and then increased further after 240 minutes of polishing.

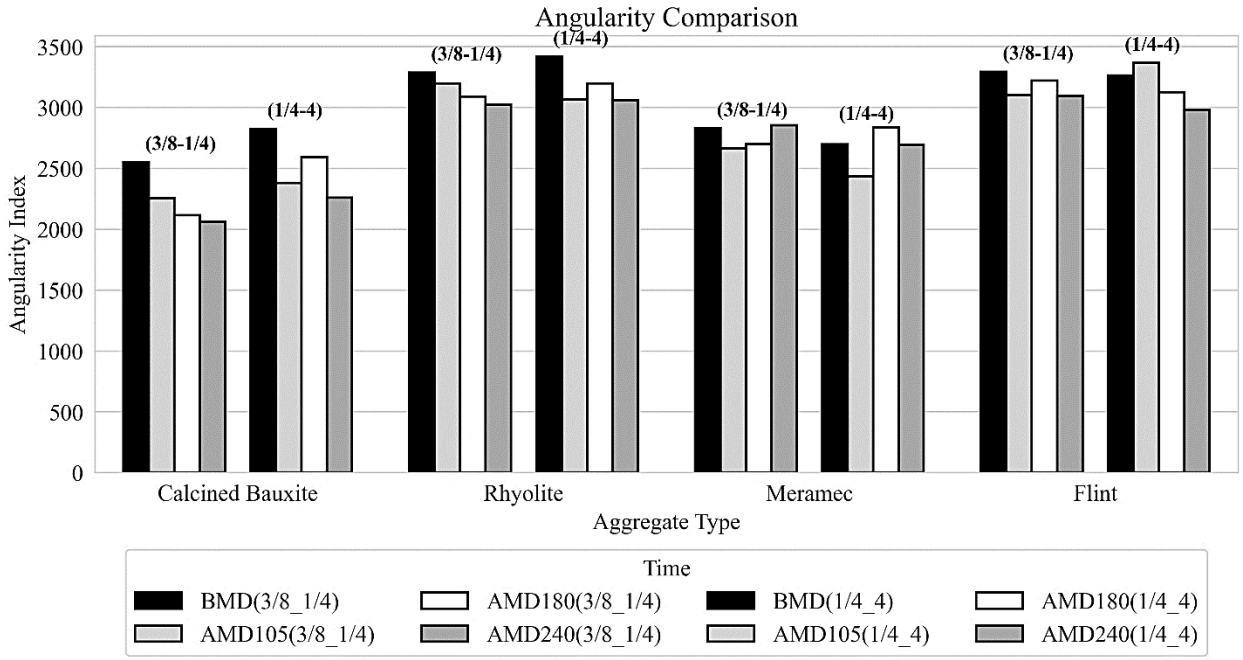

Figure 5.4 Aggregate angularity indices

For the 1/4″ - #4 size range, a similar pattern was observed for Calcined Bauxite and Rhyolite, with the angularity decreasing initially and then increasing after 180 minutes of polishing. However, in the case of Flint, there was an initial increase in angularity after 105 minutes, followed by a decrease. As for Meramec, its GA showed a decrease after 105 minutes of polishing, followed by an increase after 180 minutes, and then a slight decrease.

The increase in the aggregates' TX and GA indices after Micro-Deval (MD) polishing time may be attributed to several factors:

-Breaking of Particles: It is likely that during the MD polishing process, some particles within the aggregates broke, exposing their internal surfaces. This increased surface roughness can contribute to higher TX and GA indices.

-Exposure of Textured Surfaces: MD polishing might have uncovered textured surfaces that were previously covered by smoother surfaces. This exposure of previously hidden textures can lead to an increase in both TX and GA indices as the rougher surfaces become more prominent.

-Effect on Aggregates with Low TXs: Interestingly, Micro-Deval polishing did not have the anticipated effect on aggregates with low TX values. This suggests that the polishing process may not be as effective in altering the texture and angularity of aggregates that already have low initial TX values.

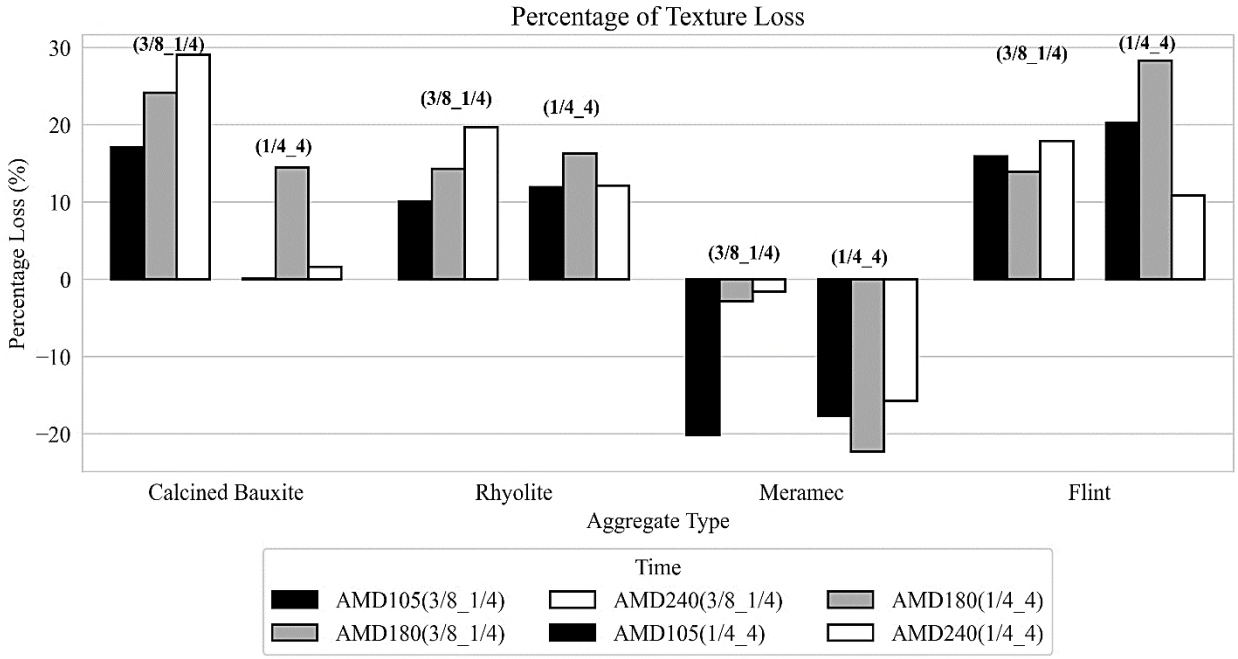

Figure 5.5 Percentages change in the texture indices

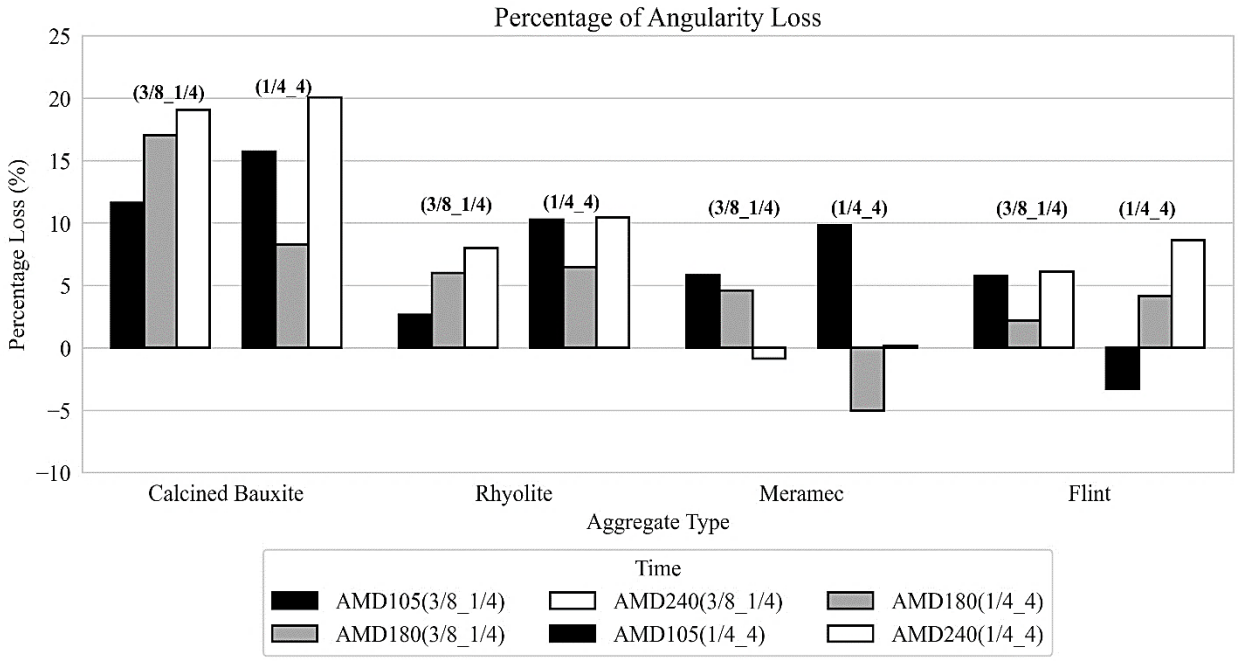

Figure 5.6 Percentages change in the angularity indices

Figures 5.7 and 5.8 depict the relationships between Texture (TX) and Gradient Angularity (GA) indices at different stages of Micro-Deval polishing for two aggregate sizes, namely 3/8″ - 1/4″ and 1/4″ - #4. Here are some key observations:

Rhyolite Performance: Rhyolite consistently exhibited the highest TX and GA values both before Micro-Deval polishing (BMD) and after 105 and 180 minutes of polishing (AMD 105 and AMD 180). This indicates that Rhyolite maintained its texture and angularity even after extended polishing.

Calcined Bauxite and Flint: For the 3/8″ - 1/4″ size range, Calcined Bauxite showed the lowest angularity after 240 minutes of polishing (AMD 240). Similarly, Flint had the lowest texture values after 240 minutes of polishing indicating that prolonged polishing had a more significant impact on Calcined Bauxite's angularity and Flint's texture. For the 1/4" - #4 size range, after 240 minutes of polishing (AMD 240), Calcined Bauxite exhibited the least angularity, and the lowest texture related to Flint after 180 minutes of polishing (AMD 180).

Lowest Angularity and Texture: For the 3/8″ - 1/4″ size range, Rhyolite exhibited the highest Texture (TX) and Gradient Angularity (GA) indices during BMD, while Flint had the lowest TX and highest GA indices for AMD 180 and AMD 240. In the 1/4" - #4 size range, Rhyolite showed the highest TX and GA indices during BMD and AMD 240, while Meramec had the lowest TX and GA indices during BMD.

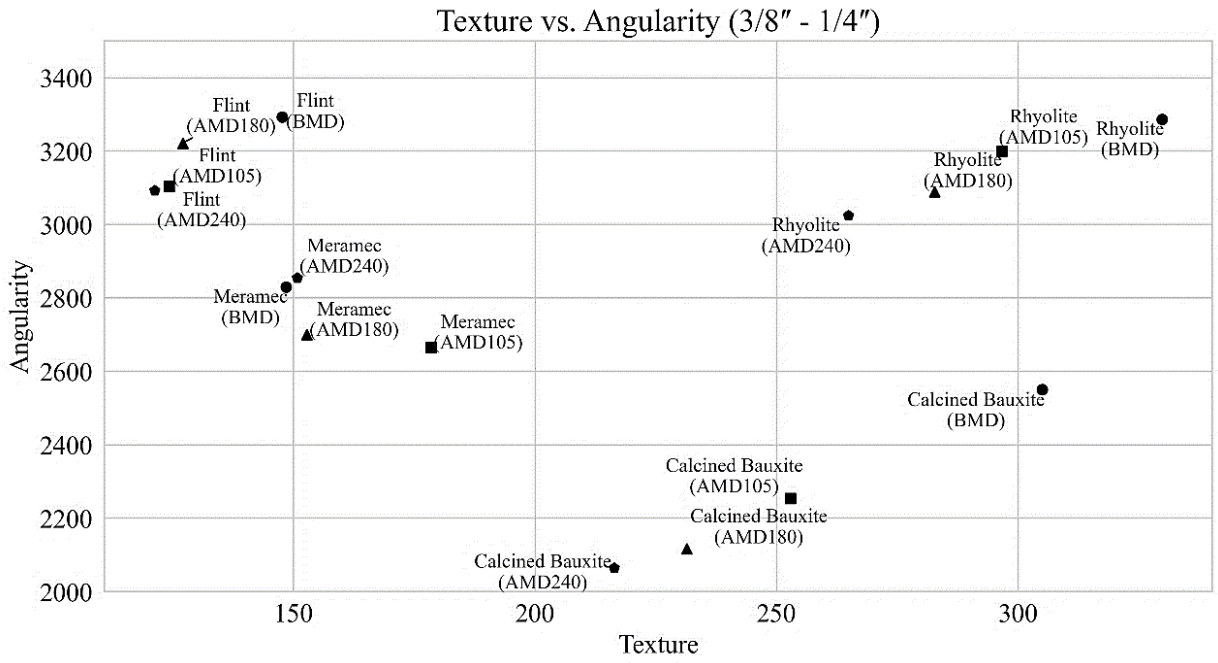

Figure 5.7 The relationships between Texture (TX) and Gradient Angularity (GA) indices (3/8″ - 1/4″)

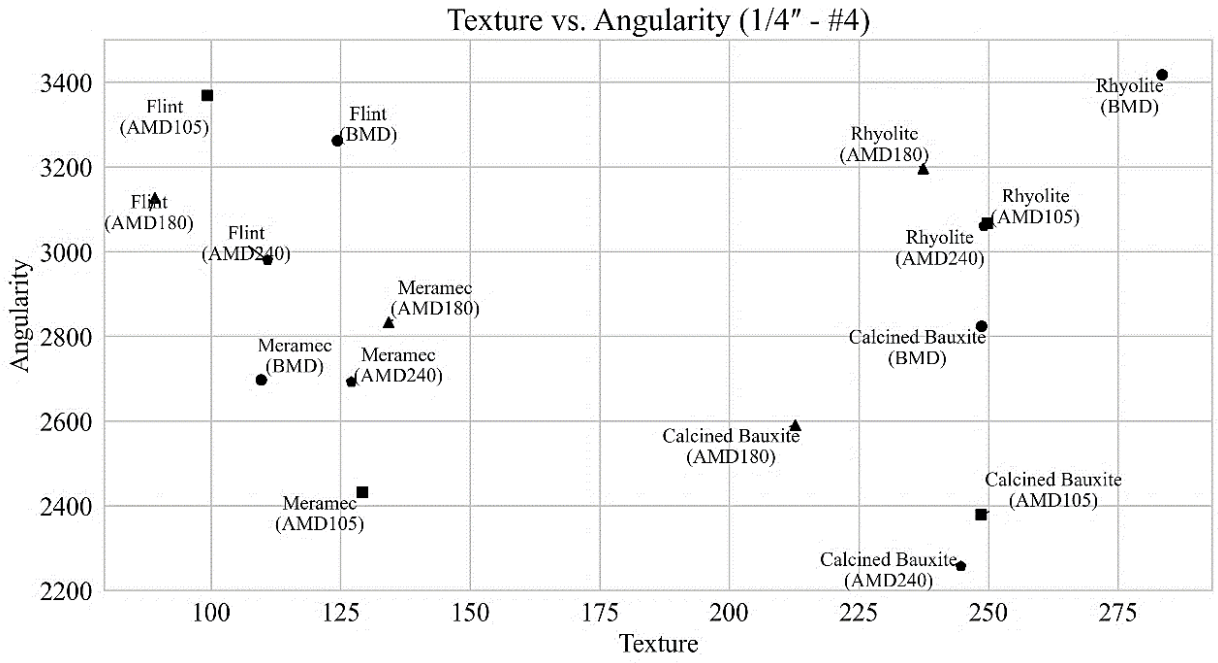

Figure 5.8 The relationships between Texture (TX) and Gradient Angularity (GA) indices (1/4″ - #4)

5.3.2 Relationships between Micro-Deval and Aggregate Image Measurement System Results

5.3.2.1 Relationships between Micro-Deval Polishing Times and Texture and Angularity Indices

Average AIMS TX indices, and average AIMS GA indices based on Micro-Deval abrasion times before polishing and after 105, 180, and 240 minutes were assessed. Figure 5.9 displays the relationships between MD abrasion times and average AIMS TX indices for each aggregate type. The MD test was carried out on aggregates with 3/8″ - #4 gradation, and subsequently, the AIMS TX indices were derived from the outcomes of two different sizes, specifically 3/8″ - 1/4″ and 1/4″ - #4, as detailed in Table 3-5.

Based on the scatter plot and the observed relationship between MD polishing times and average AIMS TX indices, it was noted that Calcined Bauxite, Rhyolite, and Flint exhibited exponential decay relationships. The formula for exponential decay is expressed Equation 5.1.

$$TX = a_{TX} + b_{TX} \times e^{(-cTX \times t)} \quad \text{Equation 5.1.}$$

where TX represents the texture index, t is the MD polishing time, a_{TX} is the terminal texture index (greater than or equal to zero), (a_{TX} + b_{TX}) is the initial texture index, and c_{TX} is the rate of texture change.

For Meramec, which did not exhibit an exponential decay trend, a polynomial showed better fit. The fit curve equation for Meramec is given by Equation 5.2.

$$TX = a_{TX} + b_{TX} \times t + (-c_{TX} \times t\text{^}2). \quad \text{Equation 5.2.}$$

where TX represents the texture index, t is the MD polishing time (a_{TX} + b_{TX}) is the initial texture index, and c_{TX} is the rate of texture change.

Table 5-1 displays the fitting parameters, along with the estimated Sum of Squares Error (SSE) and coefficient of determination (R-squared), for the (TX-MD t) model.

Table 5-1 Fitting parameters for (TX-MD t) model

Aggregate Type	a_{TX}	b_{TX}	c_{TX}	SSE	R^2
Calcined Bauxite (CB)	210.34	67.30	6.28E-3	159.82	0.91
Rhyolite	248.65	58.03	8.46E-3	2.53	1.00
Meramec	129.92	0.32	1.2E-3	40.72	0.87
Flint	112	24.03	0.2789	31.62	0.93

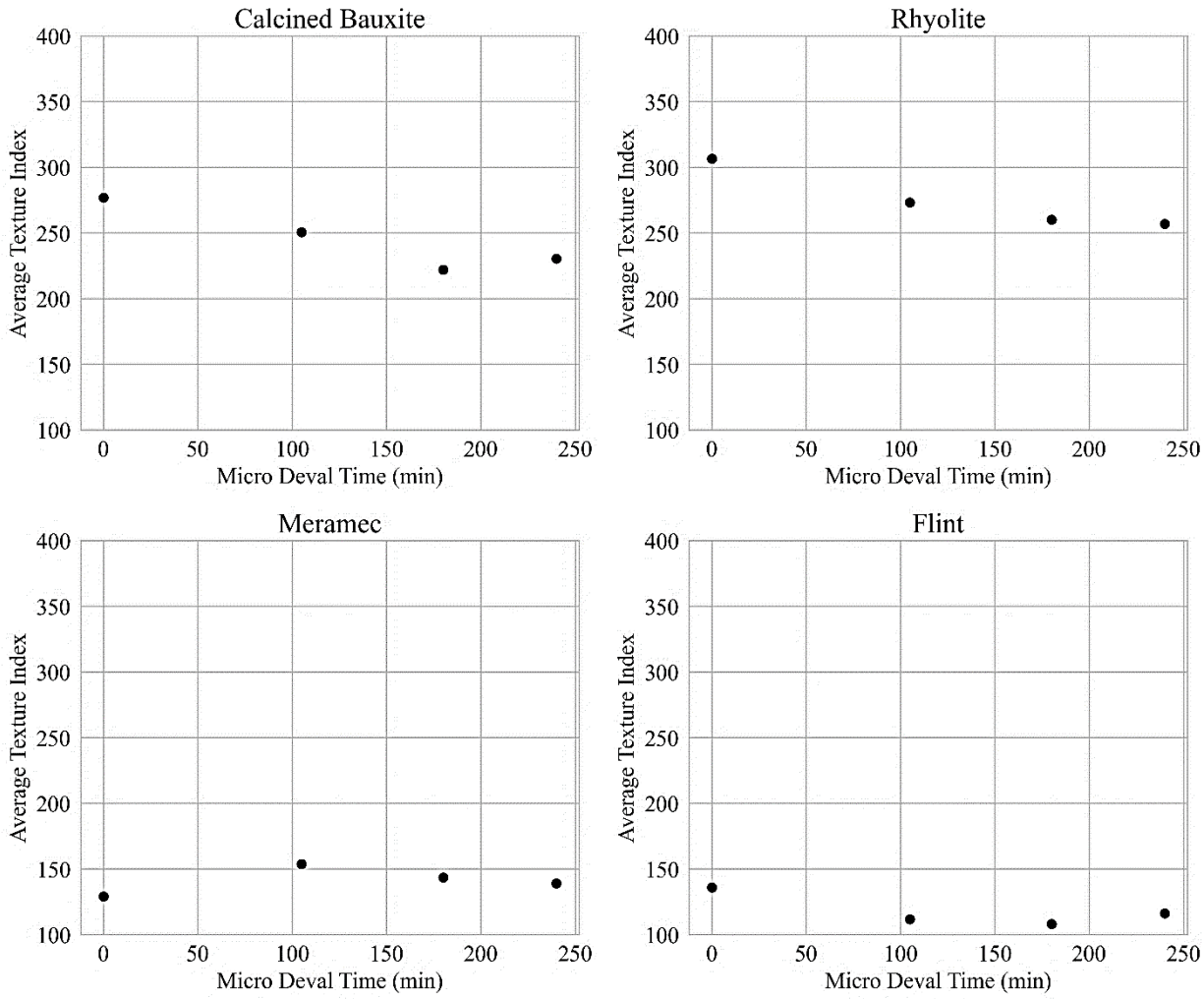

Figure 5.9 Relationships between MD Polishing time and average Texture indices

In Figure 5.10, the relationships between the Gradient Angularity (GA) indices and Micro-Deval (MD) polishing times for aggregates are depicted. Equations 5.3 and 5.4 represent the fitted curves for these relationships. Table 5-2 presents the fitting parameters, along with the estimated SSE and R^2 values for the (GA-MD t) model.

Since Meramec and Flint did not show an exponential decay trend, a polynomial fit formula was considered for these aggregates.

The formula for exponential decay for Calcined Bauxite and Rhyolite is expressed as Equation 5.3.

$$GA = a_{GA} + b_{GA} \times e^{(-c^{GA} \times t)} \qquad \text{Equation 5.3.}$$

where GA represents the angularity index, t is the Micro-Deval (MD) polishing time, a_{GA} is the terminal texture index (which should be greater than or equal to zero), (a_{GA} + b_{GA}) represents the initial texture index, and c_{GA} is the rate of angularity change over time.

For Meramec and Flint, the fit curve equation is given by Equation 5.4.

$GA = a_{GA} + b_{GA} \times t + (-c_{GA} \times t\text{^}2)$ Equation 5.4.

where GA represents the angularity index, t is the MD polishing time (a_{GA}+ b_{GA}) is the initial texture index, and c_{GA} is the rate of angularity change.

Table 5-2 Fitting parameters for (GA-MD t) model

Aggregate Type	a_{TX}	b_{TX}	c_{TX}	SSE	R^2
Calcined Bauxite (CB)	2144.31	537.07	8.5E-3	13709	0.91
Rhyolite	3032.82	316.35	9.00E-3	3455	0.93
Meramec	2746.75	2.39	1.1E-2	14763	0.59
Flint	3274.25	0.31	5.2E-3	455.38	0.99

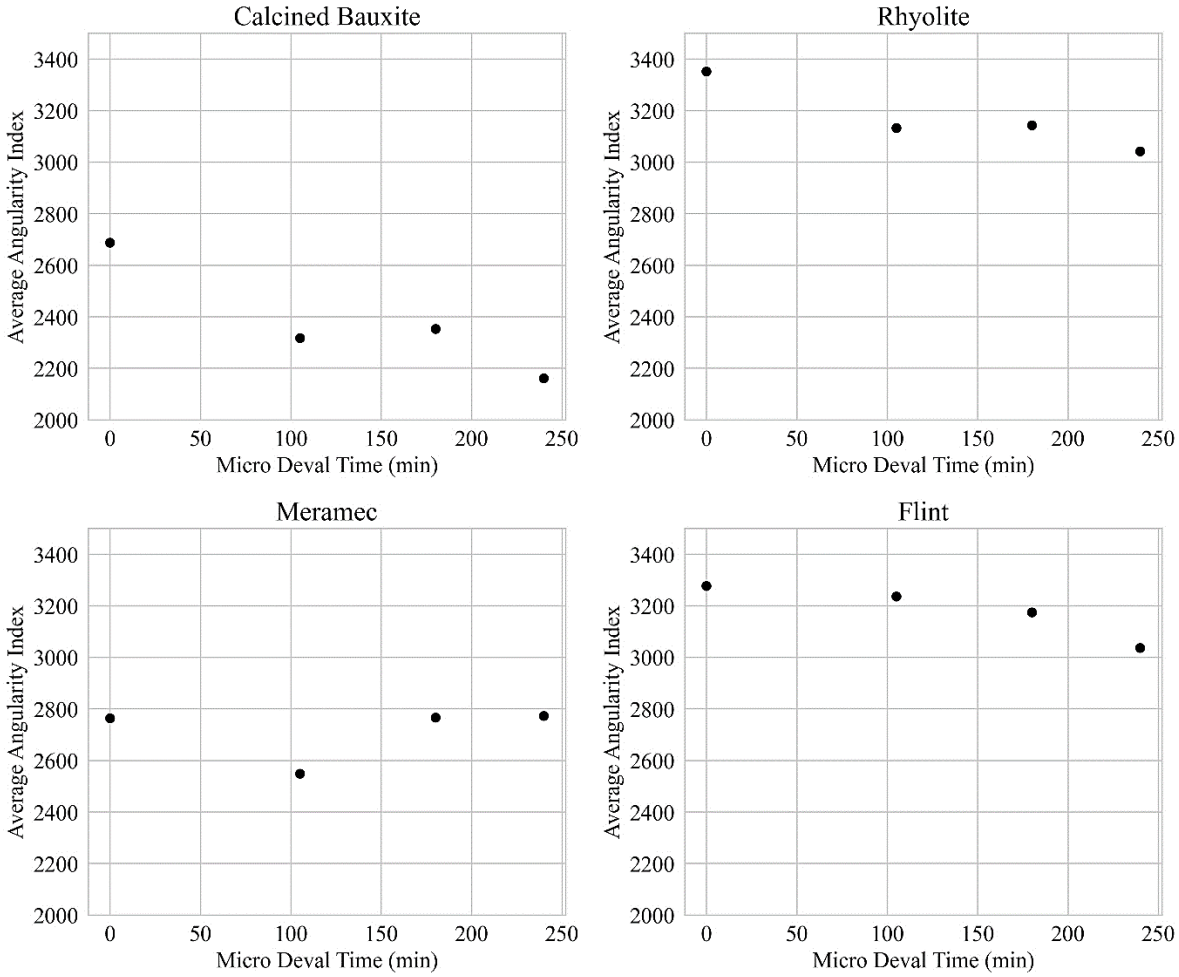

Figure 5.10 Relationships between MD Polishing time and average Angularity indices

5.3.3 Relationships between Micro-Deval and Los Angeles Mass Losses

The relationships between Los Angeles Abrasion (LAA) (grading D) and Micro-Deval (MD) mass losses for coarse sizes are illustrated in Figure 5.11. Four MD polishing times (105, 120, 180, and 240 minutes) were used for coarse gradation, and all the aggregates are shown in the figures. It can be observed that there is no specific relationship between LAA and MD at different times and for different aggregates. Meramec consistently showed the lowest LAA and MD values across different times, while Calcined Bauxite exhibited the highest MD and lowest LAA values after Meramec.

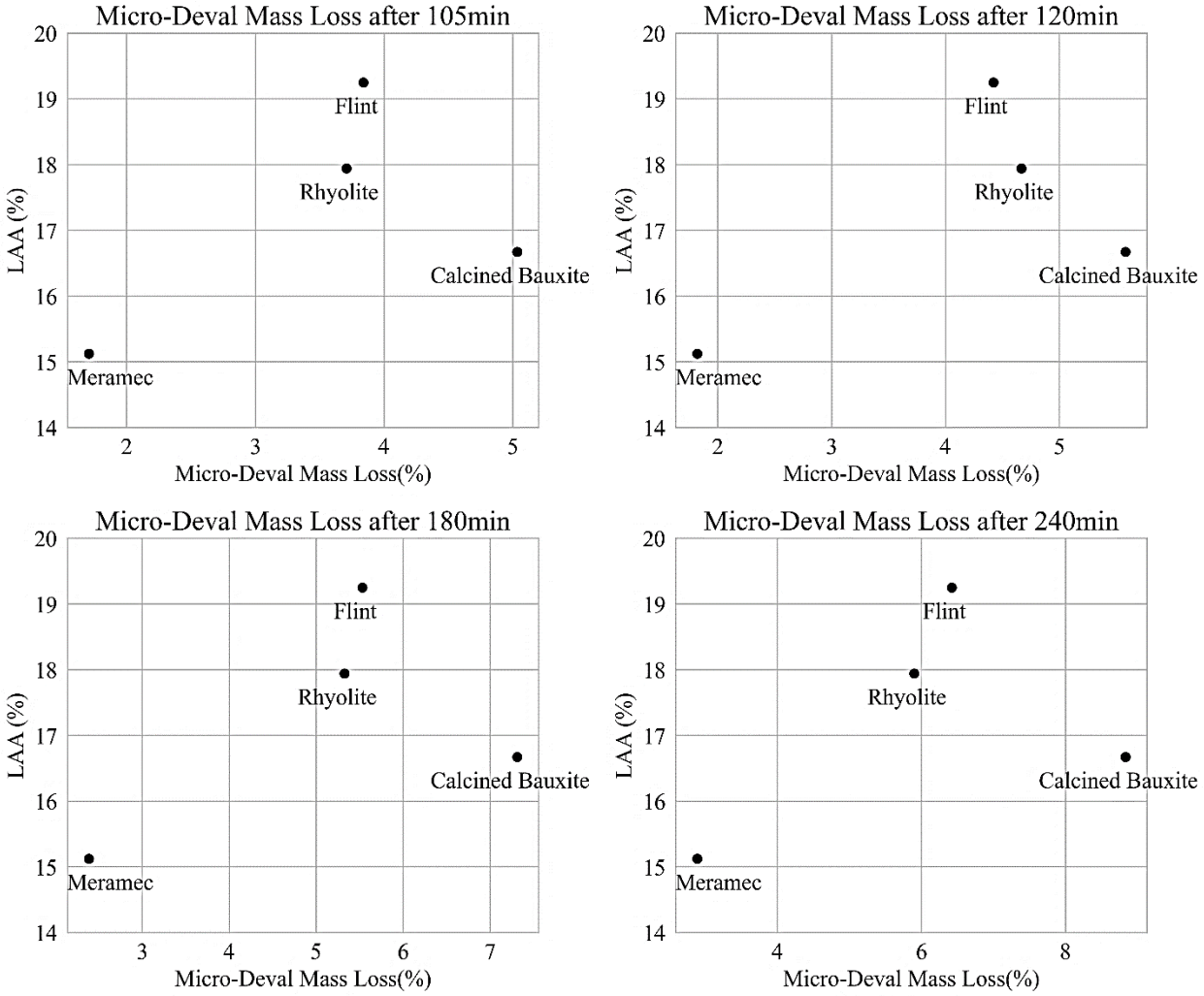

Figure 5.11 Relationships between Micro-Deval and Los Angeles Mass Losses for different aggregates indifferent polishing times

5.3.4 Relationship between Uncompacted Void Content, Micro-Deval times and Aggregate Image Measurement System Results

5.3.4.1 Effect of Micro-Deval Polishing Time on the Uncompacted Void Content Percentages

Figure 5.12 illustrates the percentages of Uncompacted Void Content (UVC) for aggregates using HFST gradation. These percentages were calculated for the aggregates at various stages: Before Micro-Deval polishing (BMD), after 15 minutes of Micro-Deval polishing time (AMD 15), and after 30 minutes of Micro-Deval polishing time (AMD 30). It is evident that UVC decreased and reached its lowest value after 30 minutes of MD polishing time. Flint Chat showed the highest percentages of UVC both before and after polishing, while Meramec consistently exhibited the lowest percentages of UVC, maintaining steady low values after polishing.

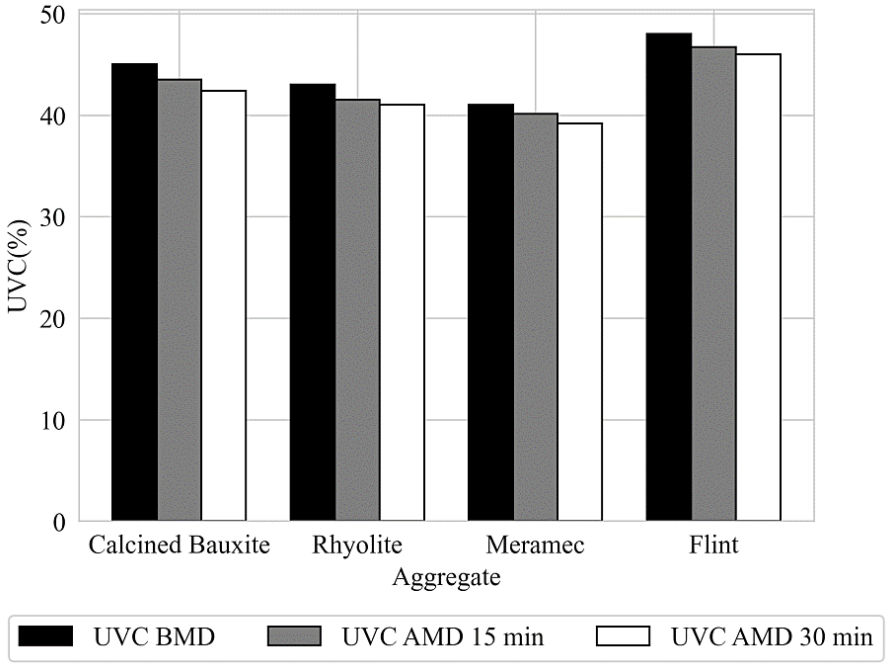

Figure 5.12 Relationship between UVC and MD polishing times

The relationship between the times of MD polishing and the percentages of UVC is further depicted in Figure 5.13. From the fitted line, it is observed that Meramec demonstrated a linear decrease in UVC with increasing polishing time, whereas other aggregates showed a quadratic relationship with polishing time.

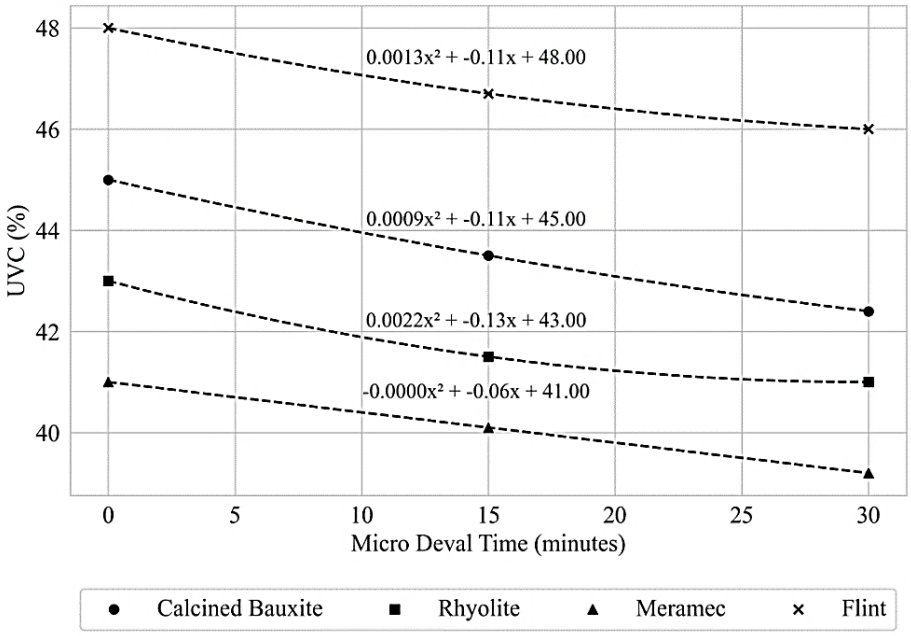

Figure 5.13 Relationship between the MD polishing times and the UVC (%) different aggregates

5.4 Summary

This chapter presented the aggregate performance testing results. The Micro-Deval (MD) test was conducted for coarse aggregates with a 3/8″ - #4 gradation and fine aggregates with a #6 - #16 gradation. Regarding the coarse gradation (3/8″ - #4), Calcined Bauxite exhibited the most significant mass loss percentages, while Meramec River Aggregate displayed the least mass loss percentages. Rhyolite and Flint demonstrated comparable mass loss percentages for AMD 105, 120, and 180. However, for AMD 240, Rhyolite showcased a lower mass loss compared to Flint. In terms of the fine gradation (#6 - #16), Meramec River Aggregate had the lowest mass loss percentages. For AMD 15, Calcined Bauxite, Rhyolite, and Flint exhibited similar mass loss percentages, but Calcined Bauxite displayed a lower mass loss compared to Flint and Rhyolite. Overall, Rhyolite showed the highest percentage of mass loss for AMD 15 and AMD 30.

The Aggregate Image Measurement System (AIMS) was used to measure Texture (TX) and Gradient Angularity (GA) indices for aggregates of two different sizes, 3/8″ - 1/4″ and 1/4″ - #4, during the polishing stages of BMD, AMD 105, AMD 180, and AMD 240. The reduction in aggregate sizes from 3/8″ - 1/4″ to 1/4″ - #4 led to a decline in TX indices across BMD, AMD 105, AMD 180, and AMD 240 phases. However, Calcined Bauxite exhibited elevated texture with AMD 240 in the 1/4″ - #4 size range compared to the 3/8″ - 1/4″ size range. Additionally, Calcined Bauxite, Rhyolite, and Flint displayed diminishing texture trends as the polishing time increased for aggregates of size 3/8″ - 1/4″. Conversely, for size 1/4″ - #4, their texture initially decreased and then experienced an upturn in AMD 240. On the other hand, Meramec demonstrated an increase in texture for both sizes following polishing to AMD 105, followed by a subsequent decrease in texture. For the 1/4″ - #4 size range, Calcined Bauxite and Rhyolite followed a similar pattern, with angularity initially decreasing and then increasing after 180

minutes of polishing. Flint, on the other hand, showed an initial increase in angularity after 105 minutes, which was followed by a decrease in subsequent time domains. As for Meramec, its GA decreased after 105 minutes of polishing, increased after 180 minutes, and then experienced a slight decrease after 240 minutes.

Among all the aggregates, Rhyolite displayed the highest TX and GA indices for both sizes, while Meramec showcased the lowest angularity values among the aggregates. The TX and GA indices for Calcined Bauxite increased at 105, 180, and 240-minute Micro-Deval polishing times as the size of the aggregate was reduced.

No specific relationship was observed between the changes in Average Texture Index and Average Angularity Index across different Micro-Deval (MD) polishing times. Before polishing in Micro-Deval (BMD), the highest average texture and angularity were observed for Calcined Bauxite and Rhyolite. However, Meramec had the highest texture and lowest angularity after 105 minutes of polishing (AMD 105), and the highest angularity observed at AMD 240. The relationship between Uncompacted Void Content (UVC) and Micro-Deval (MD) polishing times in the fine aggregates showed that UVC decreased and reached its lowest values after 30 minutes of MD polishing. Flint Chat exhibited the highest UVC percentages both before and after polishing, while Meramec consistently had the lowest UVC percentages, maintaining steady low values after polishing.

CHAPTER 6: BINDER PERFORMANCE TESTING

6.1 Introduction

This chapter discusses binder performance testing results, focusing on comparing different binders based on their characteristics and performances. Supplied asphalt binders were tested and graded by the suppliers. Selected testing was independently conducted to verify the grade and properties of the binders. This additional testing was intended to confirm that the supplied binders met the specific project requirements and aligned with the desired performance criteria. The sampling and testing methods for asphalt PG binders, emulsion binders, and modified binders were carried out according to MoDOT Standards, specifically according to Section 1015 Bituminous Material. Table 6-1 presents the sampling and test methods employed for this research.

Table 6-1 Bituminous material testing

Property	Method	PG	Emulsion
Sampling	AASHTO T 40	X	X
Water	AASHTO T 55	X	X
Flash Point (Cleveland Open Cup)	AASHTO T 48	X	
Viscosity, SSF @ 50 C	AASHTO T 201		X
Distillation	AASHTO T 78		X
Penetration	AASHTO T 49		X
Ductility	AASHTO T 51		X
Solubility in Trichlorethylene	AASHTO T 44	X	
Ash in Bituminous Material	AASHTO T 111		X
Viscosity (Rotational)	ASTM D 4402	X	
Dynamic Shear	AASHTO 315	X	
Rolling Thin Film Oven Test	AASHTO T 240	X	
Pressure Aging Test	AASHTO R28	X	
Creep Stiffness	AASHTO T 313	X	
Direct Tension	AASHTO T 314		

6.2 Performance Grade (PG) and Modified Binders testing

Several rheological tests were conducted on both unmodified (PG82-16 and PG88-16) and modified binders PG64-22+8% Kraton D0243K (PG82-22 (PM) and PG76-22 + 6% Kraton D0243K (PG88-16 (PM). These tests included evaluating the dynamic shear modulus (G*) and phase angle (δ) using Dynamic Shear Rheometer (DSR) tests, following AASHTO 315, measuring the binder's viscosity through rotational viscometer (RV) tests, following ASTM D 4402, and estimating the low-temperature stiffness (S(t)) and m-values via bending beam rheometer (BBR) tests, following AASHTO T 313. The short-term aging was simulated by following AASHTO T 240 standards, while long-term aging was simulated according to AASHTO R 28 guidelines. The summary of performance grade (PG) and modified binders are presented in Table 6-2.

Table 6-2 Performance grade (PG) and modified binders

Binder	Description
PG82-16	50% PG94-10 + 50% PG76-22
PG88-16	60% PG94-10 + 40% PG76-22
PG82-22 (PM)	PG64-22 + 8% Kraton D0243K
PG88-16 (PM)	PG76-22 + 6% Kraton D0243KT

6.3 Emulsions testing

CRS-2P and CRS-2PSC asphalt emulsions, which are cationic rapid-setting and high-viscosity types, were used in this study following the Missouri Department of Transportation (MoDOT) recommendations. The physical properties of CRS-2P and CRS-2PSC, along with the MoDOT specifications, are summarized in Table 6-3.

Table 6-3 Asphalt emulsion properties

Parameter	Test Procedure	Result		Required*	
		CRS-2P	CRS-2PSC	Min	Max
Viscosity, Saybolt Furol, 122°F (sec)	ASTM D-7496	222	340	100	400
Sieve test (%)	ASTM D-6933	0.15%	0.15%	-	0.3
Storage stability, 1 day (%)	ASTM D-6930	0.50%	0.50%	-	1
Particle charge	ASTM D-7402	Positive	Positive	Positive	
Residue by distillation (% by weight)	ASTM D-244	65.65%	65.70%	65	-
Oil distillate (% by volume of emulsion)	ASTM D-6997	Trace	Trace	-	3
Penetration, 77°F, 100g, 5 sec. (dmm)	ASTM D-5	106	123	100	200
Ductility, 39.2°F, 5 cm/min. (cm)	ASTM D-113	40	40	30	-
Elastic recovery, 50°F (%)	ASTM D-6084	58.75	68.75	58	-

*According to the section 1015.20.5.1 Polymer Modified Asphalt Emulsion, Missouri standard specifications for highway construction, 2023

6.4 Binder Bond Strength Test (BBS)

The BBS test in this project was conducted based on AASHTO T361-22 using the Positest AT-A apparatus to investigate the adhesion strength of different binders. The adhesion tester applies a pneumatic load via a pressure ring to a pull-off stub fixed to a rigid substrate with asphalt binder. The binder is adhered to the substrate and subjected to different curing conditions. In the BBS test, the loading rate was controlled at 690 kPa/s (100 psi/s), and the asphalt thickness was

maintained at 0.2 mm by the stubs, following AASHTO recommendations. The specimen preparation and BBS test procedure steps are summarized in Figure 6.1. The steps were as follows:

1. Rhyolite substrates were cleaned using an ultrasonic cleaner and subsequently dried alongside the pull-out stubs at 170°C for a minimum duration of 1 hour. The binders were heated to their application temperatures—170°C for PG and modified binders, and 80°C for emulsions—for at least 1 hour.

2. A silicone mold measuring approximately 40 mm by 40 mm (1.6 in by 1.6 in.), featuring an 8-mm (0.32-in.) diameter cavity and a depth of 2.0 mm (0.08 in.) for PG and modified binders, and silicone rings with a 21 mm diameter hole in the center for emulsions, were prepared on base substrates. A small drop of binder was placed into the hole of the silicone rings, then pressed with pull-out stubs to ensure a uniform asphalt thickness of 0.2 mm.

3. All specimens were allowed to cool to room temperature for 1 hour. Subsequently, some specimens were cured under ambient conditions (25°C, 30% humidity) for 24 hours and then tested to determine the Binder Bond Strength (BBS) under dry conditions (BBS_{dry}). Additionally, other specimens were submerged in a 40°C water bath for 24 and 48 hours, followed by a 1-hour curing period before testing. The BBS test was then performed on these immersion specimens to assess the BBS under wet conditions (BBS_{wet})

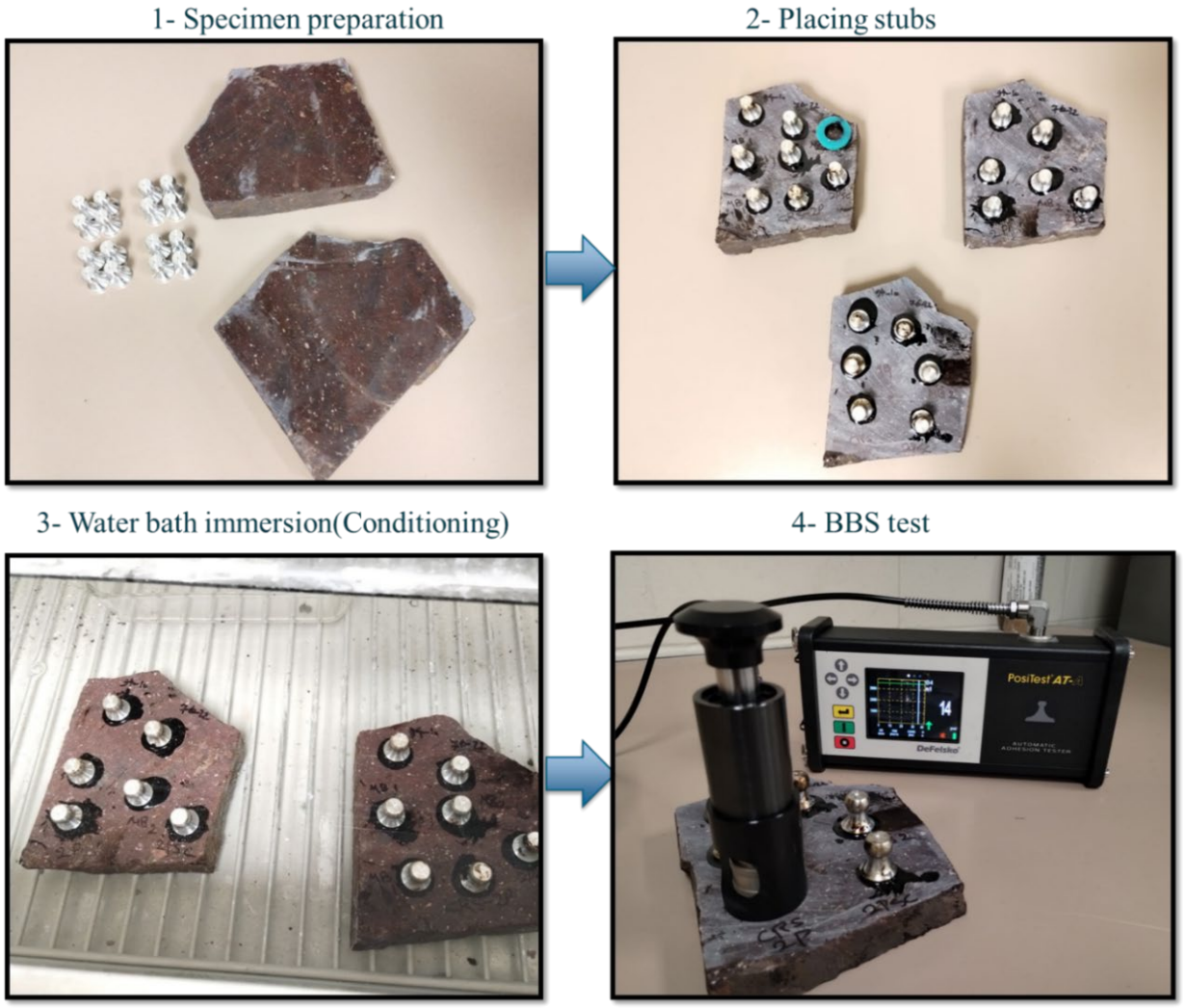

Figure 6.1 BBS test procedure

The Binder Bond Strength (BBS) results of different binders under dry and wet conditions, along with the failure modes, are depicted in Figure 6.2. Epoxy Resin showed the highest BBS values, which were significantly higher than those of other binders. Additionally, during wet conditions, the BBS of epoxy resin increased slightly, whereas the BBS of other binders decreased.

Under dry conditions, excluding epoxy, PG88-16 (PM) followed by PG82-22 (PM) and PG88-16 showed the highest BBS values. After conditioning for 24 and 48 hours in a water bath at 40°C, all binders exhibited a decrease in BBS values. This decrease was lower in both modified binders and higher in the emulsions.

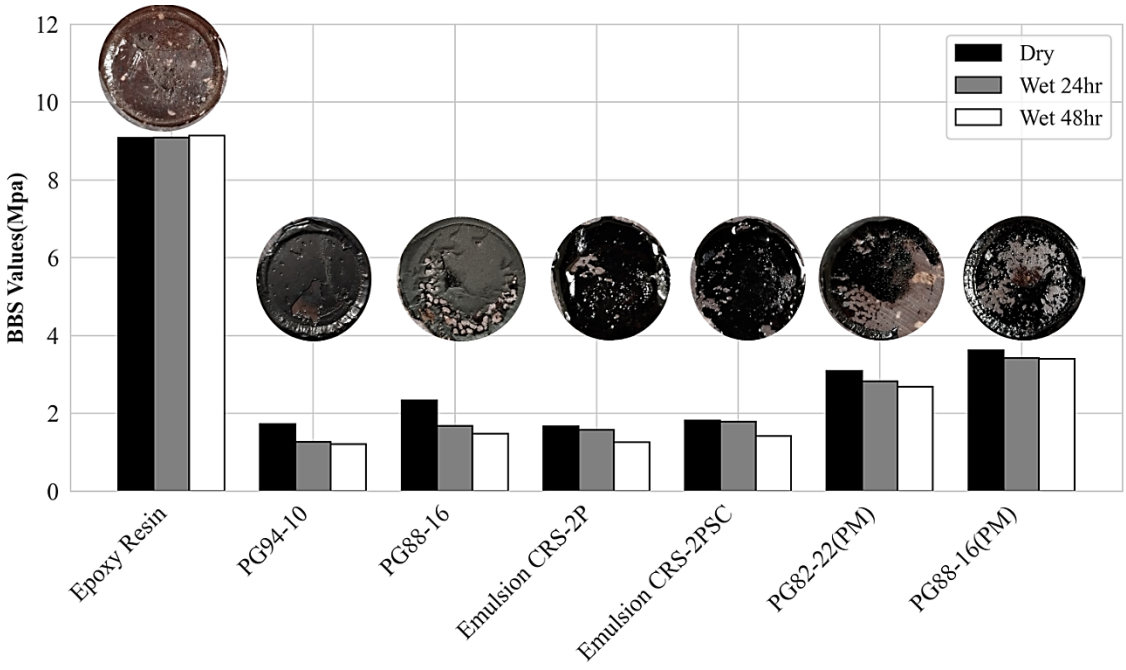

Figure 6.2 BBS values in different binders

6.5 Summary

The results for PG binders, modified binders, and emulsions indicate that all binders met the required standards. In the Binder Bond Strength (BBS) test, epoxy resin displayed the highest values, significantly outperforming the other binders. Additionally, epoxy resin showed a slight increase in BBS under wet conditions, whereas the other binders exhibited a decrease. Under dry conditions, excluding epoxy, PG88-16 (PM) had the highest BBS values, followed by PG82-22 (PM) and PG88-16. After 24 and 48 hours of conditioning, all binders demonstrated decreased BBS values, with modified binders experiencing less decline compared to emulsions.

CHAPTER 7: HIGH FRICTION PERFORMANCE TESTING

7.1 Introduction

This chapter delves into the results of high friction performance testing, emphasizing the comparison of various samples comprising different binders and aggregates of varying sizes. The performance assessment included several tests such as accelerated friction testing using the Circular Track Meter (CTM) and Dynamic Friction Test (DFT), as well as the British Pendulum (BP) and Polishing Stone Value (PSV) tests. Different combinations of binders and aggregates were utilized for each set of samples (coupons and slabs) in the CTM, DFT, BP, and PSV tests to evaluate their overall performance.

7.2 British Pendulum Test Results

The data collected from the British Pendulum tests were examined to evaluate the friction-enhancing capabilities of various binder-aggregate mixes. The results of these analyses were compared to determine which combinations exhibited the best performance based on both BPT and PSV criteria. Different binder types and aggregates of varying sizes were considered in assessing the performance of the samples (coupons).

7.2.1 Effect of Different Binders and Aggregate Size on the British Pendulum Number Values

Figures 7.1 through 7.3 display the British Pendulum Number (BPN) values measured before and after 10-hour polishing cycles on the British Wheel for different binders and aggregates. Three sizes of aggregates were used in the tests: the original HFST size, a medium size, and a coarse size, as noted in Table 3-5. For each size category, two aggregate coupons were created using various binders and aggregates selected for this study.

Five BPN measurements were taken for each aggregate coupon before and after the polishing process, and the average BPN was subsequently calculated. Figure 7.1 illustrates the BPN values before and after the polishing process for HFST size. Calcined Bauxite consistently showed the highest BPN values across all binders, both before and after polishing, followed by Rhyolite and Flint, which yielded comparable results. When the epoxy binder was replaced with PG binders, the initial BPN numbers were comparable across all samples. However, after 10 hours of polishing, samples with the PG94-10 binder exhibited a more significant decrease in BPN. Samples with the blended PG binder PG88-16 performed better than those with PG82-16, suggesting that binder stiffness may interfere with effective bonding between the aggregate and binder. This interference could lead to aggregate dislodgement and, consequently, lower BPN values post-polishing.

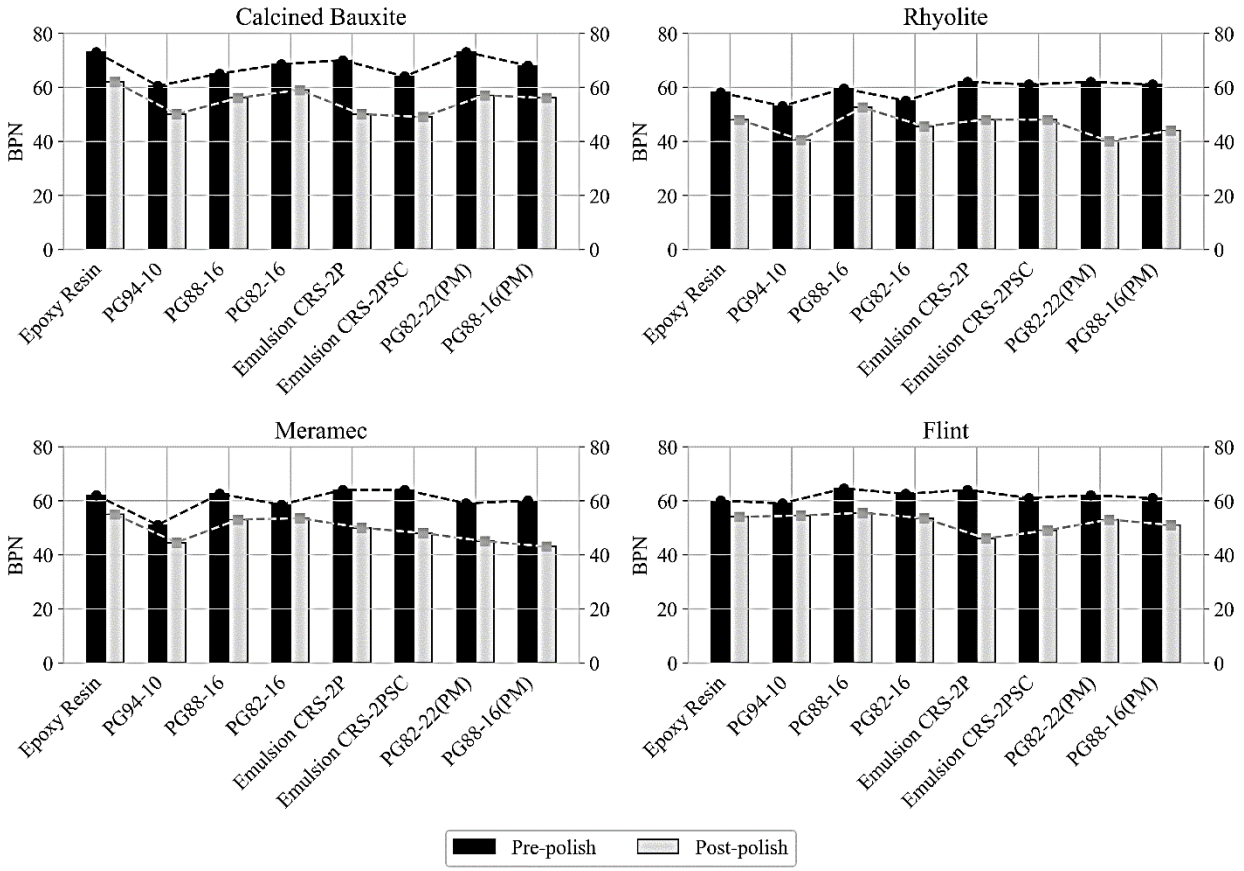

Figure 7.1 Average BPNs with different binders and aggregates for HFST size

Both emulsions showed lower BPN numbers after polishing compared to other binders, potentially due to bleeding and rutting during the polishing process. The flushing and bleeding observed in Figure 7.2 primarily occurred in the wheel paths, indicating a connection to the stiffness of the emulsions. Both Modified Binders exhibited comparable performance. For example, with Calcined Bauxite, Meramec, and Flint, PG82-22 (PM) achieved higher BPN values after polishing. However, with Rhyolite, PG88-16 (PM) led to higher BPN values.

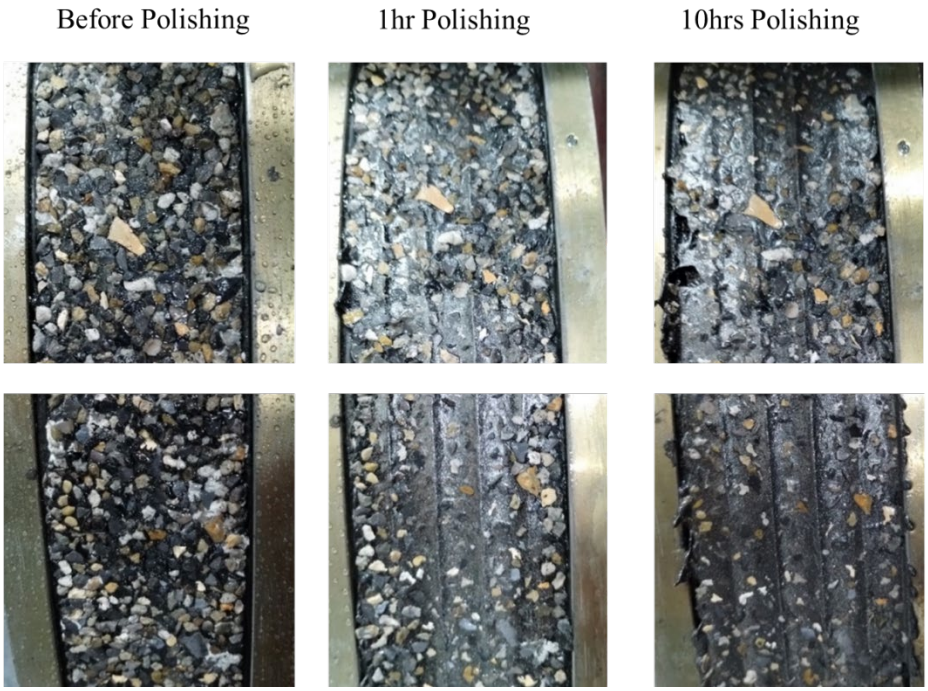

Figure 7.2 Calcined Bauxite HFST size (top: CRS-2P) (bottom: CRS-2PSC)

Figure 7.3 displays the BPN values before and after the polishing process for medium-sized aggregates. Similar to earlier findings, after the epoxy resin, the PG binders and both modified binders exhibited comparable results. Both types of emulsion demonstrated similar performances; however, they exhibited the lowest BPN values for all aggregates after the polishing process. The trend illustrated in the line graph shows that BPN values decrease slightly when transitioning from Epoxy to PG binders. A slight decrease in BPN values was observed in the line graph when transitioning from Epoxy to PG binders. For example, before polishing, a decrease of approximately 10% from Epoxy to PG94-10 was noted, and after polishing, a decrease of around 23% was observed. The decrease in BPN values is more pronounced between PG binders and Emulsions.

Figure 7.4 shows the BPN values before and after polishing for coarse-sized aggregates. The observed trend indicates a more moderate decrease in BPN values across all binders compared to those seen with HFST and medium-sized aggregate, particularly for both emulsions, suggesting that emulsions perform better with coarser aggregate. Epoxy, again, showed the lowest decrease in BPN after the polishing process, followed by the PG binders and the modified binders. Both emulsions and modified binders exhibited comparable results for Rhyolite. This similarity could be attributed to the influence of aggregate shape and texture characteristics.

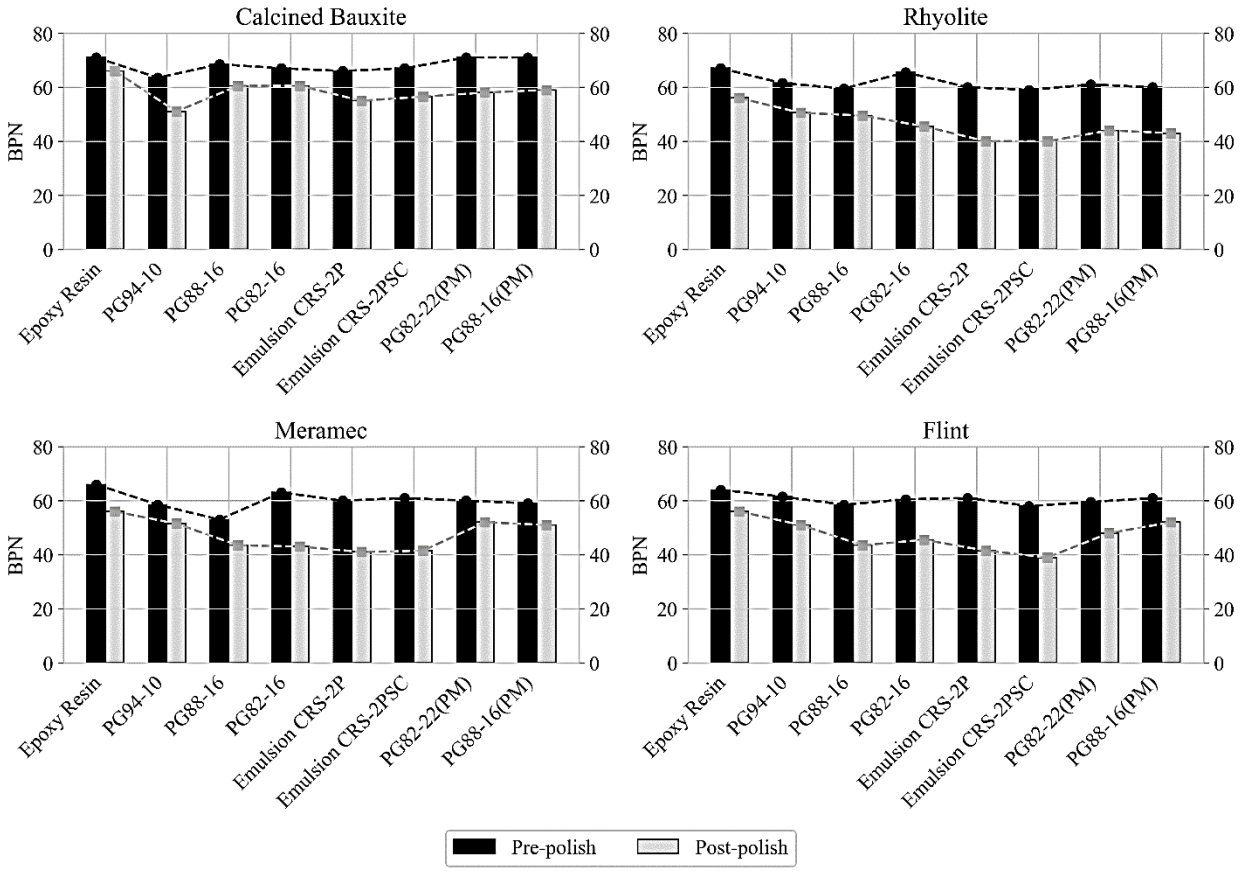

Figure 7.3 Average BPNs with different binders and aggregates of medium size

Figure 7.5 compares coarse-sized coupons at different polishing times with both emulsions. Compared to Figure 7.2, which depicted HFST sizes, there is less bleeding and rutting observed with the coarser aggregates, contributing to better BPN numbers in this scenario. These results imply that larger aggregates are more resistant to deformation and are better at resisting in the wheel path during the polishing process, enhancing performance when emulsions are used. Moreover, Figure 7.5 differentiates the performance between coupons made with CRS-2P emulsion and those with CRS-2PSC emulsion. While CRS-2P seems to have a higher stiffness due to lower bleeding, CRS-2PSC shows superior aggregate retention. When selecting an emulsion, it is crucial to consider the specific properties and objectives desired for the application, as each emulsion type offers distinct advantages.

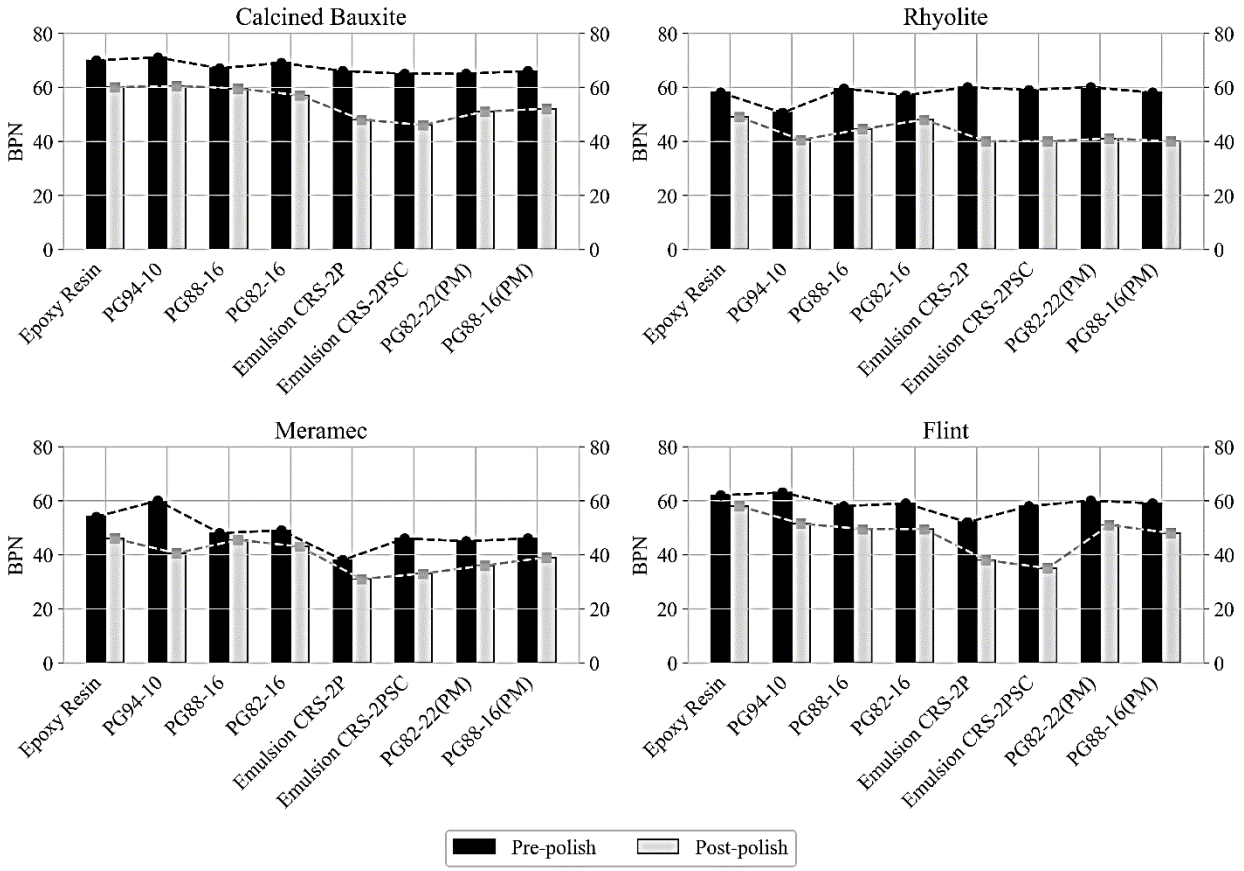

Figure 7.4 Average BPNs with different binders and aggregates of coarse size

Based on the data from Figure 7.4, coarse-sized Rhyolite showed comparable results for both emulsions and modified binders. Further evaluation, regarding BPN values before and after polishing all the binders, was conducted on extra-large-sized Rhyolite. The results, shown in Figure 7.6, revealed that for the extra-large-sized aggregate, the PG binder PG82-16 and both modified binders yielded higher BPN values, with emulsions showing comparable BPN values to other binders. Notably, epoxy resin exhibited the lowest percentage of BPN lost after the polishing process, followed by PG82-16 binder, PG82-22 (PM), and PG88-16(PM).

The analysis of BPN values before and after polishing revealed that PG94-10 had the highest percentage of BPN loss, likely due to its higher stiffness, causing more aggregate loss during polishing. This observation is supported by Figure 7.7, which shows chip loss in the coupon with PG94-10 before and after the polishing process.

Figure 7.5 Calcined Bauxite coarse size (top: CRS-2P) (bottom: CRS-2PSC)

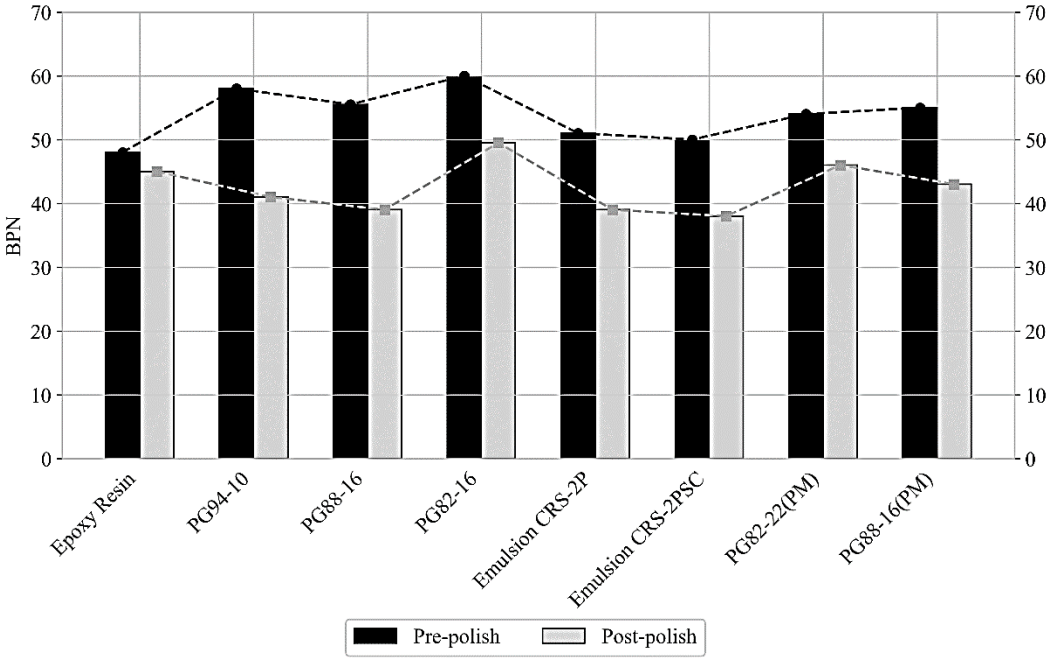

Figure 7.6 BPN values with different binders and extra-large-sized Rhyolite

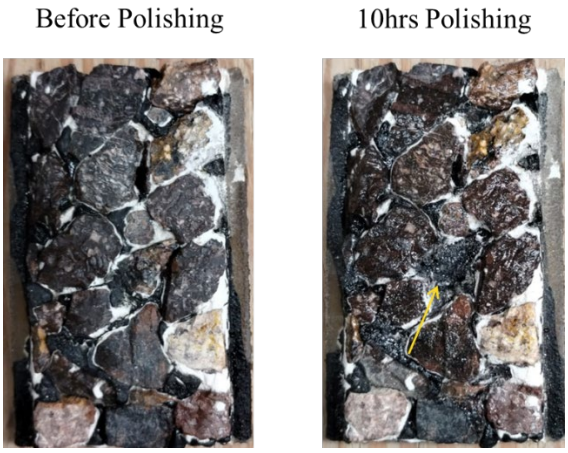

Figure 7.7 coupon with PG94-10 before and after the polishing process

7.2.2 Average British Pendulum Number Values

In Figure 7.8, the average British Pendulum Number (BPN) values for different binders and aggregates of varying sizes are displayed. Once again, epoxy resin demonstrated higher BPN values both before and after polishing. The trend in the line graph indicates a decrease in BPN from epoxy resin to the PG94-10 binder, followed by an increase for the PG binder PG88-16 and PG binder PG82-16, then a decrease again for both emulsions, and finally a rise for the modified binders.

PG88-16 (PM) exhibited better performance than PG82-22 (PM) in terms of a decrease in BPN values after polishing. The PG blended binder PG88-16 showed a smaller decrease in BPN values compared to PG82-16 when comparing results before and after polishing. Both emulsions showed comparable results and did not demonstrate superior performance over each other.

In Figure 7.9, the percentage decrease in average British Pendulum Number (BPN) values after polishing is shown for different combinations:

- For Calcined Bauxite, epoxy resin exhibited the lowest decrease at 12%, while emulsion CRS-2P showed the highest decrease at 22%.
- Regarding Rhyolite, epoxy showed the lowest decrease at 16%, whereas PG82-22 (PM) had the highest decrease at 31%.
- For Meramec and Flint, epoxy resin showed the lowest decrease, while CRS-2PSC had the highest decrease in BPN values.

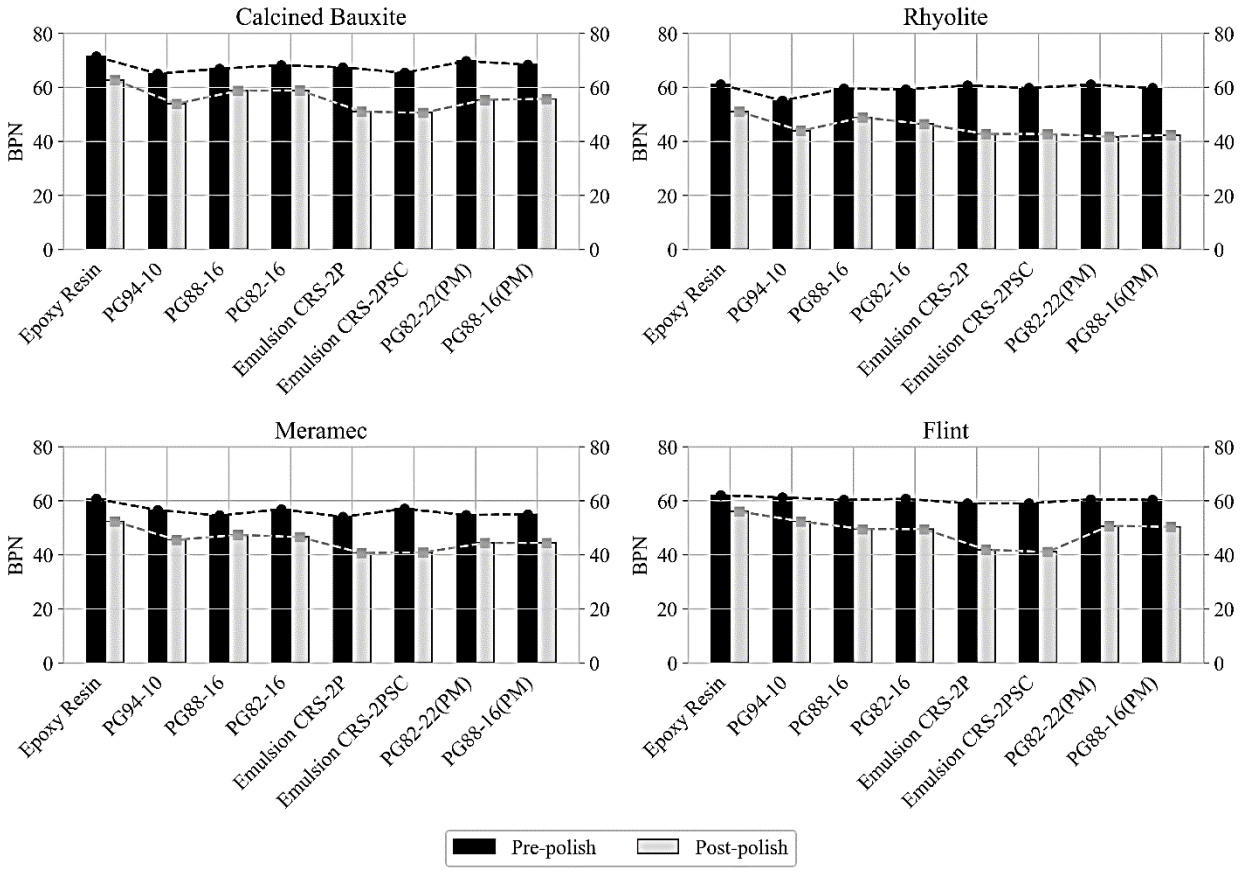

Figure 7.8 Average BPNs

7.3 Accelerated Friction Testing Results

Accelerated friction testing was utilized to assess how different binders and aggregate sizes performed in terms of surface friction. This accelerated evaluation involved using the Circular Track Meter test to measure Mean Profile Depth (MPD) and the Dynamic Friction Tester (DFT) to measure the Coefficient of Friction (COF). To simulate real-world conditions, a Three-Wheel Polishing Device (TWPD) was utilized to polish the test surfaces, mimicking the polishing process seen in High Friction Surface Treatment (HFST) applications under typical traffic conditions. The DFT was employed to measure COF at varying speeds (e.g., 20, 40, 50 km/hr) and across different numbers of polishing cycles, including 0 cycles (initial), 30 cycles, 70k cycles, and 140k cycles (considered terminal).

The researchers selected two aggregates, CB and Rhyolite, for the accelerated friction testing, based on their superior performance in physical durability and British Pendulum tests. Meramec and Flint were excluded from the selection due to their lack of comparable texture and angularity indices, as well as BPN results. Among the binders, epoxy resin, PG88-16, CRS-2P, PG82-22(PM), and PG88-16(PM) demonstrated better overall performance in BPT values before and after the polishing process, and thus were selected for evaluation.

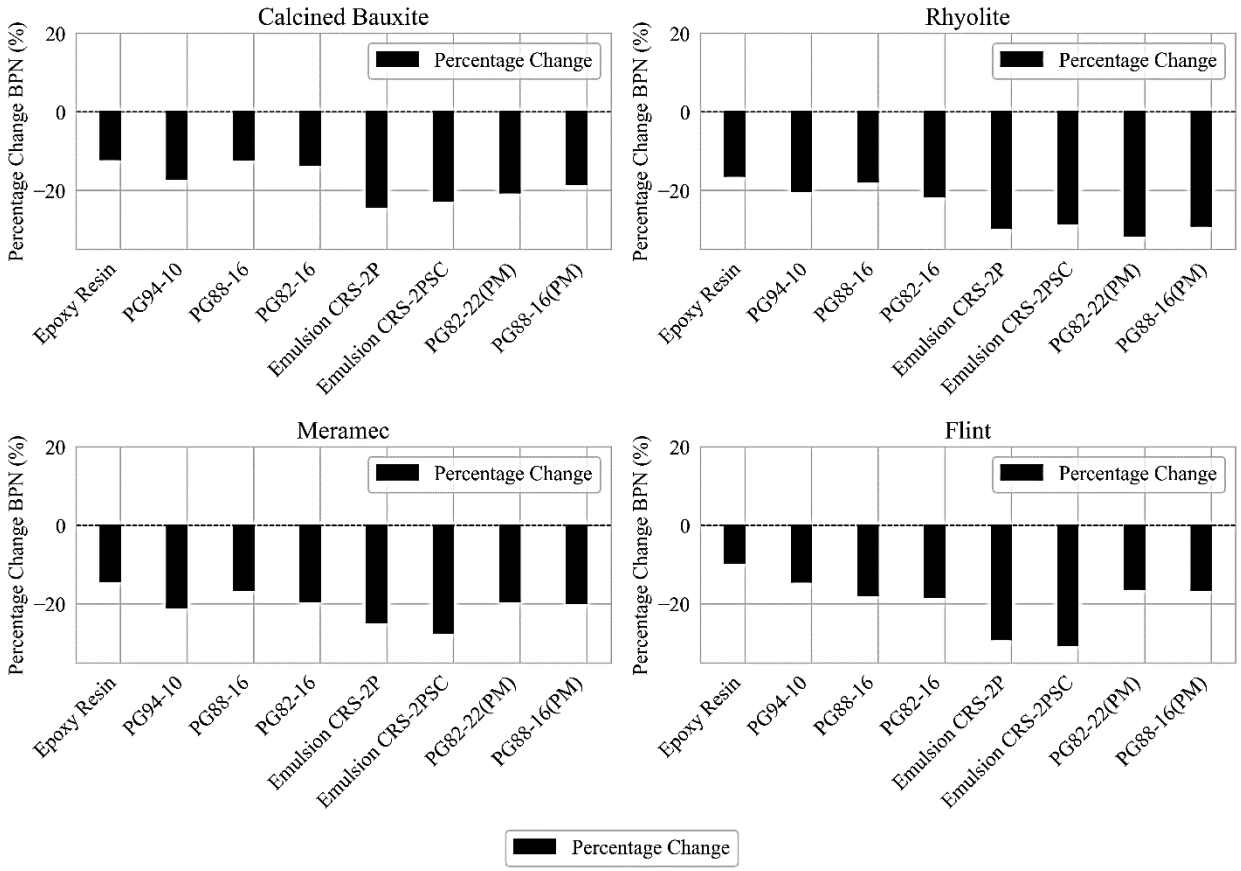

Figure 7.9 Percentages of decrease in the average BPNs after the polishing process

7.3.1 Dynamic Friction Test

Coefficient of Friction (COF) values were assessed at varying speeds (20, 40, and 50 km/hr) and across multiple polishing cycles (0 cycles (initial), 30K cycles, 70k cycles, and 140k cycles (terminal friction)) for two aggregates of three different sizes (HFST, medium, and coarse). Five binders selected for accelerated friction testing were also included in the evaluation. The COF values represent the average of two replicates, with one friction measurement taken using the Dynamic Friction Tester (DFT) for each combination of polishing cycle and speed. Figure 7.10 illustrates the COF values measured by the DFT for HFST aggregate size. The Three-Wheel-Polisher, that prepares slabs for the DFT test, is more aggressive on the HFST application, as compared to the BP wheel. Figure 7.11 illustrates an example of the damage to the emulsion slabs experienced under the DFT test. Figures 7.12 and 7.13 illustrate the COF values measured by the DFT at different speeds for the medium and coarse sizes, respectively. As indicated in Figure 7.10, the COF at 20, 40, and 50 km/hr before polishing the slabs exhibited comparable values across all binders, with Calcined Bauxite showing a higher COF compared to Rhyolite. However, after 30K polishing cycles, the COFs for emulsion CRS-2P dramatically decreased. This issue is attributed to the stiffness of the emulsions at the time of testing, as indicated in the BPT results. Both emulsions showed high flushing and rutting during the polishing process, especially in the wheel path. Furthermore, in the TWPD polishing process depicted in Figure

7.11, the slabs experienced significant aggregate and binder loss, leading to the appearance of the substrate after 30k cycles, which in turn resulted in a drop in COF.

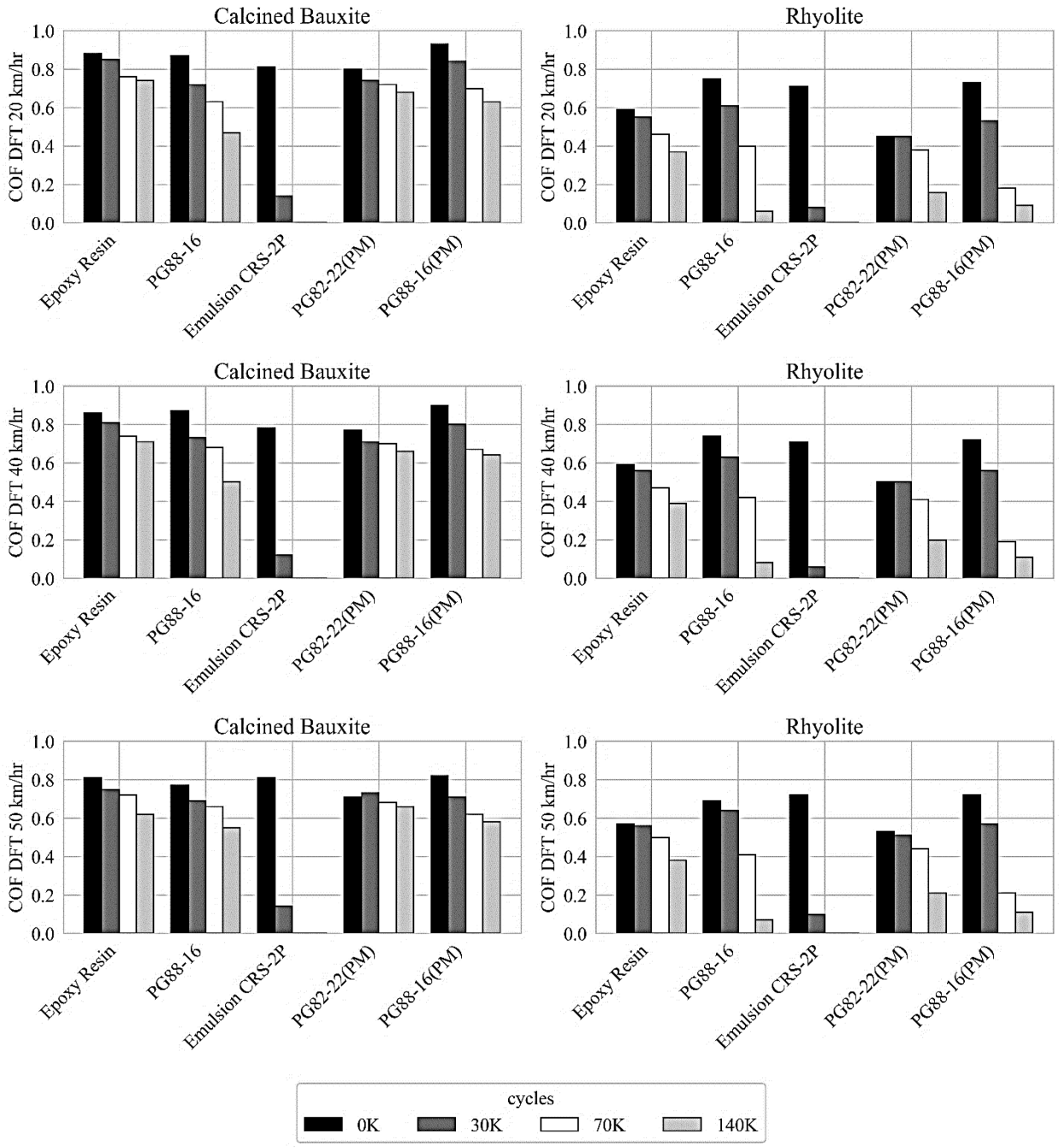

Figure 7.10 Coefficient of Friction values using DFT at 20, 40, and 50 km/hr for HFST size

After 30K polishing cycles on Calcined Bauxite, PG88-16 (PM) demonstrated comparable results to epoxy resin for COF at 20, 40, and 50 Km/hr. However, as the cycles increased to 70K and 140K, PG82-22 (PM) exhibited better performance compared to epoxy resin and other binders.

Figure 7.11 Severe bleeding and rutting in Emulsion CRS-2P slab after 30K polishing

For Rhyolite, after 30K polishing cycles, PG88-16 demonstrated results comparable to and sometimes better than epoxy resin. However, as the cycles increased to 70K and 140K, the COF dropped, with epoxy resin showing better performance at 140K cycles for the HFST size. In Figure 7.12, the COF values at 20, 40, and 50 km/hr for both aggregates of medium size are displayed for various binders across different polishing cycles. For Calcined Bauxite, after 30K polishing cycles, epoxy resin exhibited a higher COF at 20, 40, and 50 km/hr compared to other binders. Among PG binders, PG88-16 (PM) showed improved performance after 30K polishing cycles, but after 70K cycles, PG82-22 (PM) demonstrated the highest COF values. After 140K polishing cycles, epoxy exhibited the best performance overall, followed by PG88-16 (PM).

The tested slab with Rhyolite and PG82-22 (PM) exhibited superior performance compared to epoxy resin, especially at initial and after 30K polishing cycles. However, as the cycles increased to 70k and 140K, epoxy resin again showed better performance. This difference in performance can be attributed to the aggregate loss that occurred during the polishing process with PG and Modified binders. CRS-2P showed a similar trend after 30K polishing cycles, with severe bleeding and aggregate loss occurring on the slabs with this binder. It is evident that increasing aggregate size from HFST to medium results in a smaller drop in COF with increasing polishing cycles. This can be attributed to the effect of gradation on the performance of PG and modified binders.

In Figure 7.13, the COF values at 20, 40, and 50 km/hr for both aggregates of coarse size are presented with various binders across different polishing cycles. Before polishing, all the binders showed comparable COF and, in some cases, revealed higher COF for Modified binders and PG binders. However, after polishing, the COF values of coarse aggregates differed from those of HFST and medium sizes. The COF of the slabs made with modified binders and PG binders showed comparable COF to those made with epoxy. For Calcined Bauxite, PG88-16 (PM) exhibited the highest COF at 20, 40, and 50 km/hr after 30K polishing cycles. Increasing the cycles to 140K, PG88-16 continued to show higher COF and better performance. This trend suggests that increasing the aggregate size of Calcined Bauxite enhanced the friction performance of PG and modified binders. For Rhyolite, the results were similar, with PG88-16 showing slightly better performance.

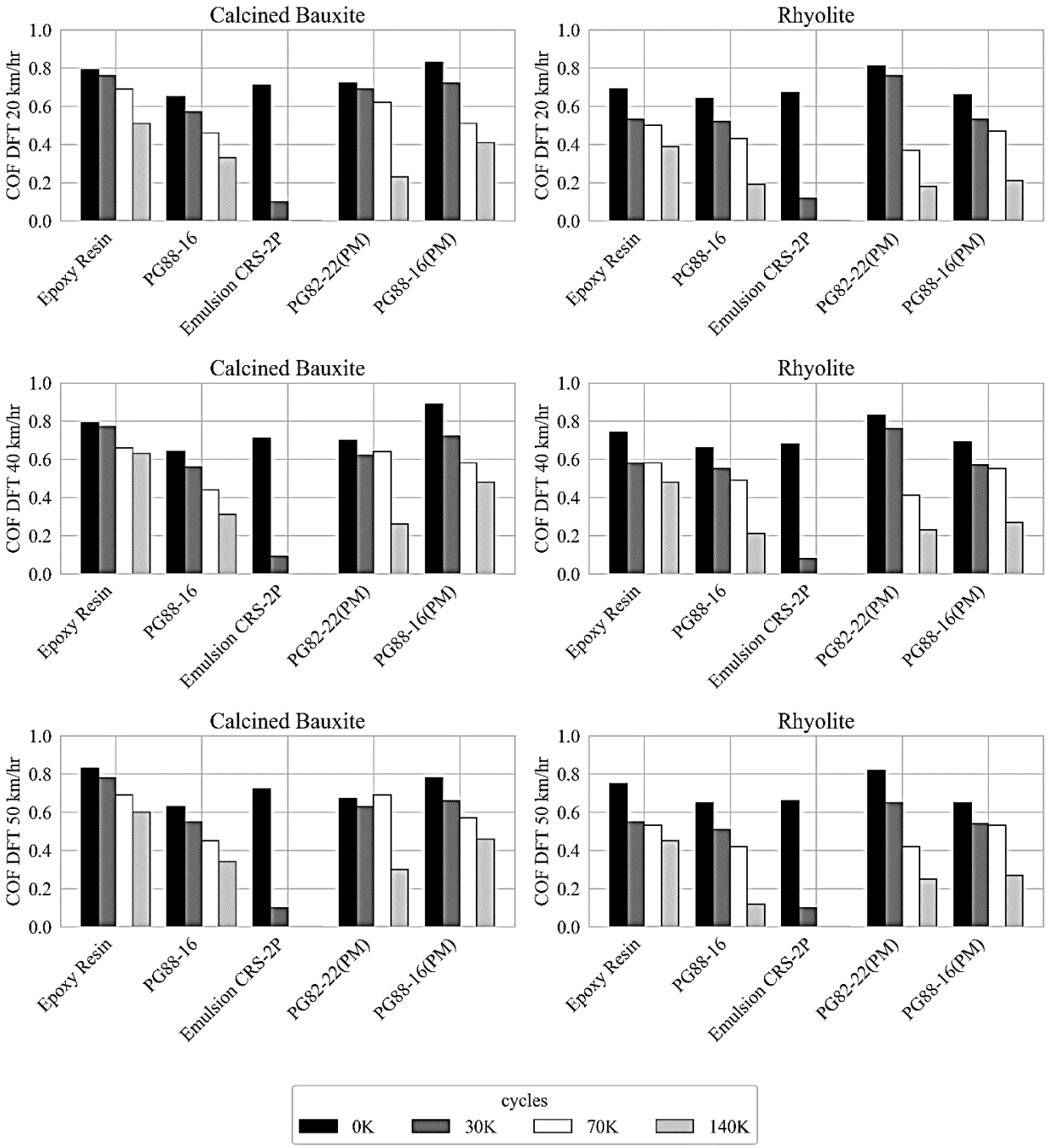

Figure 7.12 Coefficient of friction values using DFT at 20, 40, and 50 km/hr for medium-sized aggregate

CRS-2P again showed high rutting and bleeding during the 30k polishing cycles, as depicted in Figure 7.14. Figure 7.15 shows severe bleeding and rutting in the emulsion CRS-2P slab with new gradation after 30K polishing cycles.

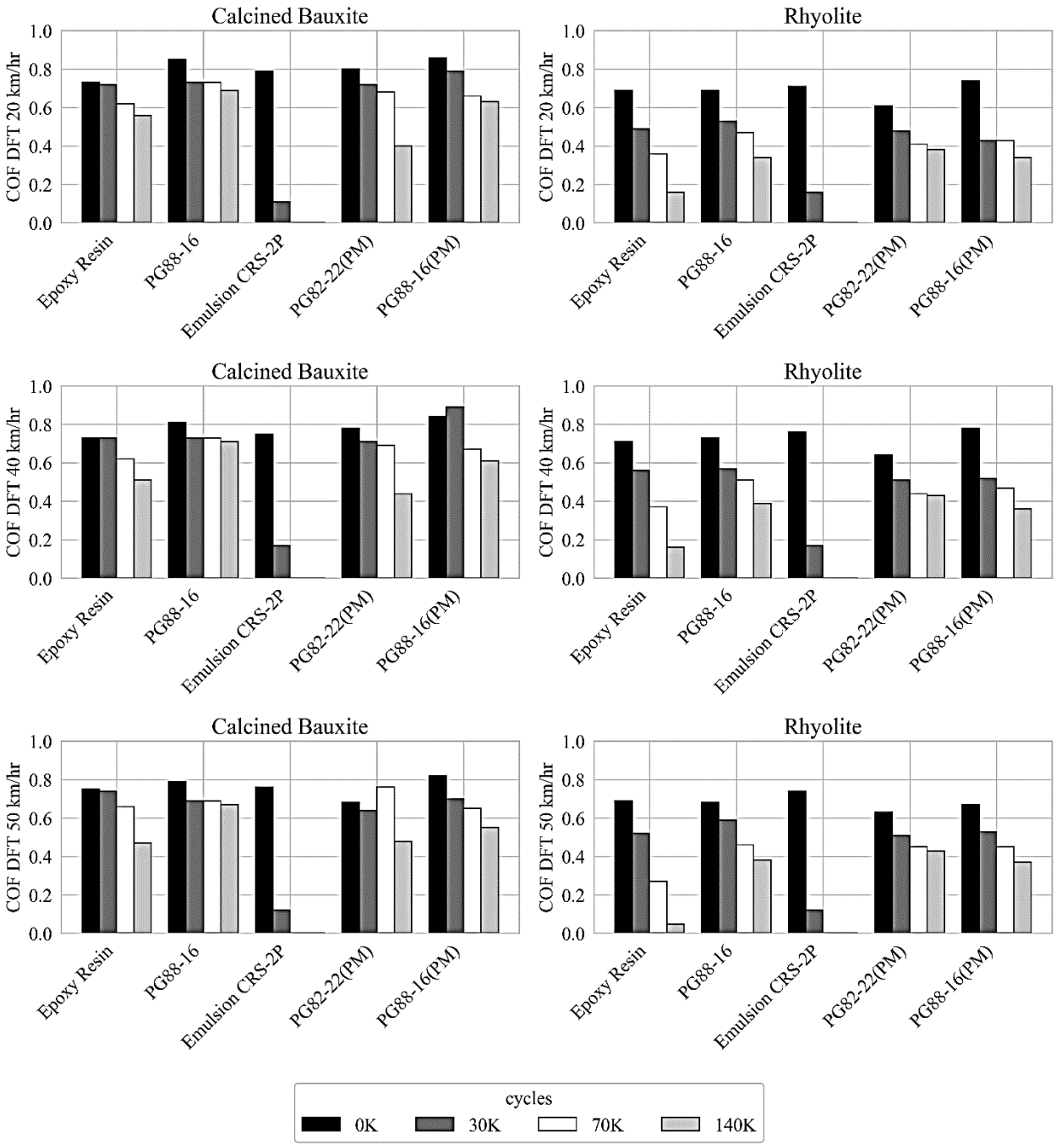

Figure 7.13 Coefficient of Friction values using DFT at 20, 40, and 50 km/hr for coarse-sized aggregate

Figure 7.14 Severe bleeding and rutting in emulsion CRS-2P slab after 30K polishing cycles

To assess the impacts of emulsion rate and aggregate gradation, a mix comprised of 50% coarse and 50% medium-sized aggregate was utilized. However, after several cycles of polishing, severe bleeding, aggregate loss, and rutting were observed in the slabs due to low stiffness at the time of testing. This issue was attributed to the emulsion sticking to the TWPD Device tires and peeling off the slabs. Figure 7.15 shows a slab with a 50% mix of coarse-sized and 50% medium-sized aggregate, showcasing these concerns.

Figure 7.15 Severe bleeding and rutting in emulsion CRS-2P slab with new gradation after 30K polishing cycles

7.3.2 Circular Track Meter Results

The surface macrotexture of the test specimen was measured using a Circular Track Meter (CTM) with a charge-coupled laser, which provided a vertical resolution of 3 mm (0.126 inches). The Mean Profile Depth (MPD) was the primary parameter of interest. Figure 7.16 displays the MPD measurements for various slab combinations using both Calcined Bauxite and Rhyolite aggregates in three different sizes across multiple polishing cycles. The results for Calcined Bauxite, of different sizes, with epoxy binder exhibited slight changes in MPD values during each cycle. Notably, the MPD increased and then decreased for the HFST size upon increasing

the cycles to 30K, while for medium and coarse aggregate sizes, the MPD slightly decreased with increasing cycles.

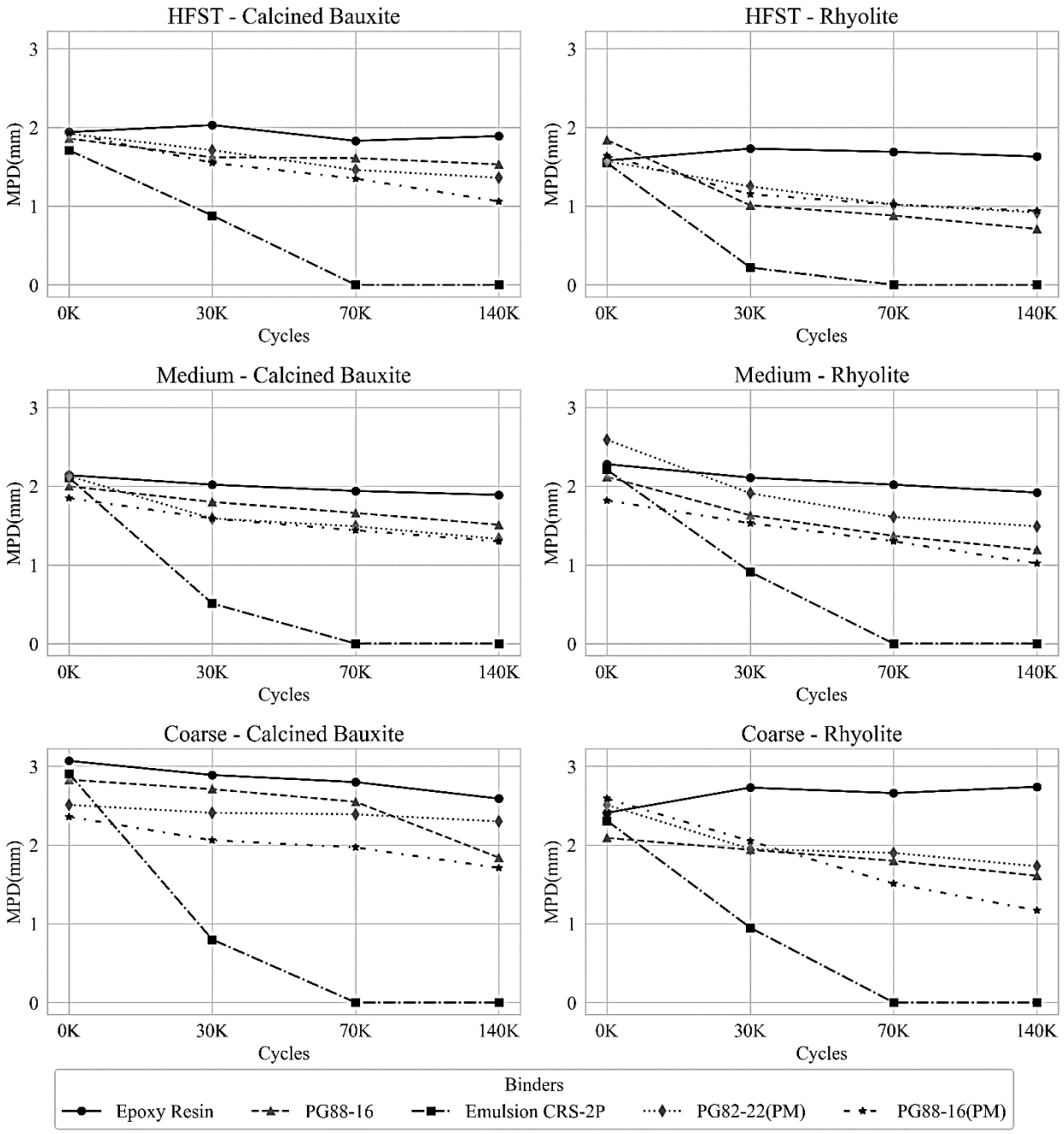

Figure 7.16 MPD values for various slab combinations

Similar trends were observed for Rhyolite, with the coarse aggregate size showing a slight increase and then decrease. These trends were attributed to the stiffness of the epoxy, indicating that as the cycles increased, only the texture of the aggregate changed, and after reaching the terminal polishing, it became stable. For the other binders, both aggregates of HFST size showed

comparable values to each other, with PG82-22 (PM) exhibiting slightly higher MPD. For the medium aggregate size, Calcined Bauxite with PG88-16 had the second highest MPD, after epoxy resin, and For Rhyolite, PG82-22 (PM) demonstrated better performance compared to other binders after epoxy resin. For the coarse aggregate size, Calcined Bauxite with PG88-16 exhibited the second highest MPD, following epoxy resin, up to 70K cycles. After this cycle, PG82-22 (PM) showed better results. For Rhyolite, PG82-22 (PM) displayed higher MPD, following epoxy resin.

7.3.3 Estimated Skid Number and International Friction Index

Figure 7.17 presents the skid number estimation at 40 mph, assessed using a skid trailer with ribbed tires (SN40R) and calculated using the equation provided in Appendix D. This estimation was derived from COF values measured by DFT at 40 km/hr (DFT40) and is pertinent for High Friction Surface Treatment (HFST) applications.

The initial SN40R values based on DFT40, for all combinations of binders and aggregates of different sizes, were above 45, except for Rhyolite of HFST size with epoxy, which showed SN40R of 41 compared to Calcined Bauxite. The results indicated that Calcined Bauxite (CB) with epoxy had the highest terminal SN40R value for HFST and medium-sized aggregate at 51 and 44, respectively. However, for the coarse-sized aggregate, Calcined Bauxite, PG88-16 exhibited the highest value of 51. Rhyolite showed a similar trend for HFST and medium aggregate sizes, but for the coarse size, the highest terminal SN40R value resulted from the modified PG82-22 (PM) and was 25.

In accordance with ASTM E1960, the COF values recorded by the DFT at 20 km/hr (DFT20) and Mean Profile Depth (MPD) measurements were employed to calculate the International Friction Index (IFI) values as outlined in the equation provided in appendix D. The IFI was established during the Permanent International Association of Road Congresses (PIARC) International Experiment to compare and harmonize texture and skid resistance measurements. This index facilitates the standardization of friction measurements across various types of equipment to a unified calibrated index.

Figure 7.18 displays the IFI values for various aggregates across different sizes and polishing cycles. Notably, the initial IFI values for all binders showed comparable results. Specifically, for Calcined Bauxite in the HFST and medium aggregate sizes, PG88-16 (PM) recorded the highest initial IFI, and for the coarse aggregate size, PG88-16 achieved the highest initial IFI. For Rhyolite, the highest initial IFI for the HFST aggregate size was attributed to PG88-16, whereas PG82-22 (PM) led for the medium aggregate size, and PG88-16 (PM) ranked highest for the coarse aggregate size.

At the terminal phase, epoxy resin showcased the highest IFI values for both HFST and medium aggregate sizes across Calcined Bauxite and Rhyolite. For the coarse aggregate size, PG88-16 attained the highest terminal IFI with Calcined Bauxite, while modified PG82-22 (PM) achieved the highest terminal IFI with Rhyolite. This suggests that exploring alternatives to epoxy resin for HFST applications with coarser aggregate sizes is possible and could improve frictional performance after prolonged polishing cycles.

Based on the Skid Number (SN) obtained using a skid trailer with smooth tires and the International Friction Index (IFI) calculated following ASTM E 1960, the modified SN (50) values can be calculated (Masad et al, 2011). The detailed calculation process and the formula used for this calculation are presented in the Appendix D.

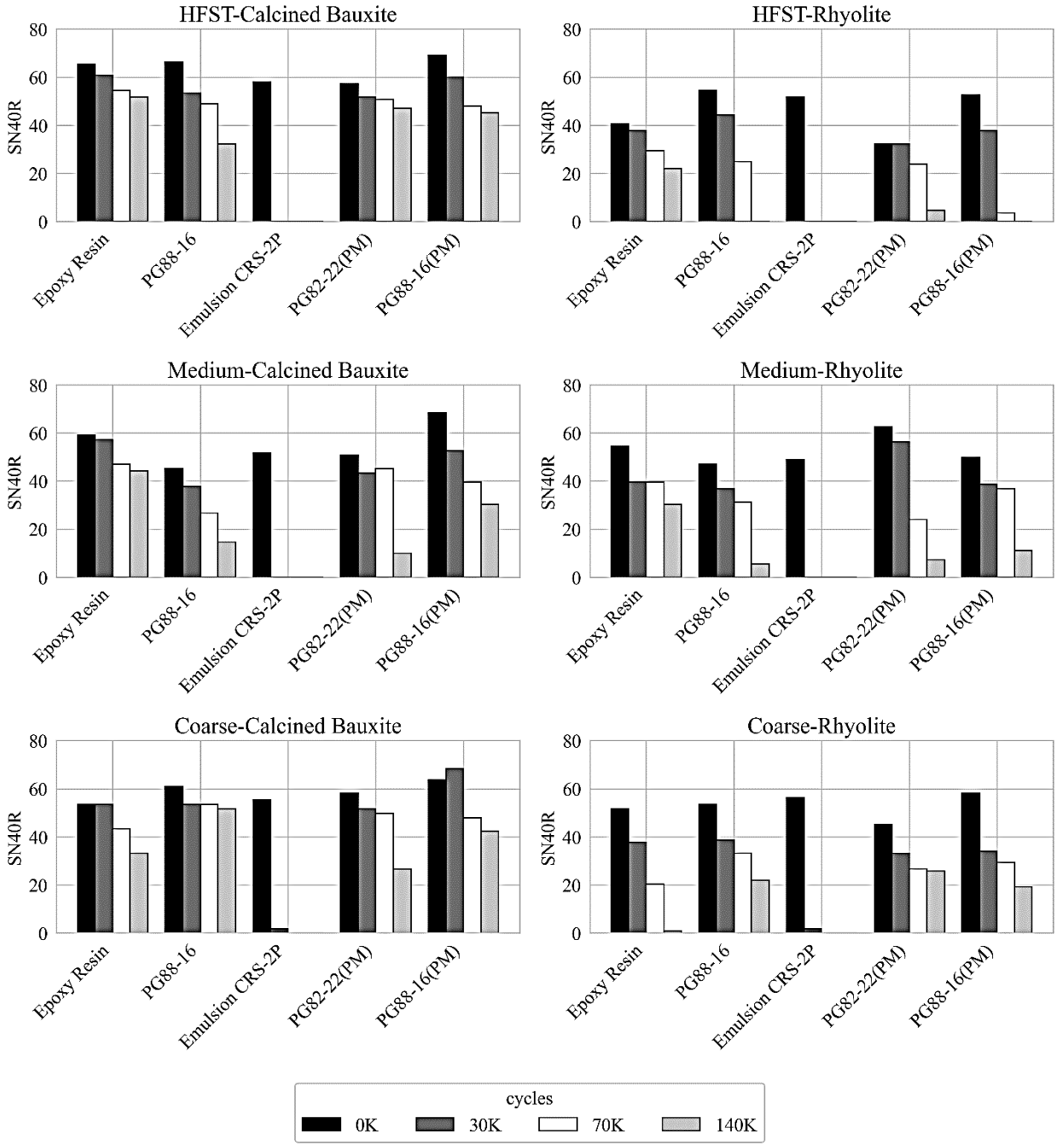

Figure 7.17 SN40R values for HFST applications with different binders

SN (50) represents the Skid Number measured at 50 miles per hour (mi/hr) by a skid trailer with smooth tires. Figure 7.19 illustrates the SN (50) values calculated based on the IFI, Dynamic Friction Tester (DFT), and Circular Track Meter (CTM) results.

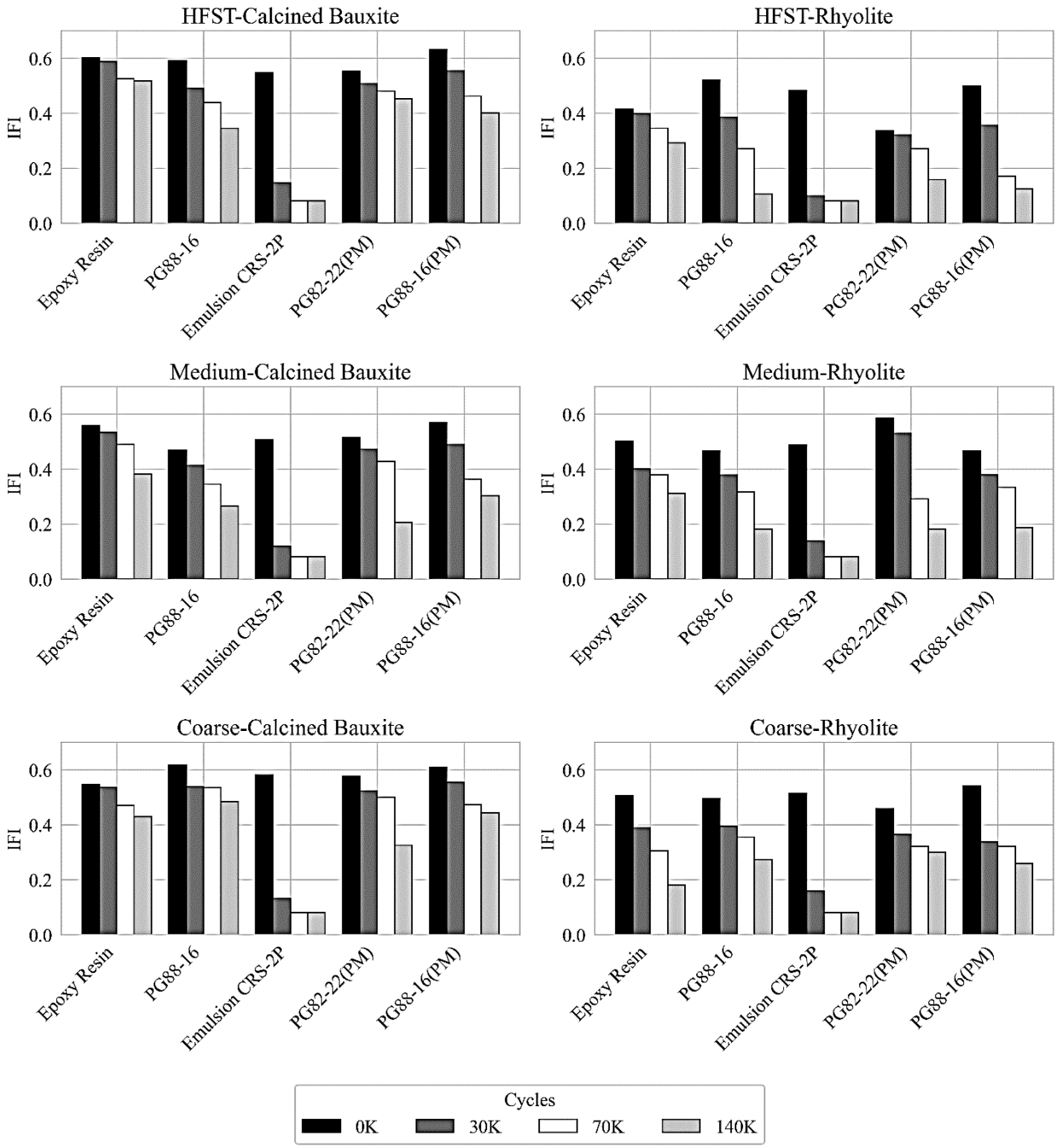

Figure 7.18 IFI values for HFST applications with different binders

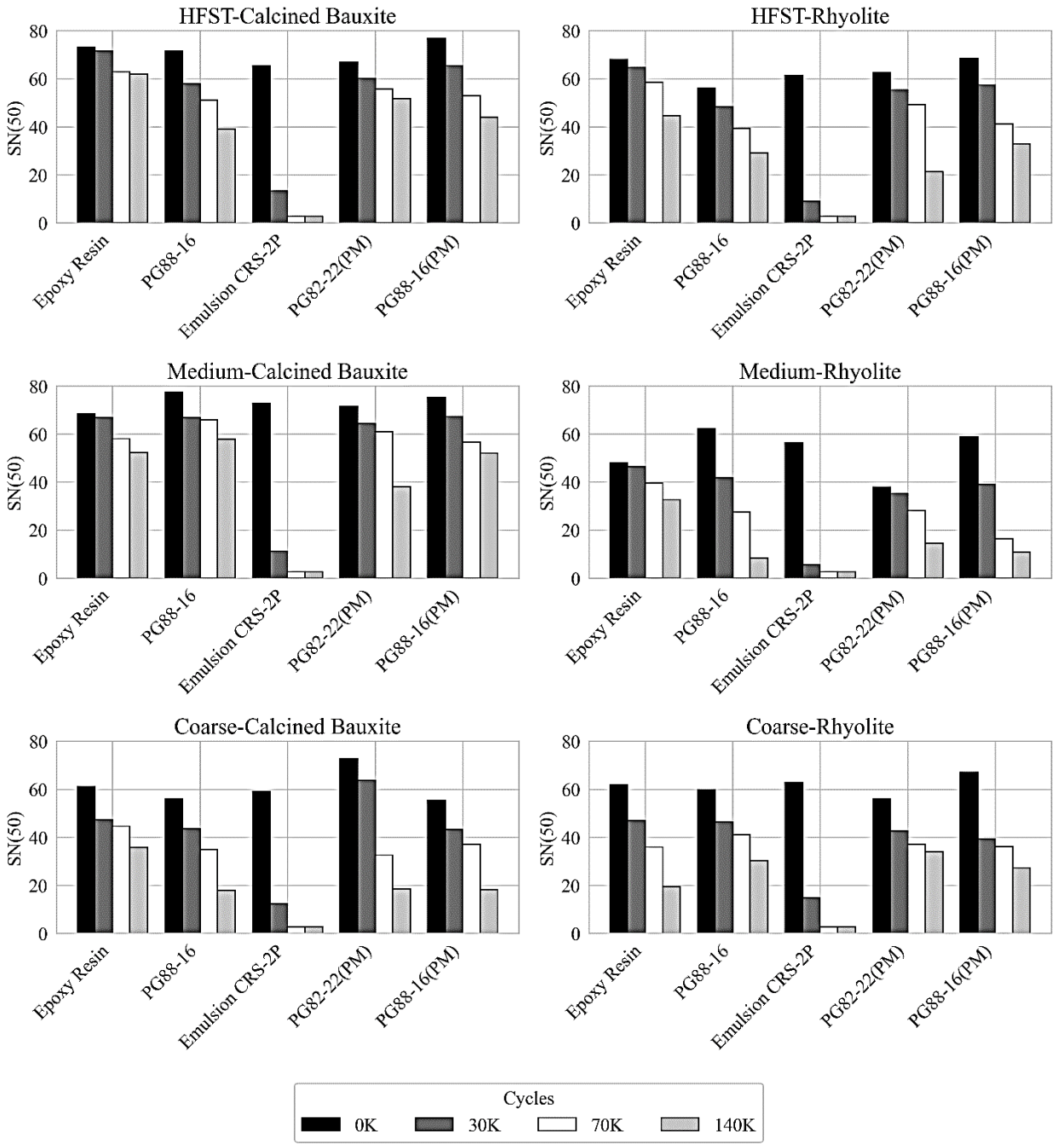

Figure 7.19 SN (50) values for HFST applications with different binders

The results indicate that the initial SN (50) values for binder-aggregates combinations did not show varying outcomes. For the HFST aggregate size, PG88-16 (PM) exhibited the highest value with both Calcined Bauxite and Rhyolite aggregates. For the medium aggregate size, PG88-16 performed well, and for coarse aggregate size, PG82-22 (PM) showed favorable results. However, the terminal values after 140,000 polishing cycles revealed different trends. Epoxy resin generally showed the highest value, except for the CB medium aggregate size where PG88-

16 performed better, and for Rhyolite coarse size where PG82-22 (PM) showed superior performance.

It should be noted that the estimated initial SN (50) values were relatively higher compared to the SN40R, which was the opposite of what was expected. Therefore, these formulas should be calibrated with High Friction Surface Treatment (HFST) aggregates before being used to estimate SN (50) (Deef-Allah and Abdelrahman 2021).

7.3.4 Relationship between Aggregate Image Measurement System and British Pendulum Test Results

Figures 7.20 and 7.21 present a comparison between the average Aggregate Image Measurement System (AIMS) Texture (TX) and Gradient Angularity (GA) indices for aggregate sizes of 3/8″ - 1/4″ and 1/4″ - #4 with the average British Pendulum Number (BPN) values across different aggregate sizes. The average pre-polish BPN values were compared with the average AIMS TX and GA indices before Micro-Deval polishing (BMD), while the average post-polish BPN values were contrasted with the average AIMS TX and GA indices after 240 minutes of Micro-Deval polishing time (AMD 240).

In Figure 7.20 there is no specific relationship observed in the average texture and average BPN results before and after polishing. This trend reflects fluctuations in results among different aggregates. Meramec exhibited the lowest BPN and texture before polishing, while Calcined Bauxite displayed the highest BPN and second-highest texture before and after polishing.

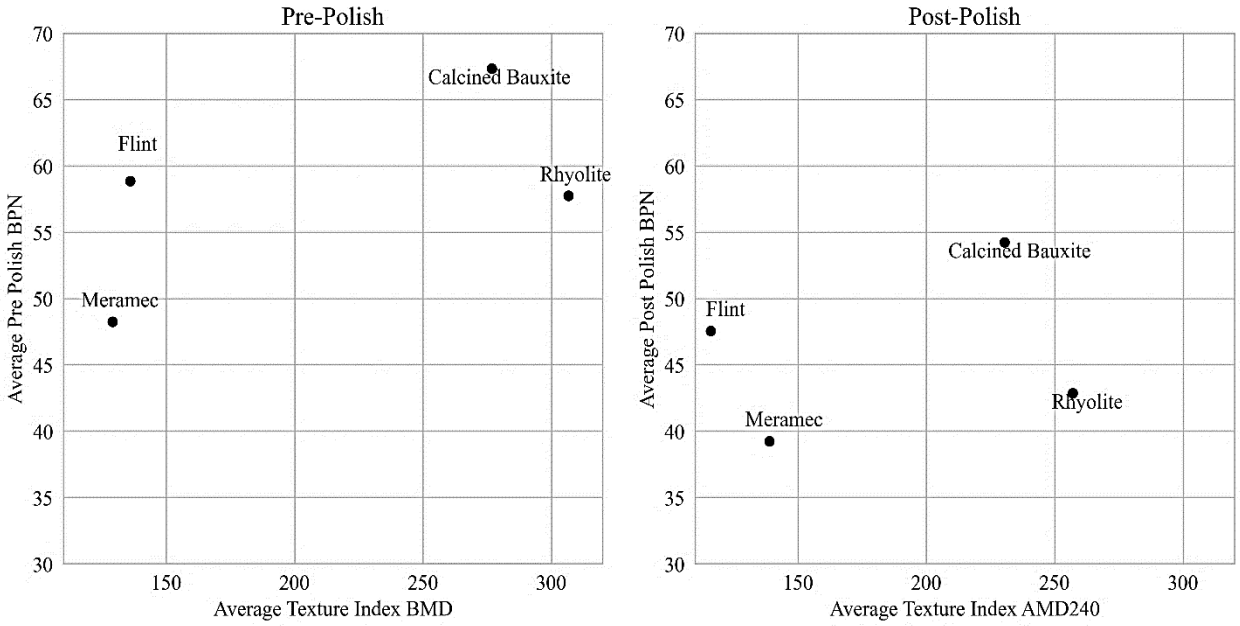

Figure 7.20 Relationship between Average Texture Index and BPN Pre and Post polishing

In Figure 7.21, there is no specific relationship between the angularity index and BPN before and after polishing. It can be observed that Meramec once again displayed the lowest BPN, while

Calcined Bauxite had the highest BPN. Rhyolite and Flint showed comparable results both before and after polishing.

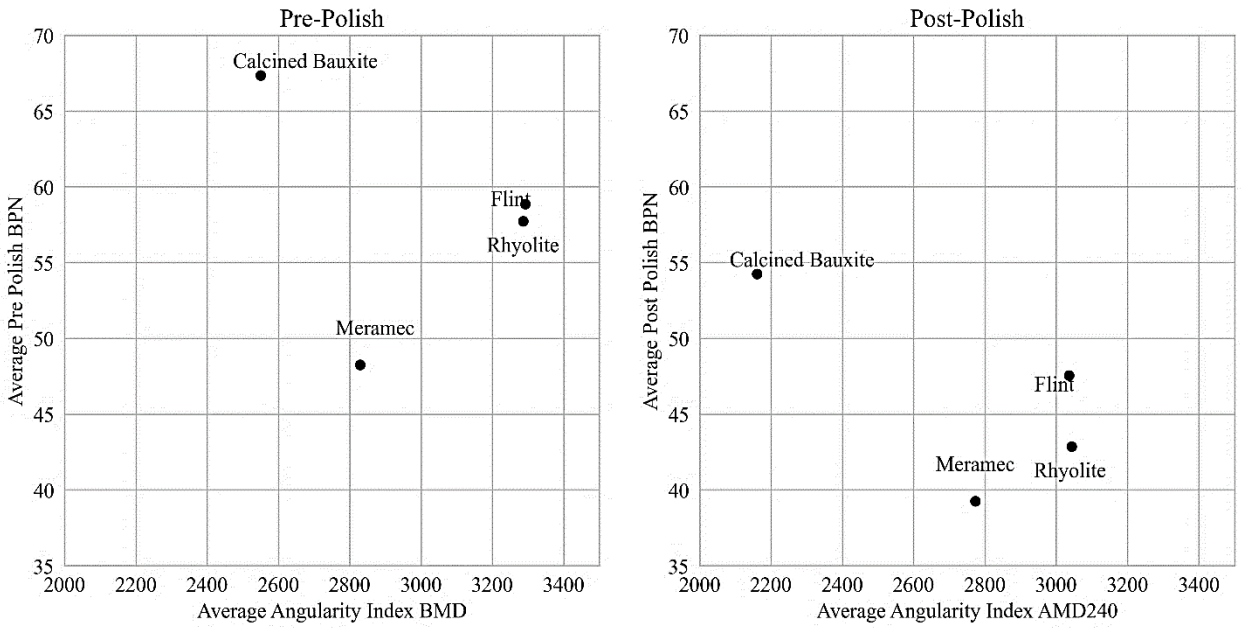

Figure 7.21 Relationship between Average Angularity Index and BPN Pre and Post polishing

7.3.5 Comparing British Pendulum Test and Dynamic Friction Test Results

In Figure 7.22, the relationship between average BPN values and COF for DFT at 40 km/hr before and after polishing for various binders and aggregates was depicted. There is no specific relationship observed between data points. However, after polishing and at 140K cycles, regardless of emulsion CRS-2P, which caused data fluctuation, both aggregates showed similar trends. Specifically, the epoxy binder resulted in the highest DFT40 and BPN after polishing for both aggregates. Before polishing for Calcined Bauxite and Rhyolite, PG88-16 (PM) exhibited the highest DFT40 value. In Table 7-1, the rankings of binders based on British Pendulum Number (BPN) and Coefficient of Friction (COF) values measured by DFT at 40 km/hr (DFT40) are presented. The binders are ranked from 1 to 5 based on their average BPN values and average DFT40 values, with binders having the highest average BPN or DFT40 values receiving a ranking of 1.

Table 7-1 Binders ranking based on British Pendulum Number (BPN) and Coefficient of Friction (COF) values measured by DFT at 40 km/hr (DFT40)

Binder Type	Ranking							
	DFT40 (0K)	DFT40 (0K)	DFT40 (140K)	DFT40 (140K)	BPN PrePolish	BPN PrePolish	BPN PostPolish	BPN PostPolish

	CB	Rhyolite	CB	Rhyolite	CB	Rhyolite	CB	Rhyolite
Epoxy Resin	2	4	1	1	1	1	1	1
PG88-16	3	3	3	4	5	5	2	2
Emulsion CRS-2P	5	2	5	5	4	3	5	3
PG82-22 (PM)	4	5	4	2	2	2	3	5
PG88-16 (PM)	1	1	2	3	3	4	4	4

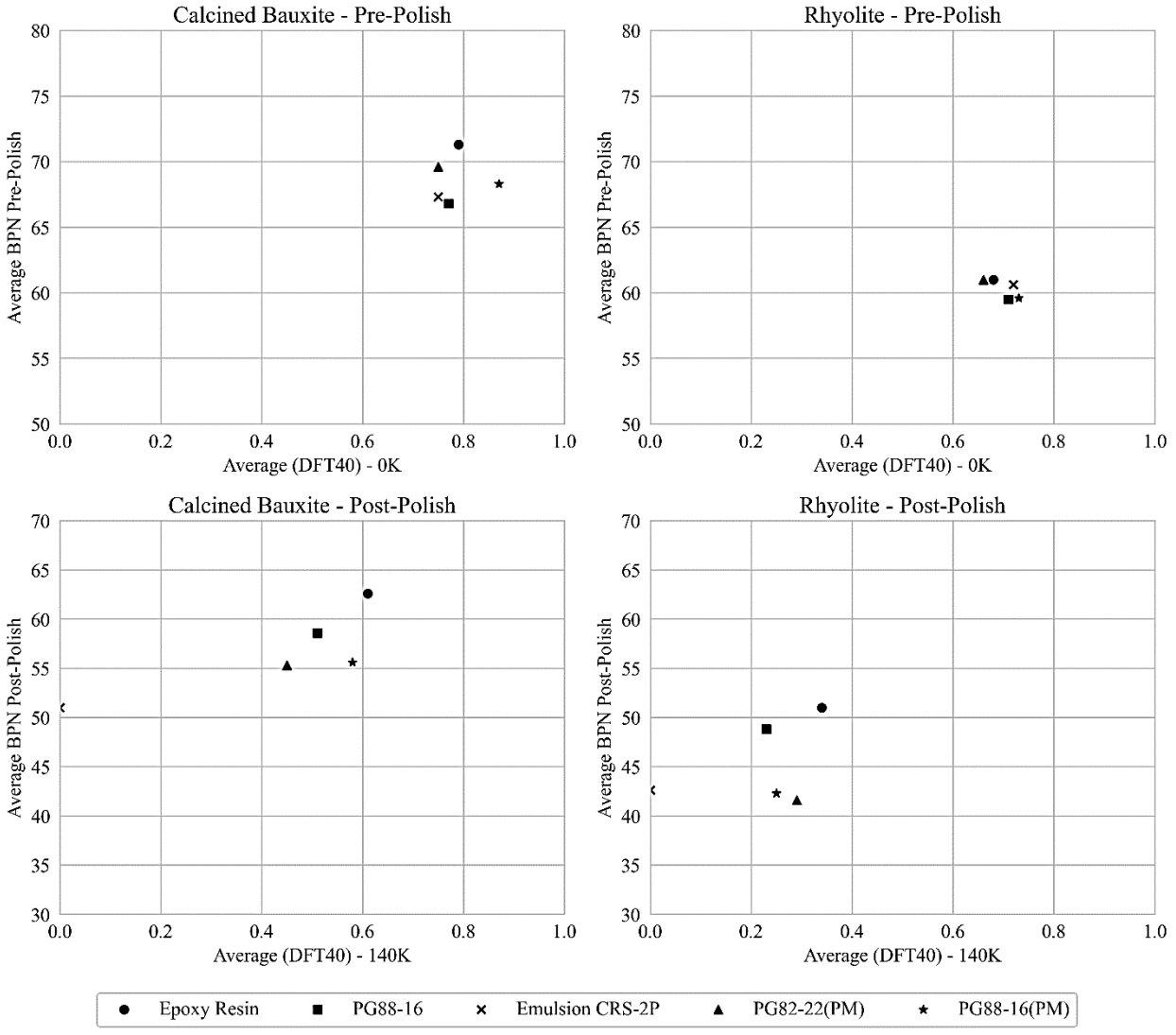

Figure 7.22 Relationship between Average BPN and DFT40 pre and post polishing

The overall binder ranking based on DFT40 and BPN before and after polishing for both aggregates indicates that epoxy resin exhibited the best friction performance, followed by PG88-16 (PM). PG82-22 (PM) and PG88-16 showed comparable performance, while emulsion CRS-2P exhibited the lowest performance.

7.3.6 Comparing between Dynamic Friction Test (DFT20) and CTM(MPD) Results

Figure 7.23 depicts the relationship between Coefficient of Friction (COF) values measured by DFT at 20 km/hr (DFT20) and Mean Profile Depth (MPD) values from Circular Track Meter (CTM) tests for both Calcine Bauxite and Rhyolite aggregate sources. The plot includes data for different binders with Calcined Bauxite and Rhyolite, of HFST aggregate size, across various polishing cycles. Fitted lines and R^2 values are displayed to illustrate the relationships more clearly.

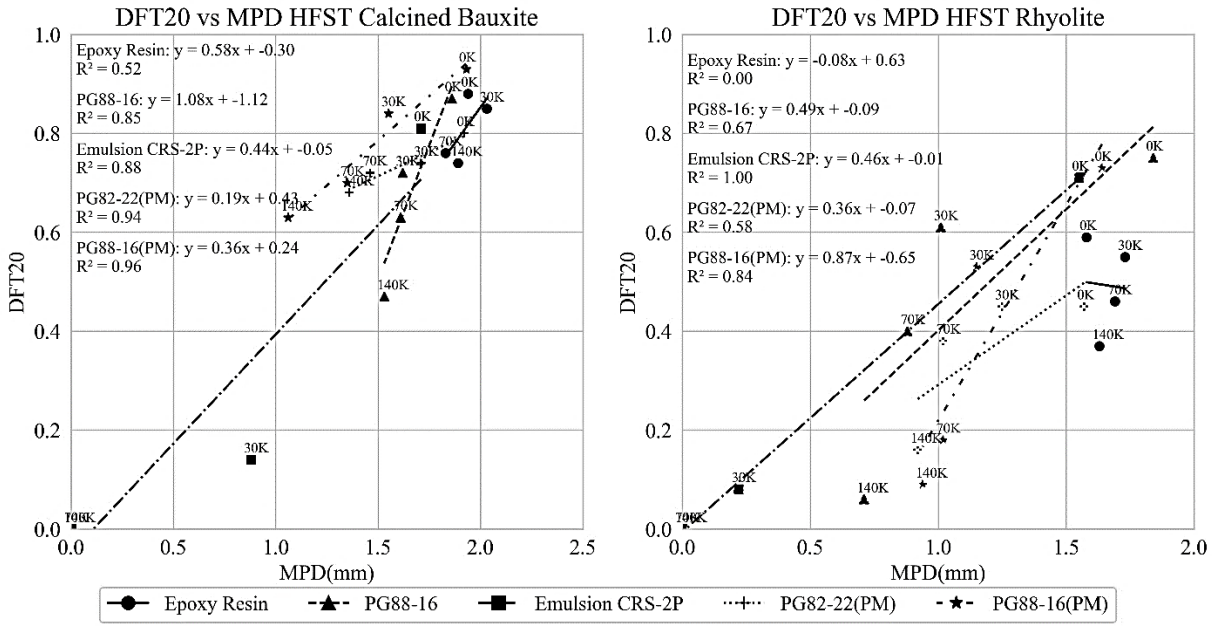

Figure 7.23 Relationship between DFT20 and MPD HFST size

In Calcined Bauxite, PG88-16 has the steeper fitted line. This indicates higher variability in DFT20 and MPD across different polishing cycles. The epoxy binder has a less steep relationship. PG82-22 (PM) has a less steep slope for both aggregates, indicating lower variability. In the case of Rhyolite, the steepest line slope is linked to PG88-16 (PM). The negative slope for epoxy resin resulted from inconsistency in the polishing cycle up to 30K cycles, leading to an increase in MPD and a decrease in DFT, which is reflected by a decreasing relationship between MPD and DFT20. Figure 7.24 depicts the relationship between DFT20 and MPD for medium aggregate size. For the medium-sized aggregate of Calcined Bauxite, the higher slope of PG82-22 (PM) indicates greater variability between the data points and DFT20 and MPD values in this sample. This trend is followed by epoxy and PG88-16 (PM), while PG88-16 shows the lowest slope and a high R-squared value, indicating a good fit to the data regardless of CRS-2P. For Rhyolite, the steepest slope is attributed to epoxy. There is a similar trend and fit line between both Modified Binders, followed by PG88-16.

The relationship between DFT20 and MPD for coarse aggregate size in both aggregate types with different binders is shown in Figure 7.25. In Calcined Bauxite, better performance and lower variability were observed with PG88-16, PG88-16 (PM), and PG82-22 (PM) compared to epoxy. The highest R-squared value in PG88-16 (PM) was attributed to a good fit between DFT20 and MPD. In Rhyolite, better performance and lower variability were related to PG88-16 (PM) and PG82-22 (PM). A negative slope was observed for epoxy, indicating a decrease in DFT20 with increasing MPD and cycles. This trend was attributed to the high stiffness of epoxy, resulting in lower aggregate loss during polishing cycles and primarily affecting aggregate polishing, which in some cases led to changes in the angularity and texture of the aggregate, increasing the MPD.

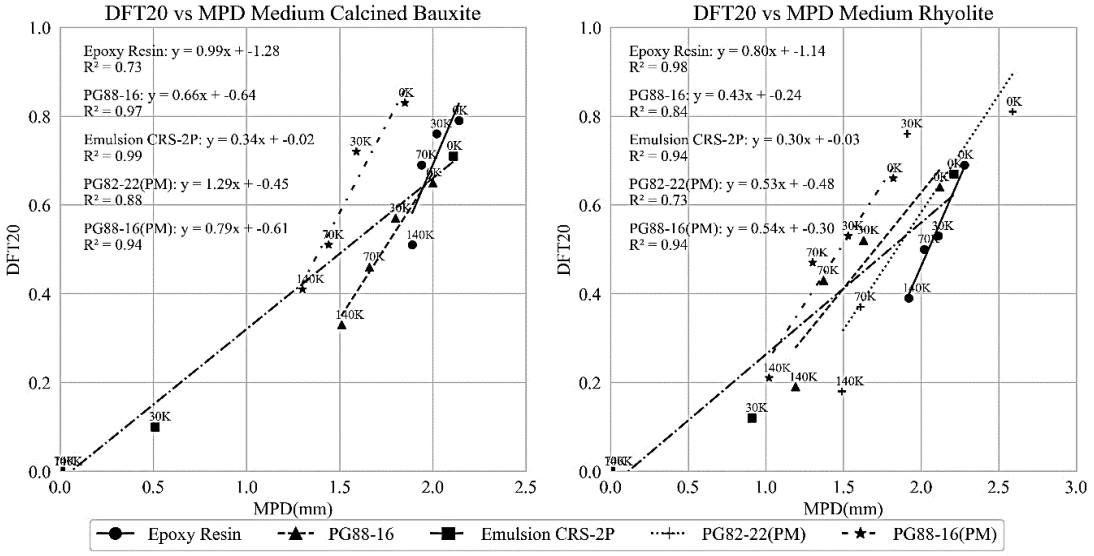

Figure 7.24 Relationship between DFT20 and MPD medium size

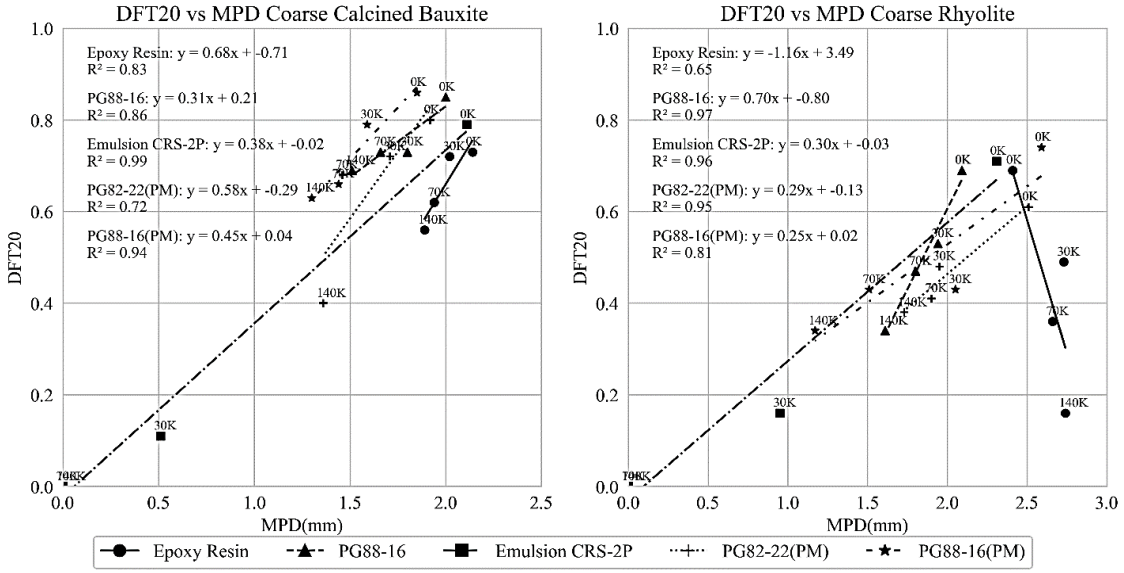

Figure 7.25 Relationship between DFT20 and MPD coarse aggregate size

7.4 Summary

The impact of binders and aggregate sizes on BPN varied. Initially, PG binders for HFST aggregate size matched the epoxy binder's BPN values. However, PG94-10 declined more after polishing. Blended PG binders show PG88-16 might outperform PG82-16 due to stiffness differences affecting post-polishing BPN. For the HFST size, both emulsions showed lower BPN values, likely due to bleeding and rutting. Modified binders showed different results with aggregate types. For instance, with Calcined Bauxite, Meramec, and Flint, PG82-22 (PM) achieved higher BPN values after polishing. However, with Rhyolite, PG88-16 (PM) resulted in higher BPN values. Medium size aggregates showed a milder decrease in BPN, particularly for emulsions, indicating better performance with coarser aggregates. Epoxy exhibited the least BPN loss, followed by the PG88-16 and modified binders. The coarse aggregate size exhibited better resistance to deformation and performed well with emulsions. The percentage decrease in average BPN values after polishing is shown for different combinations. In Calcined Bauxite, epoxy resin exhibited the lowest decrease at 12%, while emulsion CRS-2P showed the highest decrease at 22%. For Rhyolite, epoxy showed the lowest decrease at 16%, whereas PG82-22 (PM) had the highest decrease at 31%. For Meramec and Flint, epoxy resin showed the lowest decrease, while CRS-2PSC had the highest decrease in BPN values.

The COF values, which were assessed using the DFT at different speeds, across multiple polishing cycles for two aggregates of three different sizes. For HFST-sized aggregate, before polishing, slabs had comparable COF values across all binders, with Calcined Bauxite showing higher COF than Rhyolite. After 30K polishing cycles, PG88-16 (PM) matched epoxy resin's performance, but at 70K and 140K cycles, PG82-22 (PM) performed better. For Rhyolite, after 30K polishing cycles, PG88-16 demonstrated results comparable to and sometimes better than epoxy resin. However, as the cycles increased to 70K and 140K, the COF dropped. For medium-sized Calcined Bauxite, epoxy resin had higher COF at 20, 40, and 50 km/hr after 30K polishing cycles. PG88-16 (PM) improved after 30K cycles but showed higher COF at 70K cycles, while PG82-22 (PM) had higher COF at 140K cycles. Epoxy performed best at 140K cycles, followed by PG88-16 (PM). For Rhyolite, PG82-22 (PM) initially outperformed epoxy, but epoxy performed better at 70K and 140K cycles. This difference is attributed to aggregate loss during polishing with PG and Modified binder. For coarse aggregate size, initially, all binders had comparable COF, with Modified and PG binders sometimes showing higher values. After polishing, COF varied notably across binder types and aggregate sources. Modified and PG binders approached epoxy's COF levels. In Calcined Bauxite, PG88-16 (PM) had the highest COF at 20, 40, and 50 km/hr after 30K cycles, maintaining superiority at 140K cycles. This suggests a size-related improvement in friction for PG and modified binders.

The decrease in MPD percentage from HFST to coarse aggregate size for modified binders indicates improved performance with larger aggregates as the polishing cycle increases. The comparison of DFT40 and BPN values before and after polishing for both aggregates shows that epoxy resin performed the best, followed by PG88-16 (PM). PG82-22 (PM) and PG88-16 showed similar performances, whereas emulsion CRS-2P had the lowest performance.

CHAPTER 8: ECONOMIC STUDY

8.1 Introduction

This chapter presents the development and applications of Life Cycle Cost Analysis (LCCA) to assess the economic effectiveness, both in the short and long term, among competing HFST asphalt-aggregate combinations, as developed in this research. In this regard, the developed LCCA application considers the initial costs as well as discounted future expenses accrued by the agency throughout the lifespan of the proposed alternatives. The LCCA approach utilized in this study aimed to accurately estimate the service life of High Friction Surface Treatments (HFST) and alternative aggregates and binders, enabling precise analyses. Skid number analysis software designed for asphalt pavement, primarily focused on Hot Mix Asphalt (HMA) and seal coat surfaces, was adapted for this research (Chowdhury et al., 2016). The estimated service life of HFST, alternative aggregates, and binders was compared to existing records from MoDOT to ensure accuracy and consistency. The estimation of Skid Number (SN) relied on factors such as aggregate type, gradation, polishing cycles, and traffic levels. Additionally, other prediction models were employed to establish correlations between SN and results from the Dynamic Friction Tester (DFT), Circular Track Meter (CTM) or British Pendulum (BP). The research team developed simplified procedures using an Excel application based on the performance modeling of HFST, intended for use by MoDOT to assess alternative aggregates and binders. Net Present Values (NPVs) were calculated for HFST applications, aiding in the selection of the most optimal HFST application based on these values. The primary goal of this LCC program was to provide a rational method for translating diverse input data (including material and project specifics) into comparable output data (NPV), facilitating effective comparisons between different alternatives.

8.2 Calculation Process of LCCA

The researchers developed a straightforward Life Cycle Cost (LCC) program using Excel to perform Life Cycle Cost Analysis (LCCA) for High Friction Surface Treatment (HFST) applications, utilizing data from British Pendulum (BP), Dynamic Friction Tester (DFT) and Circular Track Meter (CTM) results. The LCC Analysis Calculation Process, including input data, Skid Performance Prediction Models, and output data, as well as the LCC program's interfaces based on DFT20 and CTM input data, are detailed in Appendix D. The material details and project-specific input data are illustrated in Figure D.1, and the output data is depicted in Figure D.2. This program was instrumental in predicting Net Present Values (NPVs) for HFST applications. Figure 8.1 illustrates the LCCA calculation process, with major input data categorized into material and project specifics. Performance prediction models were then used to convert these inputs into Skid Number (SN) values.

8.3 Performance Prediction

The research team attempted to use the collected friction data to calibrate existing performance models based on earlier research. Of particular interest was using the Dynamic Friction Tester

(DFT) measurements at 20 km/hr (DFT20) and Mean Profile Depth (MPD) measurements for different binders. The International Friction Index (IFI) and Skid Number (SN) predicted by this model showed a higher value than those developed by models found in the literature; indicating a more conservative prediction of the friction performance of the developed asphalt-based binders. Therefore, the previously published models were adopted in compliance with earlier research documented in the literature. The developed LCC program employed specific performance prediction models discussed in Appendix D. The first model (Equation D.1) correlated British Pendulum (BP) results with SN40R, as documented by John Jewett Henry and Wambold in 1992. These models were crucial in predicting and evaluating the skid resistance performance of HFST applications under various conditions and polishing stages.

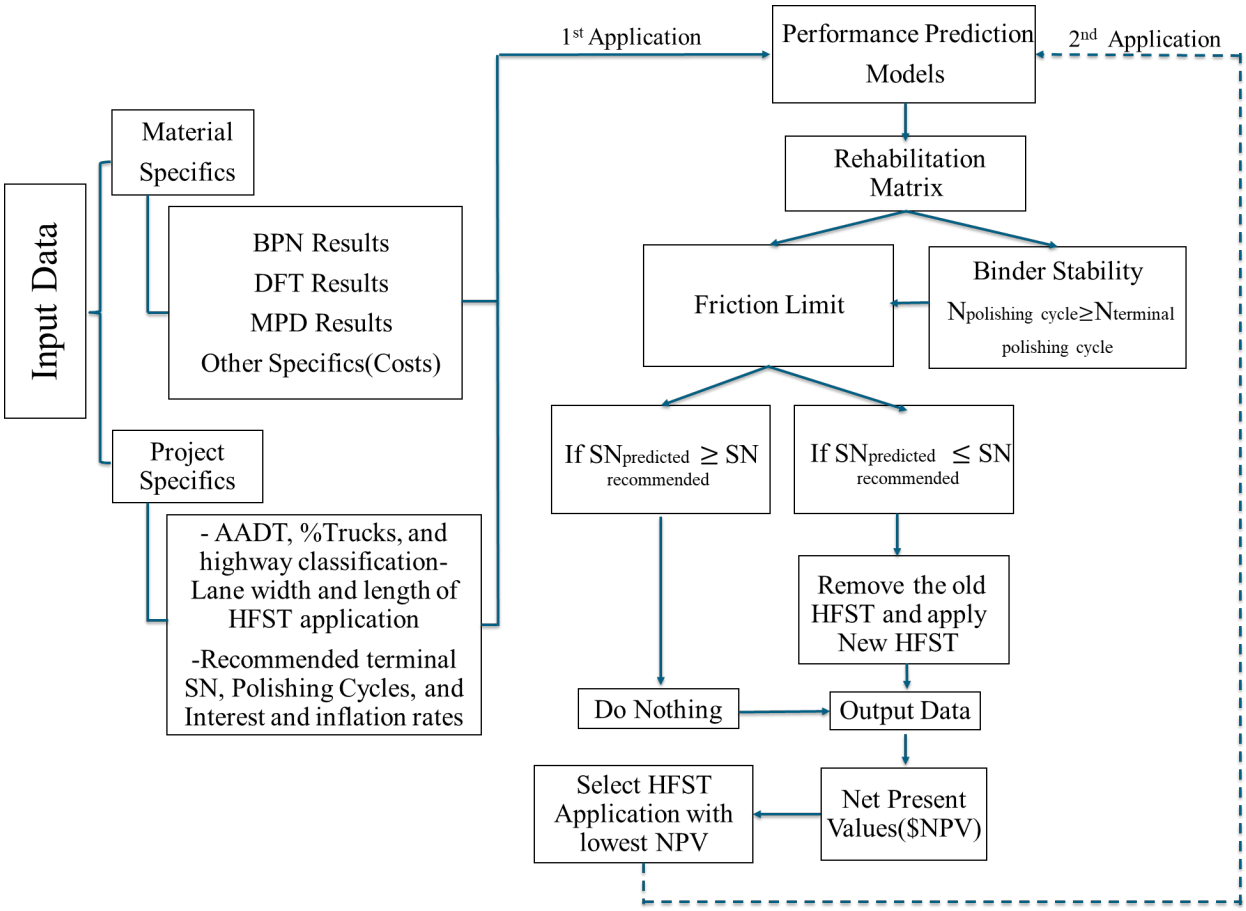

Figure 8.1 LCCA calculation process

The second model (section D.2.2) aimed to predict the Skid Number measured at 40 mi/hr by a skid trailer with Ribbed tires (SN40R) using Coefficient of Friction (COF) values measured by the Dynamic Friction Tester (DFT) at 40 km/hr (DFT40) before and after polishing. This model, presented in Equation D.2, was developed by Heitzman et al. (2015).

The third model (section D.2.3) in accordance with ASTM E1960, was used to calculate the International Friction Index (IFI) values. Based on the Skid Number (SN) obtained from using a

skid trailer with smooth tires, according to ASTM E 274, the modified SN (50) values were calculated as outlined in Appendix D and developed by Masad et al. (2011).

As discussed in Chapter 7 and depicted in appendix C, slabs with emulsion binders have shown severe damage and rutting after 30K polishing cycles in the TWPD. For the developed LCCA application, the predicted and recommended SN values were calculated after 140K polishing cycles. Therefore, for the rehabilitation matrix, the process starts with confirming if the samples reached the terminal polishing cycle (140,000 cycles) without damage. Since the samples with emulsion had not met the 140K cycles without damage, a new binder (PG binder selected for the calculation) type was considered for the emulsion samples. Table 8-1 outlined the actions for the LCCA.

Table 8-1 Rehabilitation matrix for HFST applications

What if?	Action
$N_{\text{polishing cycle}} \leq N_{\text{terminal polishing cycle(140K)}}$	Remove the old HFST and add a new one
Predicted terminal Skid Number (SN) ≥ recommended terminal SN	Do nothing
Predicted terminal SN < recommended terminal SN	Replace the old HFST application and add a new one

8.4 Life Cycle Cost Analysis (LCCA) Results

The following subsections present the economic analysis results derived from the LCC program, using input data. Subsequently, a comparative economic study was conducted based on the Net Present Value (NPV) obtained from Life Cycle Cost Analysis (LCCA) studies.

8.4.1 Net Present Value

Figure 8.2 exhibits the Net Present Values (NPVs) for the HFST applications based on the BP input data for different aggregates of HFST and medium sizes across different binders. The best choice with Calcined Bauxite was epoxy resin, which had the lowest NPV value. In contrast, for Rhyolite, Meramec, and Flint, the worst binder was epoxy resin, with the highest NPVs value. This is because the cost of Epoxy Resin is higher than other binders, leading to HFST application replacements when the aggregates reached their terminal Skid Number measured at 40 mi/hr by a skid trailer with ribbed tires (SN40R) values. Other binders showed comparable NPV values, with slightly better performance for PG88-16. There's a notable contrast between the coarse aggregate size and both HFST and medium sizes. The PG88-16 binder emerges as the optimal choice, with the lowest NPV recorded for Calcined Bauxite. Figure 8.3 displays the Net Present Values (NPVs) for HFST applications, utilizing BP input data, across various aggregates with

coarse size and different binders. Other aggregates yielded similar results with HFST and medium aggregate size.

The NPVs for the HFST applications based on DFT40 and SN40R input data are shown in Figure 8.4. The best choice for Calcined Bauxite, HFST size, was PG82-22 (PM), which had the lowest NPV value, followed by PG88-16 (PM) with comparable NPV. For Rhyolite, PG88-16 showed the lowest NPV, while the worst binder was epoxy, with the highest NPV value. As mentioned, the emulsion did not meet the terminal polishing cycle requirements, therefore, it was assumed that a PG binder would be used as a replacement after the first application of emulsion.

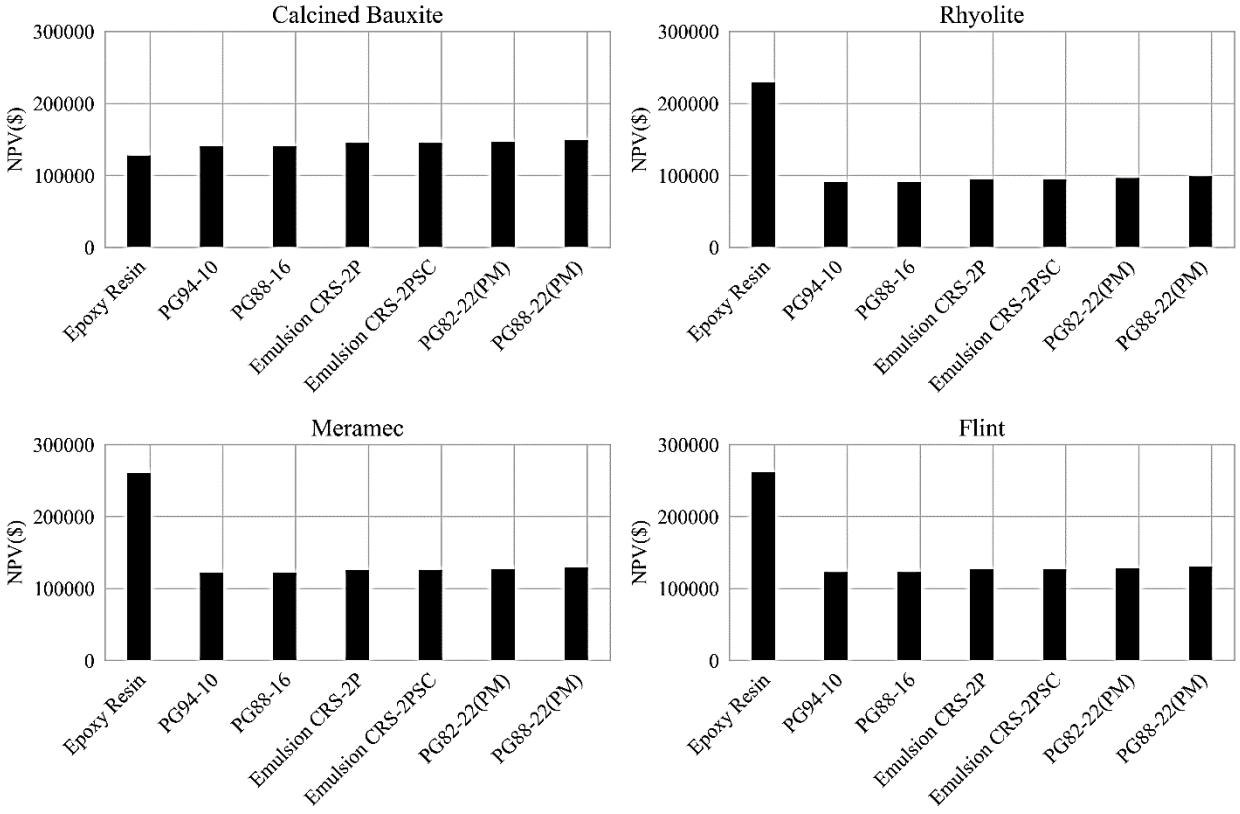

Figure 8.2 Net present values for HFST applications with different binders and HFST and medium sizes based on the BP input data

For the medium aggregate sizes, the best choice was epoxy resin for Calcined Bauxite and PG 88-16 for Rhyolite, because they produced the lowest NPV values. For the coarse aggregate size, for both aggregates, PG88-16 was the best choice. The worst binder was epoxy, with the highest NPV values for both aggregates.

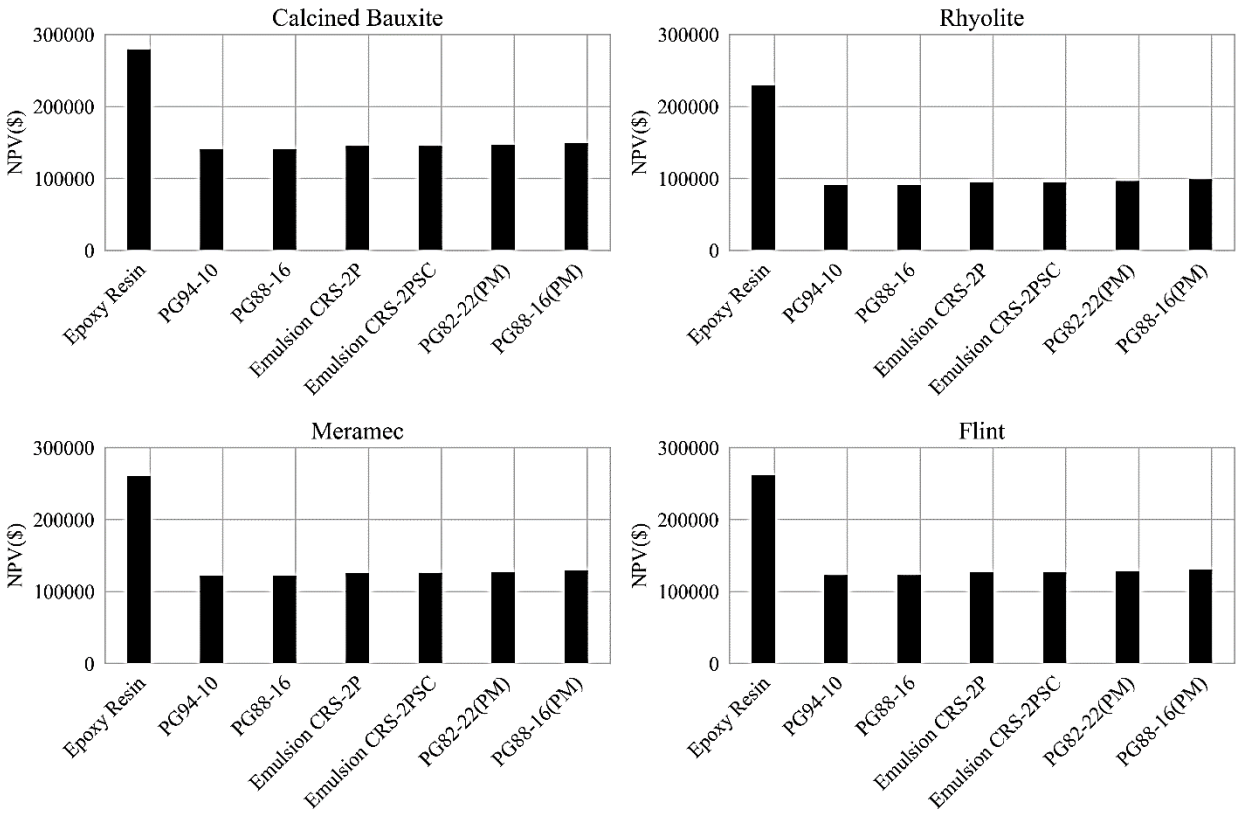

Figure 8.3 Net present values for HFST applications with different binders and coarse size aggregates based on the BP input data

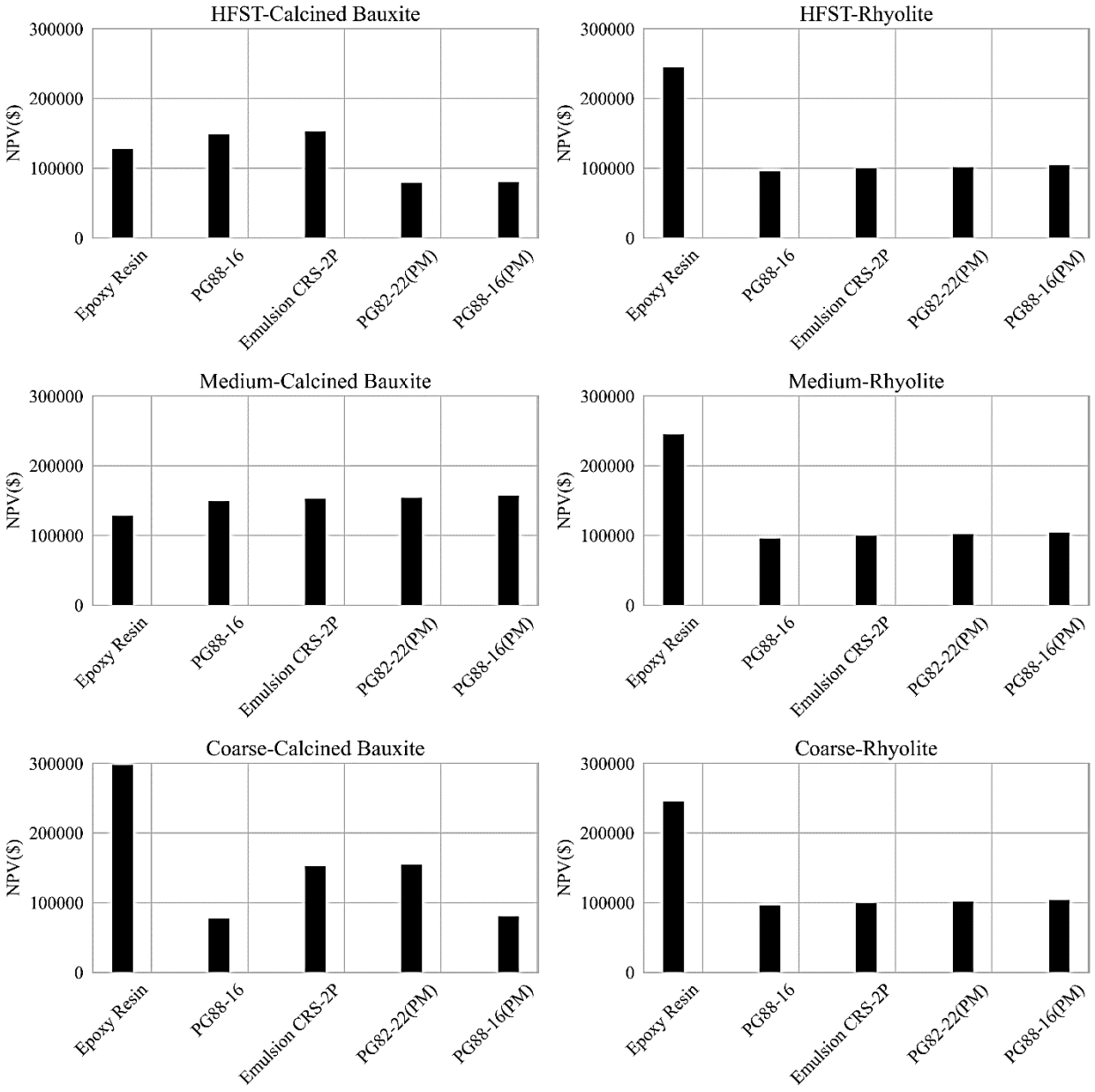

Figure 8.4 Net present values for HFST applications with different binders and aggregates based on the DFT40 input data

Figure 8.5 shows the NPVs for HFST applications with different binders and aggregates based on the DFT20 and CTM input data. For the Calcined Bauxite HFST aggregate size, the best choice was PG88-16 with the lowest NPV value, followed closely by both modified binders. The worst choice was emulsion, with the highest NPV value. A similar trend was exhibited in the HFST-sized Rhyolite. As mentioned before, it was assumed that a PG binder would be used as a replacement after the first application of emulsion.

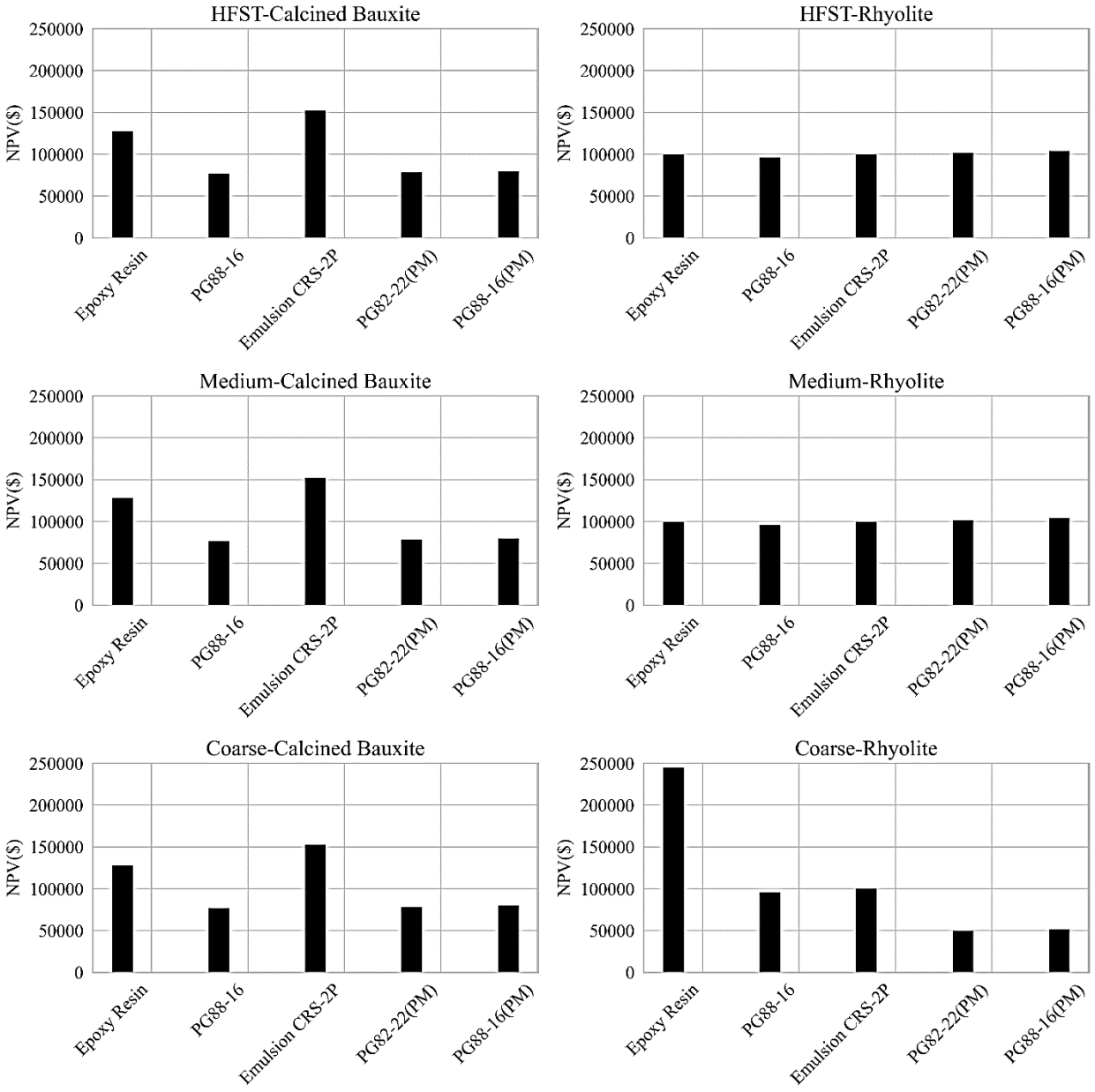

Figure 8.5 Net present values for HFST applications with different binders and aggregates based on the DFT20 and CTM input data

For the medium aggregate size, both aggregates showed similar results, with the best choice being PG88-16, followed closely by modified binders. The worst choice for Calcined Bauxite was attributed to the emulsion, which had the highest NPV values. For the coarse aggregate size, the lowest NPV for Calcined Bauxite was in conjunction with PG88-16, followed closely by PG82-22 (PM) and PG88-16 (PM), with the worst results from emulsion. For Rhyolite, PG82-22 (PM) and PG88-16 (PM) showed the lowest NPV, followed by PG88-16, and finally epoxy, with the highest NPV.

8.5 Comparative Economic Study

In this section, the Net Present Value (NPV) data obtained from the LCC program is compared to the High Friction Surface Treatment (HFST) applications. The NPV rankings for HFST, based on the LCC using BPN which predicted SN (40R), ranged from 1 to 7. The HFST application with the lowest NPV was ranked 1, and the HFST application with the highest NPV was ranked 7. Table 8-2 presents the rankings of HFST applications based on BPN for HFST and medium aggregate sizes.

Table 8-2 Binder rankings based on BPN for HFST and medium aggregate sizes

Binder Type	Aggregate Type			
	Calcined Bauxite	Rhyolite	Meramec	Flint
Epoxy Resin	1	7	7	7
PG94-10	3	2	2	2
PG88-16	2	1	1	1
Emulsion CRS-2P	4	3	3	3
Emulsion CRS-2PSC	5	4	4	4
PG82-22 (PM)	6	5	5	5
PG88-16 (PM)	7	6	6	6

The BPN LCC results, based on the predicted SN (40R), indicate that for Calcined Bauxite, the lowest NPV was associated with epoxy resin. For other aggregate sources, epoxy resin yielded the highest NPV due to its necessity for replacement falling below the threshold. PG88-16 demonstrated superior performance among the binders, achieving rank 2 with Calcined Bauxite and the lowest NPV with other aggregates.

Table 8-3 presents the rankings of HFST applications based on BPN for the coarse aggregate size. For Calcined Bauxite, the PG88-16 binder emerges as the optimal choice, with the lowest NPV recorded, thus ranking first. Conversely, epoxy resin for this aggregate size exhibited the highest NPV. For other aggregates, the results are consistent, with all binders showing comparable NPVs, and the PG88-16 binder offering the lowest cost.

Table 8-3 Binder rankings based on BPN for coarse aggregate size

Binder Type	Aggregate Type			
	Calcined Bauxite	Rhyolite	Meramec	Flint
Epoxy Resin	7	7	7	7
PG94-10	2	1	1	1
PG88-16	1	2	2	2
Emulsion CRS-2P	3	3	3	3
Emulsion CRS-2PSC	4	4	4	4
PG82-22 (PM)	5	5	5	5
PG88-16 (PM)	6	6	6	6

The LCC utilizing DFT40, which predicted SN (40R), ranked from 1 to 5. The HFST application with the lowest NPV was assigned rank 1, while the HFST application with the highest NPV was allocated rank 5. Table 8-4 illustrates the rankings of HFST applications based on DFT40 and SN (40R).

Table 8-4 Binder rankings based on DFT40

Binder Type	Aggregate Type					
	Calcined Bauxite			Rhyolite		
	HFST	Medium	Coarse	HFST	Medium	Coarse
Epoxy Resin	3	1	5	5	5	5
PG88-16	4	2	1	1	1	1
Emulsion CRS-2P	5	3	3	2	2	2
PG82-22 (PM)	1	4	4	3	3	3
PG88-16 (PM)	2	5	2	4	4	4

The results suggest that in DFT40 analysis, for Calcined Bauxite, the lowest NPV was linked to PG82-22 (PM) for HFST aggregate size, while epoxy was associated with the lowest NPV for medium aggregate size and PG88-16 was associated with the lowest NPC for coarse aggregate size. Conversely, for Rhyolite, PG88-16 exhibited the lowest NPV. Epoxy showed the highest NPV across all the gradations.

The LCC based on DFT20 and CTM, which predicted SN50, encompassed rankings from 1 to 5. The HFST application with the lowest NPV received rank 1, whereas the one with the highest NPV was placed at rank 5. Table 8-5 presents the rankings of HFST applications derived from DFT20 and CTM results.

Table 8-5 Binder rankings based on DFT20 and CTM

Binder Type	Aggregate Type					
	Calcined Bauxite			Rhyolite		
	HFST	Medium	Coarse	HFST	Medium	Coarse
Epoxy Resin	4	4	4	2	2	5
PG88-16	1	1	1	1	1	3
Emulsion CRS-2P	5	5	5	3	3	4
PG82-22 (PM)	2	2	2	4	4	1
PG88-16 (PM)	3	3	3	5	5	2

The findings from the DFT20 and CTM analysis indicate that for Calcined Bauxite, PG88-16 was consistently associated with the lowest NPV across all sizes, while emulsion demonstrated the highest NPV. Following the PG binder, PG82-22 (PM) and PG88-16 (PM) were second and third ranked. For Rhyolite, PG88-16 exhibited the lowest NPV in HFST and medium aggregate sizes but in the coarse aggregate size the lowest NPV related to PG82-22 (PM) and PG88-16 (PM).

8.6 Summary

In this chapter, the economic analysis of HFST applications was presented. The researchers developed a simple LCC program using Excel to predict the NPV for HFST applications. The predicted terminal Skid Number (SN) values for the HFST applications were compared with the recommended terminal SN values to inform maintenance decisions. Based on BPN input data for various aggregates with HFST and medium aggregate sizes across different binders, epoxy resin emerged as the best choice for Calcined Bauxite, exhibiting the lowest NPV value. Conversely, for Rhyolite, Meramec, and Flint, epoxy resin was the least favorable binder, showing the highest NPV values. This discrepancy is attributed to epoxy resin's higher cost, leading to the

need for HFST application replacements when aggregates reached their terminal Skid Number, measured at 40 mi/hr (SN40R), values using a skid trailer with ribbed tires. Other binders displayed comparable NPV values, with slightly better performance noted for PG88-16. Notably, there was a significant contrast between the coarse aggregate size and both HFST and medium aggregate sizes, with PG88-16 emerging as the optimal choice, showcasing the lowest NPV for Calcined Bauxite.

Based on the DFT40 and SN40R input data, the optimal choice for Calcined Bauxite HFST aggregate size was PG82-22 (PM), boasting the lowest NPV value, followed closely by PG88-16 (PM) with a comparable NPV value. Conversely, for Rhyolite, PG88-16 exhibited the lowest NPV, while epoxy was identified as the worst binder, producing the highest NPV value. In terms of medium aggregate size, epoxy resin was the top choice for Calcined Bauxite, while PG88-16 performed best for Rhyolite. In the coarse aggregate size category, for both aggregates, PG88-16 emerged as the optimal choice, whereas epoxy was again the worst binder, displaying the highest NPV values for both aggregates.

Based on the DFT20 and CTM input data, PG88-16 emerged as the best choice for Calcined Bauxite HFST aggregate size, showcasing the lowest NPV value, closely followed by both modified binders. Conversely, emulsion was identified as the worst choice, displaying the highest NPV value. A similar pattern was observed for HFST Rhyolite. Moving to the medium aggregate size, both aggregates yielded comparable results, with PG88-16 being the preferred choice, followed closely by modified binders. However, the worst choice for Calcined Bauxite was attributed to emulsion, with the highest NPV values. In terms of the coarse aggregate size, the lowest NPV for Calcined Bauxite was associated with PG88-16, followed closely by PG82-22 (PM) and PG88-16 (PM), while emulsion represented the worst binder. For Rhyolite, PG82-22 (PM) and PG88-16 (PM) demonstrated the lowest NPV, followed by PG88-16, with epoxy exhibiting the highest NPV values.

The LCCA of different binder-aggregate combinations shows a wide range of NPV values. This variety is mainly due to comparing different binder-aggregate combinations and involving a wide range of rehabilitation costs. The outcomes of the LCCA allowed the research team to provide the analysis on alternative aggregates or blends that provide comparable frictional performance at reduced cost. The presented LCCA is an updated version compared to the LCCA application of MoDOT project #TR202005 “Evaluation of Alternatives to Calcined Bauxite for Use in HFST” with additional binder-aggregate alternatives and additional material and performance testing as outlined.

CHAPTER 9: SUMMARY, CONCLUSIONS, AND RECOMMENDATIONS

9.1 Summary

High Friction Surface Treatment (HFST) is an effective and economical solution that has proven its ability to increase pavement friction and reduce crash rates in various scenarios worldwide. However, the relatively high cost of constructing and removing HFST with polymer resins, coupled with durability concerns due to existing pavement conditions, has led state agencies to explore alternative asphalt-based binders that use the same hard, highly angular fine aggregate; referred to as high friction chip seal (HFCS). This research focuses on testing HFST applications with asphalt-based binders as alternatives to polymer resin (epoxy) binders.

The alternative binders tested included standard PG binders, emulsions, and polymer modified binders. The performance of alternative aggregates, Rhyolite, Meramec, and Flint of three different sizes, was also evaluated, alongside Calcined Bauxite, as aggregate sources to be used with these binders.

Aggregate testing encompassed three categories: physical properties, durability, and performance. Physical properties testing included aggregate gradation, specific gravity and absorption, and Uncompacted Void Content (UVC) of fine aggregates tests. Durability testing involved Los Angeles Abrasion (LAA), sodium sulfate soundness, water-alcohol freeze-thaw, and acid-insoluble residue tests. Performance testing involved Micro-Deval (MD) polishing to evaluate the aggregates' resistance to abrasion and polishing, and the Aggregate Image Measurement System (AIMS) to examine changes in Texture (TX) and Gradient Angularity (GA) indices using the gradient method. This testing was conducted on coarse aggregates before and after 105, 180, and 240 minutes of polishing in the MD. These tests were conducted to classify the aggregates and identify routine tests for evaluating their suitability as HFST materials. Asphalt binder testing was also conducted and included characterizing performance grade (PG) binders and emulsion binders and conducting Binder Bond Strength tests for each type.

Friction testing utilized the British Pendulum (BP) test to evaluate the surface frictional properties of aggregates before and after 10 hours of polishing with the British Wheel. The Dynamic Friction Tester (DFT) was used to measure Coefficient of Friction (COF) values before and after polishing with the Three-Wheel Polishing Device (TWPD). Additionally, the Circular Track Texture Meter (CT-Meter) was employed to measure Mean Profile Depth (MPD).

The researchers developed a straightforward, updated Life-Cycle-Cost (LCC) process in Excel to calculate the Net Present Value (NPV) for HFST applications, utilizing BP, DFT, and MPD results. The primary input data for the LCC program were divided into material and project specifics. Performance prediction models transformed the input data into Skid Number (SN) values. The predicted terminal SN was compared to the recommended terminal SN using a rehabilitation matrix, which was designed based on these SN values. The output data, presenting

the NPVs for the HFST applications, were then calculated. The HFST application with the lowest NPV was selected as the optimal choice.

9.2 Conclusions

9.2.1 Aggregate physical properties, durability, and performance

1. The findings on Uncompacted Void Content (UVC) of fine aggregates showed no significant difference between the #6 - #8 size and the #6 - #16 size. Calcined Bauxite (CB) had the least UVC variance, while Meramec had the highest. Flint Chat had the highest UVC percentages, while Meramec River Aggregate had the lowest.

2. In Los Angeles Abrasion (LAA) testing for Grade D, Meramec exhibited the lowest LAA percentages, followed by Calcined Bauxite, Rhyolite, and Flint. In Micro-Deval (MD) testing for coarse gradation 3/8" - #4, Calcined Bauxite had the highest mass loss, while Meramec River Aggregate had the lowest. Rhyolite and Flint showed similar mass loss, with Rhyolite having lower loss than Flint for AMD 240. Among fine gradation aggregates, Meramec had the lowest mass loss, followed by Calcined Bauxite, Flint, and Rhyolite. Soundness test results showed Calcined Bauxite with the lowest sodium sulfate loss, followed by Meramec, Flint, and Rhyolite. In water-alcohol freeze-thaw resistance, Flint had the highest loss, Calcined Bauxite was intermediate, and Rhyolite had the lowest followed by Meramec. Acid-insoluble residue tests indicated Flint had the lowest residue percentage, followed by Rhyolite.

3. AIMS results showed that reducing aggregate sizes from 3/8" - 1/4" to 1/4" - #4 led to a decline in texture indices across different phases. However, Calcined Bauxite showed higher texture in AMD 240 for the 1/4" - #4 size range compared to 3/8" - 1/4" size range. Rhyolite had the highest texture and angularity indices for both sizes, while Meramec had the lowest angularity values. Additionally, Calcined Bauxite showed increased texture and angularity indices during Micro-Deval polishing as aggregate size decreased. No specific relationship was found between changes in average texture and average angularity indices across different Micro-Deval polishing times. Before polishing, Calcined Bauxite, Rhyolite, and Flint had the highest average texture and angularity, while Meramec exhibited a different trend, with the texture slightly increasing after 105 minutes of polishing, followed by a decrease as polishing continued.

4. Strong relationships between aggregate properties, such as AIMs parameters, and HFST friction performance characteristics, that could be applied to all aggregate sources and sizes could not be established. This is due to varying properties of aggregate sources and the nature(s) of the adopted testing standards.

9.2.2 Binder performance

1. Physical rheological tests on PG binders, Modified binders, and emulsions confirmed that all binders met the specified criteria.

2. Epoxy resin showed the highest values in the BBS test, significantly different from other binders. Additionally, epoxy resin had a slight increase in BBS during wet conditions, while other binders decreased. Under dry conditions, except for epoxy, PG88-16 (PM) had the highest BBS values, followed by PG82-22 (PM) and PG88-16. After 24 and 48 hours of conditioning, all binders showed decreased BBS values, with modified binders experiencing less decline compared to emulsions.

9.2.3 High friction applications frictional performance

1. The analysis of different binders and aggregate sizes on British Pendulum Number (BPN) revealed distinctive patterns. Replacing the epoxy with PG binders for HFST-sized aggregate mixes initially resulted in comparable BPN values, but PG94-10 exhibited a sharper decrease after polishing. The BPN performance of PG binders suggests that a PG88-16 might outperform a PG82-16, possibly due to stiffness affecting post-polishing BPN. For HFST aggregate size, both emulsions showed lower BPN values, likely due to bleeding and rutting. Modified binders showed different results with different aggregate types. Medium-sized aggregates, especially for emulsions, showed a less significant decrease in BPN, suggesting improved performance with coarser aggregates. Among the binders, epoxy experienced the least BPN loss, followed by PG88-16 and modified binders. Coarse aggregates demonstrated better resistance to deformation and performed well, particularly with emulsions.
2. Binder type and aggregate size played an important role in influencing COF values, with Modified Binders showing promising performance in various scenarios. The COF values from DFT testing exhibited variability across different speeds and polishing cycles for different binders and aggregates of three sizes (HFST, medium, and coarse). Initially, COF values were comparable across all binders in the HFST size, with Calcined Bauxite having a higher COF than Rhyolite. PG88-16 (PM) exhibited comparable performance to epoxy resin after 30K cycles, while PG82-22 (PM) showed better performance at 70K and 140K cycles. For Rhyolite, PG88-16 performed similarly or better than epoxy after 30K cycles, but its COF decreased with higher cycles. The medium aggregate size displayed a similar trend in Calcined Bauxite, but for Rhyolite after epoxy, PG82-22 (PM) showed better performance. For the coarse aggregate size, COF values varied from the HFST and medium size values, with Modified and PG binders comparable to and, in some cases, better than epoxy. PG88-16 (PM) performed well for Calcined Bauxite, while PG88-16 excelled at lower speeds for Rhyolite. Coarser gradation aggregates showed a smaller decrease in COF as polishing cycles increased. This observation is attributed to the reduced aggregate loss in coarser-sized aggregates when using PG and modified binders.
3. The decline in MPD percentage from HFST to coarse aggregate size with modified binders reveals an improvement in performance with larger aggregates as the polishing cycle progresses. The relationship between DFT40 and BPN values before and after polishing for both aggregates revealed that epoxy resin exhibited superior performance,

followed by PG88-16 (PM). PG82-22 (PM) and PG88-16 showed similar performance trends, while emulsion CRS-2P exhibited the lowest performance.

9.2.4 Binder-aggregate combinations performance

The outcomes of this research show the interactions of aggregate source and size and binder selection for the optimal friction performance. The results varied depending on the friction testing system, BN vs. DFT.

1. Based on COF values from DFT in the HFST and medium aggregate sizes, epoxy resin exhibited the best performance. In initial cycles, PG88-16 (PM) and PG82-22 (PM) showed promising results, but epoxy ultimately outperformed them in extended cycles. For the coarse aggregate size, PG88-16 (PM) showed the best performance for Calcined Bauxite, while PG88-16 demonstrated better performance in the initial cycles for Rhyolite, but in the terminal cycles, PG82-22 (PM) emerged as the best choice.
2. Based on the BPN input data in the LCCA, HFST and medium aggregate size of Calcined Bauxite combined with epoxy resin emerged as the best choice, showing the lowest NPV value. For other aggregate sources, epoxy resin was the least favorable binder due to high NPV. With the coarse-sized Calcined Bauxite, PG88-16 was identified as the optimal choice.
3. Based on the DFT40 input data in the LCCA, PG82-22 (PM) was optimal for Calcined Bauxite HFST, while PG88-16 had the lowest NPV for Rhyolite HFST. For the medium aggregate sizes, epoxy resin was found to be the top choice for Calcined Bauxite, while PG88-16 performed the best for Rhyolite. In the coarse-sized category for both aggregates, CB and Rhyolite, PG88-16 was identified as the optimal choice.
4. Based on DFT20 and CTM input data in the LCCA, PG88-16 was the best choice for HFST-sized Calcined Bauxite, closely followed by the polymer modified binders, while emulsion was the worst choice. Similar trends were observed for HFST Rhyolite. With the medium aggregate size, PG88-16 exhibited the lowest NPV for both aggregates. For coarse-sized aggregate, PG88-16 had the lowest NPV for Calcined Bauxite, while PG82-22 (PM) and PG88-16 (PM) were optimal for Rhyolite, with epoxy having the highest NPV.
5. The performance of coarse gradation aggregate was optimal with modified and PG binders, indicating that these binders offer better performance compared to epoxy as alternatives for coarser gradation aggregates.

9.3 Recommendations

1. Due to the scope of this study, a limited number of asphalt-based binder types have been considered. The development of modified asphalt binders is happening rapidly and providing significantly advanced binders, including for surface treatment applications.

The research team highly recommends the exploration and testing of advanced asphalt-based binders as alternatives to epoxy for HFST applications.

2. The research team recommends the construction of High Friction Surface Treatment (HFST) field sections, using the researched asphalt-based binders. This will allow for evaluation of the field performance of the binder-aggregate combinations. Field friction performance could be compared to the results produced in the lab.
3. The research team recommends the continuation of effort on updating the developed LCCA program as a rational tool in selecting the optimum binder-aggregate combination in HFST applications. Further research will enhance the capabilities of the program to compare the asphalt-based binders in HFST applications as alternatives to the epoxy-based applications, particularly on old and deteriorated asphalt sections.

REFERENCES

Anderson, R. Michael, Gayle N. King, Douglas I. Hanson, and Phillip B. Blankenship. "Evaluation of the relationship between asphalt binder properties and non-load related cracking." *Journal of the Association of Asphalt Paving Technologists* 80 (2011).

Bennert, Thomas, Robert Blight, Vahid Ganji, Drew Tulanowski, and Susan Gresavage. "Development of high friction surface treatment prescreening protocols and an alternative friction application." *Transportation Research Record* 2675, no. 5 (2021): 345-355. https://doi.org/10.1177/0361198121990027

Bosin, Anna, Ron Martindale, and Jeanne Bowie. *High Friction Surface Treatments Supplement*. No. TRS 1802S. Alaska Dept. of Transportation and Public Facilities, 2018.

Cuelho, Eli, Robert L. Mokwa, and Keely Obert. *Comparative Analysis of Coarse Surfacing Aggregate Using Micro-Deval, LA Abrasion, and Sodium Sulfate Soundness Tests*. No. FHWA/MT-06-016/8117-27. Montana Dept. of Transportation. Research Programs, 2007.

Deef-Allah, Eslam, Korrenn Broaddus, and Magdy Abdelrahman. *Evaluation of Alternatives to Calcined Bauxite for Use in High Friction Surface Treatment (HFST) in Missouri*. No. cmr21-006. Missouri Dept. of Transportation. Construction and Materials Division, 2021.

Federal Highway Administration (FHWA). *Every Day Counts Program (EDC-2) Innovation*. 2020. https://www.fhwa.dot.gov/innovation/everydaycounts/edc-2.cfm.

FHWA (Federal Highway Administration). 2019. *High Friction Surface Treatments (HFST)*. https://safety.fhwa.dot.gov/roadway_dept/pavement_friction/high_friction.

FHWA. *High Friction Surface Treatments Frequently Asked Questions*. No. FHWA-CAI-14-019, 2014.

FHWA-SA-18-004. “Frequently Asked Questions about High Friction Surface Treatments (HFST).” FHWA. Accessed March 20, 2024.

FHWA-SA-22-016. “Frequently Asked Questions about High Friction Surface Treatments (HFST).” FHWA. Accessed March 20, 2024.

Golembiewski, G. A., Brian Chandler, and Rosemarie Anderson. *Roadway Departure Safety: A Manual for Local Rural Road Owners*. No. FHWA-SA-11-009. United States. Federal Highway Administration, 2011.

Harkey, David L. *Accident Modification Factors for Traffic Engineering and ITS Improvements*. Vol. 617. Transportation Research Board, 2008. https://doi.org/10.17226/13899

Heitzman, Michael, and Jason Moore. "Evaluation of laboratory friction performance of aggregates for high friction surface treatments." *NCAT Report* (2017): 17-01.

Heitzman, Michael, Pamela Turner, and Mary Greer. *High Friction Surface Treatment Alternative Aggregates Study*. No. NCAT Report 15-04. 2015.

Henry, John Jewett. *Evaluation of Pavement Friction Characteristics*. Vol. 291. Transportation Research Board, 2000.

High Friction Surface Treatment Site Selection and Installation Guide. FHWA-SA-21-093. https://highways.dot.gov/sites/fhwa.dot.gov/files/2022-06/HFST_Guide_HPA.pdf.

Kandhal, Prithvi S., and Frazier Parker. *Aggregate Tests Related to Asphalt Concrete Performance in Pavements*. Vol. 405. Transportation Research Board, 1998. https://doi.org/10.3141/1638-10

Kassem, Emad, Ahmed Awed, Eyad A. Masad, and Dallas N. Little. "Development of predictive model for skid loss of asphalt pavements." *Transportation Research Record* 2372, no. 1 (2013): 83-96. https://doi.org/10.3141/2372-10.

Lal Das, V. K. "Evaluation of Louisiana asphalt pavement friction (M. Sc. thesis)." *Louisiana State University and Agricultural and Mechanical College, Baton Rouge, LO* (2011).

Li, Qiang Joshua, Guangwei Yang, Kelvin C.P. Wang, You Zhan, David Merritt, and Chaohui Wang. "Effectiveness and performance of high friction surface treatments at a national scale." *Canadian Journal of Civil Engineering* 43, no. 9 (2016): 812-821. https://doi.org/10.1139/cjce-2016-0132

Li, Shuo, Peiliang Cong, Demei Yu, Rui Xiong, and Yi Jiang. "Laboratory and field evaluation of single layer and double layer high friction surface treatments." *Transportation Research Record* 2673, no. 2 (2019): 552-561. https://doi.org/10.1177/0361198119826078

Li, Shuo, Rui Xiong, Demei Yu, Guangyuan Zhao, Peiliang Cong, and Yi Jiang. "Friction surface treatment selection: Aggregate properties, surface characteristics, alternative treatments, and safety effects." (2017). https://doi.org/10.5703/1288284316509

Mahmoud, E.M. “Development of Experimental Methods for the Evaluation of the Aggregate Resistance to Polishing, Abrasion, and Breakage.” M.Sc. Thesis, Texas A&M University, College Station, TX, U.S.A., 2005.

Masad, E., A. Luce, and E. Mahmoud. “Implementation of AIMS in Measuring Aggregate Resistance to Polishing, Abrasion, and Breakage.” FHWA/TX-06/5-1707-03-1, Texas Transportation Institute, Texas A&M University, College Station, TX, U.S.A., 2006.

Masad, E., A. Rezaei, and A. Chowdhury. “Field Evaluation of Asphalt Mixture Skid Resistance and Its Relationship to Aggregate Characteristics.” FHWA/TX-11/0-5627-3, Texas Transportation Institute, Texas A&M University, College Station, TX, U.S.A., 2011.

Masad, E., A. Rezaei, A. Chowdhury, and P. Harris. “Predicting Asphalt Mixture Skid Resistance Based on Aggregate Characteristics.” FHWA/TX-09/0-5627-1. Texas Transportation Institute, Texas A&M University, College Station, TX, U.S.A., 2009.

Mayora, José M. Pardillo, and Rafael Jurado Piña. "An assessment of the skid resistance effect on traffic safety under wet-pavement conditions." *Accident Analysis & Prevention* 41, no. 4 (2009): 881-886. https://doi.org/10.1016/j.aap.2009.05.004

McGovern, Colleen M., Peter F. Rusch, and David A. Noyce. *State Practices to Reduce Wet Weather Skidding Crashes*. No. FHWA-SA-11-21. United States. Federal Highway Administration. Office of Safety, 2011.

Milstead, Robert, X. Qin, Bryan Katz, James A. Bonneson, Michael Pratt, Jeff Miles, and Paul J. Carlson. *Procedures for Setting Advisory Speeds on Curves*. No. FHWA-SA-11-22. United States. Federal Highway Administration. Office of Safety, 2011.

Missouri DOT. "High Friction Surface Treatment (NJSP-15-13B)." Standard Specifications, 2015.

Missouri Standard Specifications for Highway Construction, 2023. https://www.modot.org/sites/default/files/documents/2022%20Missouri%20Standard%20Specific%20-%20MHTC%20%28Oct%202022%29_notsigned.pdf.

Musey, K., and S. Park. "Pavement skid number and horizontal curve safety." *Procedia Engineering* 145 (2016): 828-835.

Musey, Kimberley M. *Quantifying the Safety Impact of High Friction Surface Treatment Installations in Pennsylvania*. Villanova University, 2017.

Najafi, Shahriar, Gerardo W. Flintsch, and Alejandra Medina. "Linking roadway crashes and tire–pavement friction: A case study." *International Journal of Pavement Engineering* 18, no. 2 (2017): 119-127. https://doi.org/10.1080/10298436.2015.1039005

NJDOT. DIVISION 420. https://njdotlocalaidrc.com/perch/resources/Uploads/njdot-high-friction-surface-treatment-guidelinesfinalfeb2019.docx.

Pranav, Cibi, and Yi-Chang Tsai. "High friction surface treatment deterioration analysis and characteristics study." *Transportation Research Record* 2675, no. 12 (2021): 370-384. https://doi.org/10.1177/03611981211029648

Pratt, Michael P., Srinivas R. Geedipally, Bryan Wilson, Subasish Das, Marcus A. Brewer, and Dominique Lord. *Pavement Safety-Based Guidelines for Horizontal Curve Safety*. No. FHWA/TX-18/0-6932-R1, 0-6932-R1. Texas A&M Transportation Institute, 2018.

Roshan, Alireza, and Magdy Abdelrahman. "Improving Aggregate Abrasion Resistance Prediction via Micro-Deval Test Using Ensemble Machine Learning Techniques." *Engineering Journal* 28, no. 3 (2024): 15-24. https://doi.org/10.4186/ej.2024.28.3.15

Roshan, Alireza, and Magdy Abdelrahman. "Evaluating Friction Characteristics of High Friction Surface Treatment Application Under Varied Polishing and Slippery Conditions." *Transportation Research Record* (2024): 03611981241257505.

RSTA ADEPT. *Code of Practice for High Friction Surfacing*, 2nd Edition. Road Surface Treatment Association. United Kingdom, 2017.

Torbic, Darren J., Douglas W. Harwood, David K. Gilmore, Ronald Pfefer, Timothy R. Neuman, Kevin L. Slack, and Kelly K. Hardy. "Guidance for implementation of the AASHTO strategic highway safety plan." *NCHRP Report* 500. Volume 7: A Guide for Reducing Collisions on Horizontal Curves (2004).

Wambold, J. C., J. J. Henry, R. R. Harris, and A. R. Wymer. *NCHRP Report 108: Skid Resistance of Highway Pavements*. National Cooperative Highway Research Program, Transportation Research Board, 1970.

Wambold, J. C., C. E. Antle, J. J. Henry, and Z. Rado. *International PIARC Experiment to Compare and Harmonize Texture and Skid Resistance Measurements: Final Report*. Permanent International Association of Road Congresses (PIARC), 1995.

Watson, Donald E., Robert D. Bhasin, K. Williams, and A. Jared. *Georgia Load and Resistance Factor Design (LRFD) Bridge Design Manual*. Georgia Dept. of Transportation, Office of Bridge Design, 2014.

Yap, Priscilla F., Norlida Abas, and Kahar Osman. "Effect of aggregate shape and surface texture on skid resistance of pavement surface." In *IOP Conference Series: Earth and Environmental Science*, vol. 16, no. 1, p. 012023. IOP Publishing, 2013.

APPENDIX A: HFST APPLICATION AND PERFORMANCE SPECIFICATION

A.1 AASHTO MP 41-22 Standard Specification

The current version of the AASHTO specification for High Friction Surface Treatment (HFST) for asphalt and concrete pavements, AASHTO MP 41-22, was developed through a collaborative process between agencies and industry (AASHTO 2022). This specification provides guidance for agencies looking to develop their own HFST specifications, but it can also be adopted as-is. Agencies with established HFST programs have often created their own specifications, incorporating agency-specific requirements for materials and installation practices. Key elements of an HFST specification, based on the AASHTO specification and other agency specifications, are highlighted below.

Table A-1 summarizes the required tests and corresponding specifications for resin binders (epoxy, MMA, or polyester) according to AASHTO MP 41-22. Other required tests, besides the refractory grade of CB, specifications, and their threshold for the CB are presented in Table A-2.

A.2 High Friction Chip Seal (HFCS) standard

NJDOT currently utilizes Division 420 – Pavement Preservation Treatments (Section 424 Chip Seal) as the standard specification for HFCS applications.

Asphalt Binder Application:

Apply the asphalt binder at the temperature recommended by the manufacturer. The application rate should be set between 0.30 and 0.38 gallons per square yard.

HFCS Aggregate:

The fine aggregate must be clean, dry, and composed of pure manufactured Calcined Bauxite, free from contaminants. It must meet the specifications outlined in Tables A-3 and A-4.

Table A-1 Physical Requirements for low modulus epoxy, Methyl Methacrylate (MMA), and polyester resins

Property	Test Method	Epoxy Requirements	MMA Requirements	Polyester Requirements
Viscosity	ASTM D2556	≥ 1000 centipoise (cP)[a]	1500-2500 cP	≥ 1000 cP[a]
Flash Point	ASTM D3278	See SDS	See SDS	See SDS
Gel Time	ASTM C881/M 235	≥ 10 minutes	≥ 15 minutes (ASTM D2471)	≥ 10 minutes
Compressive Modulus (7 days)	ASTM D695	≤ 130,000 psi	≤ 130,000 psi	-
Compressive Strength (3 hours)	ASTM C579	≥ 1000 psi	≥ 1000 psi	≥ 1000 psi
Compressive Strength (24 hours)	ASTM C579	≥ 3000 psi	≥ 3000 psi	≥ 3000 psi
Tensile Strength (7 days)	ASTM D638	2000-5000 psi	500-1000 psi	2000-5000 psi
Tensile Elongation	ASTM D638	≥ 30%	≥ 50%	≥ 30%
Absorption	ASTM D570	≤ 1.0%	≤ 1.0%	≤ 1.0%
Type D Hardness (7 days ± 6h)	ASTM D2240	60-80	50-60	50-60
Thermal Compatibility	ASTM C884	PASS	-	PASS
Infrared Spectrum	ASTM E573/AASHTO MP 41	Combined and Components[b]	Combined and Components[a]	Combined and Components[b]

Notes:

- a - Epoxies and polyesters with low viscosities may require additional applications to achieve desired thickness.
- b - Methodologies for comparisons should be similar.

Table A-2 Physical and chemical requirements of refractory grade Calcined Bauxite aggregate

Property	Test Method	Requirements
Resistance to Degradation	ASTM D7428 (Micro-Deval)	≤ 3% loss
Aggregate Grading	AASHTO T 27	% Passing
- No. 4 Sieve		100
- No. 6 Sieve		95-100
- No. 16 Sieve		0-5
- No. 30 Sieve		0-0.2
Moisture Content	AASHTO T 255	≤ 0.2%
Aluminum Oxide Content	ASTM E1621	≥ 85%

Table A-3 Requirements for HFCS aggregate

Property	Test Method	Requirement
Polish Stone Value	AASHTO T 279	Minimum 38.0
Resistance to Degradation (Grading D)	AASHTO T 96	Maximum 20.0% loss
Moisture Content	AASHTO T 255	Maximum 0.2%
Aluminum Oxide Content	ASTM C 25 (Section 15)	Minimum 87%

Table A-4 Gradation requirements for HFCS fine aggregate

Sieve Size	Percent Passing
No. 4	100
No. 6	95 - 100
No. 16	0 - 5

A.3 Other States' Standards for High Friction Surface Treatment (HFST)

In addition to Missouri Department of Transportation (MoDOT) requirements and the AASHTO standard, this section explores High Friction Surface Treatment (HFST) aggregate requirements from other states.

While there are significant variations in the specific tests different states require for HFST aggregates, the required values for those tests often show consistency when a particular test is used by multiple states. The two most common tests employed across these states are the Los Angeles Abrasion (LAA) test and the aluminum oxide content test. However, the recent AASHTO MP 41-22 standard replaces the LAA test with the potentially more relevant Micro-Deval (MD) test. The aluminum oxide content test is primarily relevant for Calcined Bauxite (CB) aggregate and might not be required for alternative materials.

Understanding these commonalities and differences among state standards can inform MoDOT's decisions when selecting and testing aggregates for their HFST projects, especially as they transition towards the AASHTO MP 41-22 standard.

A.3.1 Aggregate Gradation Standards

- Most states require analysis of aggregate passing the #4 sieve, ensuring a specific size range for optimal performance.
- A few states, like Michigan, replace the #6 sieve analysis with the #8 sieve.
- Table A-5 summarizes these gradation requirements across different states.

A.3.2 Physical Properties and Abrasion Testing Standards

- Every state has specifications for the physical properties of HFST aggregates.
- Tables A-6 and A-7 highlight the most common requirements by state.

State Variations:

- Alaska appears to have the most flexible HFST requirements based on the reviewed specifications.

Table A-5 High friction aggregate gradation requirements by state

State	#4 Sieve	#6 Sieve	#8 Sieve	#16 Sieve	#30 Sieve	Gradation Test Method	Reference
Alabama	100% Min	95% Min	-	5% Max	-	AASHTO T 27	Alabama DOT 2014

Alaska	-	95% Min	-	5% Max	-	AASHTO T 27	Alaska DOT 2004
California	-	95% Min	-	5% Max	-	AASHTO T 27	California DOT, n.d.
Florida	100% Min	95% Min	-	5% Max	-	AASHTO T 27	Florida DOT 2014
Georgia	100% Min	95% Min	-	5% Max	-	AASHTO T 27	Georgia DOT 2017
Illinois	100% Min	95% Min	-	5% Max	-	AASHTO T 27	Illinois DOT 2014
Indiana	100% Min	95% Min	-	5% Max	1% Max	AASHTO T 27	Indiana DOT 2017
Iowa	100% Min	95% Min	-	5% Max	-	AASHTO T 27	Iowa DOT 2011
Kentucky	100% Min	95% Min	-	5% Max	-	AASHTO T 27	Kentucky DOT, n.d.
Michigan	98% Min	-	30-70%	5% Max	1% Max	AASHTO T 27	Michigan DOT 2016
Pennsylvania	100% Min	95% Min	-	5% Max	-	AASHTO T 27	Pennsylvania DOT 2014
South Carolina	100% Min	95% Min	-	5% Max	-	AASHTO T 27	South Carolina DOT 2015
South Dakota	100% Min	95% Min	-	5% Max	-	AASHTO T 27	South Dakota DOT 2015
Tennessee	100% Min	95% Min	-	5% Max	-	AASHTO T 27	Tennessee DOT 2017
Texas	-	95% Min	-	5% Max	-	AASHTO T 27	Texas DOT 2004

Virginia	-	95% Min	-	5% Max	-	AASHTO T 27	Virginia DOT 2012
Wisconsin	100% Min	95% Min	-	5% Max	1% Max	AASHTO T 27	Wisconsin DOT, n.d.

In addition to the physical properties of the aggregates, many states have requirements for other characteristics of the delivered material. The most common requirement is a maximum moisture content, likely to ensure proper adhesion with the resin binder during HFST application. Table A-8 summarizes these moisture content requirements by state.

California has a unique requirement, specifying an additional property - cleanness value, following AASHTO CT-227. This test likely assesses the presence of fines or contaminants that might affect the bonding between the aggregate and the resin. California requires a minimum cleanness value of 75 (California DOT, n.d.).

Table A-6 Requirements of high friction aggregates' physical properties by state

State	Aggregate Type	Los Angeles Abrasion (LAA)	Threshold	LAA Specification	Aluminum Oxide Content	Threshold	Aluminum Oxide Content Specification	References
Alabama	Calcined Bauxite (CB)	Max	20%	AASHTO T 96	Min	87%	ASTM C25	Alabama DOT 2014
Alaska	Blend of CB	-	-	-	-	-	-	Alaska DOT 2004
California	Blend of CB	Max	10%	CT 211	-	-	-	California DOT, n.d.
Florida	CB	Max	10%	AASHTO T 96	Min	87%	ASTM C25	Florida DOT 2014
Illinois	CB	Max	20%	AASHTO T 96	Min	87%	ASTM C25	Illinois DOT 2014
Indiana	CB	Max	10%	AASHTO T 96	Min	87%	ASTM C25	Indiana DOT 2017
Iowa	CB	Max	20%	AASHTO T 96	-	-	-	Iowa DOT 2011
Michigan	CB	-	-	-	Min	87%	ASTM C25	Michigan DOT 2016
Pennsylvania	CB	Max	20%	AASHTO T 96	Min	87%	ASTM C25	Pennsylvania DOT 2014
South Carolina	CB	Max	20%	AASHTO T 96	Min	87%	ASTM C25	South Carolina DOT 2015

South Dakota	CB	Max	20%	AASHTO T 96	Min	87%	ASTM C25	South Dakota DOT 2015
Tennessee	CB	-	-	-	Min	87%	ASTM C25	Tennessee DOT 2017
Texas	CB	Max	10%	ASTM C131	Min	87%	ASTM C25	Texas DOT 2004
Virginia	CB	Max	20%	AASHTO T 96	-	-	-	Virginia DOT 2012
Wisconsin	Natural or Synthetic	Max	25% & 10%	AASHTO T 96	-	-	-	Wisconsin DOT, n.d.

Table A-7 Other high friction aggregates' physical properties by state

State	Fineness Modulus	Fine Aggregate Angularity (FAA)	Threshold	FAA Specification	Hardness Test	Threshold	Hardness Test Specification	References
Indiana	-	-	-	-	Mohs Scale	Min 8	-	Indiana DOT 2017
Michigan	2.28-22.81	-	-	-	-	-	-	Michigan DOT 2016
Wisconsin	-	Min 45%	AASHTO T 304	-	-	-	-	Wisconsin DOT, n.d.

Table A-8 As delivered high friction aggregates' moisture content threshold by state

State	Moisture Content Threshold	Moisture Content Specification	Reference
Alabama	0.2% Max	AASHTO T 255	Alabama DOT 2014
Florida	0.2% Max	AASHTO T 255	Florida DOT 2014
Illinois	0.2% Max	AASHTO T 255	Illinois DOT 2014
Indiana	0.2% Max	AASHTO T 255	Indiana DOT 2017
Pennsylvania	0.2% Max	AASHTO T 255	Pennsylvania DOT 2014
South Carolina	0.2% Max	AASHTO T 255	South Carolina DOT 2015
South Dakota	0.2% Max	AASHTO T 255	South Dakota DOT 2015
Tennessee	0.2% Max	AASHTO T 255	Tennessee DOT 2017
Wisconsin	0.2% Max	AASHTO T 255	Wisconsin DOT, n.d.

A.3.3 Performance and Durability Testing Standards for HFST Aggregates

High Friction Surface Treatment (HFST) applications aim to enhance friction on critical roadway locations. Here, the durability of the aggregates used becomes a significant factor. Without highly durable aggregates, the HFST application will not last for an extended period.

Importance of Durability: Since HFST targets improved friction on specific roadway sections, using durable aggregates is crucial. Aggregates with low durability would not withstand traffic wear and tear, leading to a shortened lifespan for the HFST treatment.

PSV and Micro-Deval Requirements: Table A-9 showcases the Polished Stone Value (PSV) and Micro-Deval (MD) requirements implemented by various states. These tests evaluate the aggregate's resistance to polishing under traffic, which directly affects skid resistance.

Variations in Durability Testing: Unlike the physical properties discussed earlier, there is less consistency among states regarding the specific durability tests deemed important. Tables A-10 and A-11 highlights additional durability requirements employed by some states.

Wisconsin's EFST Standard: Notably, Wisconsin utilizes an Enhanced Friction Surface Treatment (EFST) standard instead of the typical HFST standard. This distinction is highlighted

in Table A-11, which details the specifications for their EFST. These specifications might be more relevant for the current study due to potentially stricter requirements.

Table A-9 Polished Stone Value (PSV) and Micro-Deval (MD) requirements for HFST aggregates by state

State	Polished Stone Value (PSV) Threshold	PSV Specification	Micro-Deval (MD) Threshold	MD Specification	References
Alabama	Min 38	AASHTO T 279	-	-	Alabama DOT 2014
Indiana	38-44	AASHTO T 279	-	-	Indiana DOT 2017
Iowa	Min 70.0 BPN[a]	ASTM E660	-	-	Iowa DOT 2011
Pennsylvania	Min 38	AASHTO T 279	-	-	Pennsylvania DOT 2014
South Carolina	Min 38	AASHTO T 279	-	-	South Carolina DOT 2015
Tennessee			Max 5%	ASTM D7428	Tennessee DOT 2017
Virginia			Max 5%	AASHTO T-327	Virginia DOT 2012
Wisconsin			Max 15%	ASTM D7428	Wisconsin DOT, n.d.

a : BPN=British Pendulum Number

Table A-10 High friction aggregates' additional durability and performance requirements by state

State	Acid Insolubility Threshold	Acid Insolubility Specification	Magnesium/Sodium Sulfate Soundness Threshold	Magnesium/Sodium Sulfate Soundness Specification	References
California	Min 90%	ASTM D-3042	Max 30%	ASTM C88	California DOT, n.d.
Indiana	-	-	Max 12%	AASHTO T 104	Indiana DOT 2017
Texas	Min 90%	Tex-512-J	Max 30%	Tex-411-A	Texas DOT 2004
Wisconsin	-	-	-	-	Wisconsin DOT, n.d.

Table A-11 Natural/synthetic aggregates' requirements in Wisconsin (Wisconsin DOT, n.d.)

Test	Threshold Value	Specification
Fine Aggregate Micro-Deval (MD)	15% Max. loss	ASTM D7428
Los Angeles Abrasion (LAA)	10% Max. loss at 100 revolutions & 20% Max. loss at 500 revolutions	AASHTO T 96
Moisture Content	0.2% Max.	AASHTO T 255
Water-Alcohol Freeze-Thaw Soundness	9% Max. loss	AASHTO T 103

A.4 High Friction Surface Treatment Performance Testing

This section examines two key areas of High Friction Surface Treatment (HFST) performance evaluation.

A.4.1 Performance Tests for Friction Properties

Various tests assess the frictional properties of HFST aggregates and mixes. These include the British Pendulum (BP) Test paired with the British Accelerated Polishing Machine (BAPM), the Dynamic Friction Tester (DFT) with the National Center for Asphalt Technology's (NCAT) Three-Wheel Polishing Device (TWPD), and the combination of the Aggregate Image Measurement System (AIMS) and the Micro-Deval (MD) device. The BP and DFT directly measure skid resistance, while the BAPM and TWPD simulate the polishing effect of traffic. AIMS analyzes aggregate shape and texture, influencing friction, and the MD device evaluates resistance to degradation, impacting long-term performance.

A.4.2 Evaluation of Alternative binders

These performance tests play a critical role in selecting suitable binders for HFST applications.

Evaluation Criteria:

When evaluating alternative binders for HFST, several key criteria need to be considered:

- Compatibility with Asphalt Pavements: The binder should be compatible with existing asphalt surfaces to minimize the risk of thermally induced failures.
- Bond Strength and Durability: The binder must provide a strong and durable bond between the aggregate and the pavement surface to ensure long-term performance under traffic wear.
- Friction Properties: The binder should not negatively impact the frictional properties of the applied aggregates. Ideally, it might even contribute to maintaining high friction over time.
- Workability and Application: The binder should be workable at reasonable temperatures and allow for efficient application during construction.
- Cost and Availability: The cost of the binder material and its availability for large-scale projects are important considerations.
- Environmental Impact: The environmental impact of the binder material, including its recyclability and removal, should be factored into the evaluation.

A.4.3 British Pendulum Test

The British Pendulum (BP) Test is utilized to assess the resistance of coarse aggregates to polishing, both before and after they undergo a 10-hour polishing procedure with the British accelerated polishing machine (also known as the British wheel). According to ASTM D3319-11, the initial polish value (PV-i) and the value after 10 hours of polishing (PV-10) are recorded for the curved aggregate samples using the BP on the F-scale, as depicted in Figure B-2. The F-scale is applied when using a slider that measures 1.25 inches in width. Conversely, for a 3-inch-wide slider, which is preferred for flat surfaces, the main scale is employed. The resistance of coarse

aggregates to polishing is determined by the polished stone value, which is calculated using Equation A.1 (Li et al. 2017). They discovered discrepancies between the Polished Stone Value (PSV), computed according to BS EN 1097-8, and the PV-10, measured in line with ASTM D3319-11. These differences arise from the distinct methodologies and materials employed in each standard, including variations in the abrasive materials, the duration of polishing, and the rate of abrasive feed. This study noted the lack of conclusive evidence to prefer either PSV or PV-10 as the more accurate metric for assessing polish resistance. Equation A.1 for PSV is given as

$$PSV = S - C + 52.5 \qquad \text{Equation A.1}$$

where S represents the mean of four test samples of aggregates, and C is the average from four control stone samples.

A.4.4 Accelerated Friction Testing

Accelerated friction testing serves to assess the frictional properties of pavement surfaces by measuring their surface friction. This testing involves determining the Mean Texture Depth (MTD) through a sand patch test or the Mean Profile Depth (MPD) using a Circular Texture Meter (CTM), both of which evaluate the macrotexture of the surfaces. Furthermore, the Dynamic Friction Tester (DFT) is employed to gauge the Coefficient of Friction (COF) at varying speeds in accordance with ASTM E 1911, across different stages of wear indicated by the number of polishing cycles—starting from 0 cycles (initial), through 70,000 cycles, and up to 140,000 cycles (deemed terminal).

A.4.5 Micro-Deval and Aggregate Image Measurement System (AIMS)

The Micro-Deval (MD) apparatus, originating from France in the 1960s, has been utilized to evaluate the durability of aggregates and their resistance to polishing, abrasion, and grinding when exposed to water. This method, highlighting the role of water to simulate environmental impacts, offers a more representative assessment of aggregate durability compared to the Los Angeles Abrasion (LAA) test. (Li et al. 2017; Wilson and Mukhopadhyay 2016; Kassem et al. 2013). The introduction of water and the employment of smaller steel balls than those used in the LAA test lessen the effect of impact, shifting the emphasis towards surface wear through grinding and abrasion (Li et al. 2017; Cuelho et al. 2007; Wu, Parker, and Roshan et al. 2024).

Complementing the MD test, the AIMS, developed at Texas A&M University, measures the physical characteristics of aggregates such as shape, Gradient Angularity (GA), and surface Texture (TX), both prior to and following polishing in the MD apparatus. The shape of aggregates is quantified based on two-dimensional forms, angularity is assessed through the irregularities on a particle's surface using black and white images, and the surface texture is analyzed using grayscale images through wavelet analysis (Kassem et al. 2013; E. Mahmoud and Masad 2007; Masad, Luce, and Mahmoud 2006; Masad et al. 2009).

A.4.6 Previous Relevant Research

Bennert et al. (2021) explored an innovative alternative to epoxy resin in pavement surface treatments, introducing a high friction chip seal (HFCS). This novel approach retains the use of hard, highly angular fine aggregates typical of high friction surface treatments (HFSTs) but opts for an asphalt binder as the adhesive agent in the chip seal process. The research involved evaluating three different sources of aggregates applied using the HFCS method on Route 68 in New Jersey. Through both laboratory analyses of the aggregates and field evaluations of the test sections, the study discovered that HFCS presents a viable alternative in scenarios where early failure of conventional HFSTs poses a concern. This finding suggested that HFCS could offer a more durable and potentially cost-effective option for improving road surface friction and safety without the drawbacks associated with the use of epoxy resins.

(Heitzman et al., 2017) conducted a study focusing on the long-term friction loss trends (terminal friction) across 11 different types of aggregate, including basalt, copper slag, Flint 65-8, RK Bauxite 6×14C CB, Calcined Kaolin in various gradations (47 - 4×20, 60 - 4×20, 70 - 4×20), Best Sand 612 Quartz, Armor Stone Quartz, EP5-Mod Quartz, and Traction Control Feldspar Mineral. Their research methodology involved measuring the surface textures (TXs) utilizing both a Circular Texture Meter (CTM) and a Dynamic Friction Tester (DFT). The CTM assessed the macrotexture of these aggregates by providing a Mean Profile Depth (MPD), while the DFT was employed to measure the surface friction, expressed as Friction Number (FN), at speeds of 20, 40, and 60 km/hr. Additionally, the microtexture was estimated using the DFT. The friction characteristics (FN) and macrotexture (MPD) of these aggregates were evaluated both before and after they were subjected to polishing using the NCAT Three-Wheel Polishing Device (TWPD). Interestingly, the study found no correlation between the results obtained from the CTM and DFT tests. Among the tested aggregates, Calcined Bauxite (CB) stood out for its superior frictional properties, consistently showing the highest FN values across the assessments.

Heitzman et al. (2015) conducted a thorough examination of seven friction aggregates (granite, flint, basalt, silica, emery, and taconite), comparing their performances against Calcined Bauxite (CB) using the Dynamic Friction Tester (DFT). The results indicated that none matched CB's friction performance, with similar friction loss observed after 70,000 to 140,000 polishing cycles. No correlation was found between DFT and Circular Texture Meter (CTM) readings, implying these tests measure different aspects of surface texture and friction. Smaller aggregate particles led to lower surface textures, with CTM macrotexture decreasing from 2.3 mm to 1 mm when the size changed from #6 to #16. The #8 sized aggregate had the highest friction values. A significant relationship was identified between Micro-Deval (MD) mass losses and friction rankings for CB, for slag, and taconite, though flint did not follow this trend. Additionally, no correlation was found between AIMS data and friction outcomes, suggesting macroscopic physical properties measured by AIMS may not directly influence friction performance.

Wilson et al. (2016) conducted a study to compare the friction performance of two sources of Calcined Bauxite (CB) aggregate, one sourced from China and the other from India, with a third, unspecified aggregate type from the UK. The CB aggregates were noted for their high alumina content (87% Al_2O_3), while the UK aggregate was characterized by a significant presence of silica (60% SiO_2) and alumina (20% Al_2O_3). To assess friction performance, the researchers employed both the Circular Texture Meter (CTM) and the Dynamic Friction Tester (DFT),

complemented by the use of the NCAT Three-Wheel Polishing Device (TWPD) for simulating wear. Furthermore, the study also examined the shape, texture, and angularity of the aggregates using the Aggregate Image Measurement System (AIMS) both before and after processing with the Micro-Deval (MD) apparatus. The research showed that Calcined Bauxite (CB) had the lowest mass loss (5.5%) after a 50-minute wear process, indicating high durability. The UK aggregate had a higher mass loss (24.6%), showing less wear resistance. Kassem et al. (2013) evaluated the friction performance of soft limestone, intermediate limestone, and hard sandstone using AIMS, CTM, and DFT on slabs with various mix designs (PFC, SMA, Type F, Type C) and the same asphalt binder (67−22). Polishing was performed with the TWPD at intervals of 5K, 10K, 30K, 50K, and 100K cycles. Sandstone showed the highest resistance to degradation, with the lowest mass loss after 105 and 180 minutes of polishing, while soft limestone had the lowest resistance. AIMS indicated that sandstone had the highest TX and GA indices post-MD polishing. PFC mixtures had the highest MPD, indicating superior macrotexture. Sandstone had the highest DFT20 measurements, reflecting the best microtexture, though values decreased with more polishing cycles.

A.4.7 Skid Resistance Prediction Models

Kassem et al. (2013) conducted a study using a limited number of aggregates, including soft limestone, intermediate hardness limestone, and hard sandstone, to assess how aggregate source and gradation influence skid resistance. They found that the International Friction Index (IFI) effectively reflected pavement skid resistance, leading to the development of a regression model correlating IFI with Coefficient of Friction (COF) values measured by Dynamic Friction Tester (DFT) at 20 km/hr (DFT20) and Mean Profile Depth (MPD) values (Wambold et al. 1995). Other studies (Kassem et al., 2013 and Masad et al., 2006, 2007, 2009, and 2011) have also explored skid resistance prediction models. The regression coefficients (amix, bmix, and cmix) in Equation A.2 were linked with aggregate Texture (TX), aggregate Gradient Angularity (GA), and Weibull distribution parameters that characterized the aggregates. Subsequently, the Skid Number measured at 50 mph by a skid trailer with smooth tires [SN (50)] was correlated with the International Friction Index (IFI) and Mean Profile Depth (MPD) according to Equation A.3 (Rezaei and Masad, 2013).

$$I(N) = amix + bmix \times e^{(-cmix \times N)} \quad \text{Equation A.2}$$

$$SN\,(50) = 4.81 + 140.32 \times (IFI - 0.045) \times e^{(-20\,(14.2+89.7\times MPD))} \quad \text{Equation A.3}$$

Masad et al. (2011) showed the modified SN (50) values can be calculated according to Equation A.4.

$$SN\,(50) = 1.41+143.19\times (IFI-0.045) \times e^{(-20/S_P)} \quad \text{Equation A.4}$$

The Sp value is a function of MPD (see Equation A.5), which is obtained using the CT Meter device. And the IFI is calculated following ASTM E 1960, based on COF values recorded by the DFT at 20 km/hr (DFT20) (see Equation A.6).

$$Sp = 14.2 + 89.7\times MPD \quad \text{Equation A.5}$$

$$IFI = 0.081+0.732DFT_{20}\times e^{(-40/S_P)} \quad \text{Equation A.6}$$

Masad et al. (2009) established a relationship between in-situ traffic loading and laboratory polishing cycles using Equations A.7 and A.8. This relationship allows for the correlation of laboratory polishing results with actual traffic conditions. In this formula, *N* represents the number of polishing cycles, and TMF is the traffic multiplication factor (Lal Das, V. K 2011).

$$TMF = 35600/ (1+15.96\times e^{(-4.78x10-2N)}) \quad \text{Equation A.7}$$

$$TMF = AADT \times \text{Years in Service}/1000 \quad \text{Equation A.8}$$

APPENDIX B: PERFORMANCE TESTING AND SAMPLE PREPRATION PROCEDURE

B.1 Performance Testing

B.1.1 Measuring Aggregate Coupons' Surface Frictional Properties Using the British Pendulum

B.1.1.1 Preparing Aggregate Coupons

The preparation of the coupons (curved specimens) for this project involved several steps, as depicted in Figure B.1:

1. Coating the Mold Bottom: The bottom of the molds was coated with a layer of ready-mix plaster, ensuring smooth and even coverage across the mold surface.

2. Embedding Aggregates: Aggregates were carefully embedded into the plaster within the molds, ensuring proper distribution and compaction for uniformity and optimal performance of the HFST samples.

3. Pouring the Binder: The binders were proportioned according to the standard rate and poured onto the embedded aggregates, aiming for uniform coverage and strong bonding with the aggregates.

4. Curing Process: The coupons underwent a curing process to allow the binders to set and form a robust bond with the aggregates. This process ensured the development of the desired strength and properties in the HFST coupons. After curing, the plaster was stripped away to reveal the prepared surface for further testing.

In addition to the preparation steps, the application rates of the binder and aggregate were specified, as seen in section 2.6.3. These application rates ensured the appropriate quantity of binder and aggregate for achieving the desired friction-enhancing properties and performance in the high friction surface treatment application [35].

B.1.1.2 British Pendulum (BP) and Polishing Stone Value Test (PSV)

The BPT (British Pendulum Tester) is a highly regarded device utilized in a wide range of research fields. Its utilization is governed by established standards set forth by ASTM E303 and AASHTO T 278. The primary function of the BPT is to quantify frictional forces generated when a rubber pad slides across a sample surface. By simulating a velocity equivalent to 10 km/h or 6 mph the BPT enables the measurement of microtexture characteristics (AASHTO T 278).

Figure B.1 The preparation process for the aggregate coupons

In order to evaluate the resistance of binder-aggregate matrixes to polishing and wear, the British polishing wheel, depicted in Figure B.2, was utilized to simulate the polishing effects generated by vehicular traffic on aggregate. The specimens were prepared following the methods described in the previous section. To conduct the test (ASTM, 2000a), a total of fourteen specimens were securely clamped along the periphery of the road wheel to establish a continuous aggregate surface. Subsequently, the wheel was rotated at an approximate speed of 320 rotations per minute.

To apply pressure on the aggregate surface, a smooth-surfaced, pneumatic, rubber-tired wheel with a load of 88 lbs (390 N) was utilized. Throughout the entire ten-hour testing period, silicon carbide grit of size number 150 was continuously fed at a rate of 0.013 lbs (6 g) per minute. Additionally, water was supplied to the surface at a controlled rate ranging from 0.013 to 0.020 gal (50 to 75 mL) per minute.

Upon completion of the ten-hour polishing process, the road wheel was carefully dismantled, and thorough cleaning procedures were undertaken to eliminate any remaining silicon carbide grit.

Figure B.2 BPT and PSV test placement

B.1.2 Accelerated Friction Testing

B.1.2.1 Slab Preparation for High Friction Surface Treatment Performance Tests

To ensure consistency and uniformity, the samples were prepared on a plywood substrate instead of the HMA substrate, as approved by MoDOT. In addition, to compare the results and performance of different substrates, some samples were prepared using an HMA substrate.

HMA Substrate Preparation Procedure:

1. Set up the compaction mold.

2. Heat approximately 50-55 pounds of loose asphalt mixture to 320 °F.

3. Line the bottom of the compaction mold with thermal paper.

4. Evenly distribute the loose asphalt mixture into the mold.

5. Cover the top of the mixture with another sheet of thermal paper.

6. Place the compaction metal cover on top of the mold.

7. Use a plate compactor to compress the mixture for roughly 10 minutes.

8. Remove the metal cover.

9. Allow the compacted slabs to cool within the mold overnight to prevent damage or distortion.

10. Dismantle the compaction mold and extract the prepared slab after 24 hours (Heitzman M, Gu F, Welderufael A. 2019].

Slab Preparation with Epoxy Resin Procedure:

1.Clean the surface of the HMA or plywood substrate. It is recommended to use air to avoid causing damage to the surface.

2.Proportion of epoxy resin binder based on manufacturer's recommendations for the correct proportions of epoxy resin and curing agent.

3. Depending on the size of the sample or area, mix the epoxy resin binder either by hand or using a jiffy mixer. Follow the manufacturer's specified mixing time, which is typically around 3-5 minutes, to ensure proper blending.

4. Spread epoxy resin binder using, a notched neoprene squeegee, evenly onto the prepared surface. Ensure that the surface is clean and free from debris.

5. Apply the epoxy resin binder to achieve the desired target thickness, which is typically 50-65 mils (25 to 32 square feet per gallon). Most commonly, a thickness of 40-45 mils is achieved (High Friction Surface Treatments FHWA 2023].

6. Broadcast the high-friction aggregate immediately after applying the epoxy resin binder. Continue adding aggregate until reaching the point of rejection, which typically occurs when approximately 12-15 pounds of aggregate per square yard (12-15 lb/yd^2) have been applied. During this process, ensure that the aggregate is evenly distributed and embedded into the epoxy resin binder (MoDOT NJSP-15-13B, 2015).

7.After the HFST has cured, rub the surface of each slab with a wooden board to dislodge loosely bound particles, Figure B.3.

Figure B.3 Slab preparation with epoxy resin

Slab Preparation with PG and modified asphalt binder:

1.Heat the binder to a temperature range between 340 °F and 375 °F (171 °C - 190 °C) depending on type of the PG or modified binders. Allow the binder to reach the desired temperature and ensure that it is consistent throughout.

2. Apply the heated binder onto the prepared slab. Apply the binder uniformly at a rate between 0.30 to 0.38 gallons per square yard. Ensure the desired coverage rate is consistently achieved across the entire surface (NJDOT, 424 Chip Seal HFCS).

3. Broadcast the heated high-friction aggregate immediately after applying the binder. Continue adding aggregate the point of rejection is reached, which typically occurs when approximately 12-15 pounds of aggregate per square yard (12-15 lb/yd^2) have been applied. During this process, ensure that the aggregate is evenly distributed and embedded into the binder.

4. Place the heavy plate and using manual compactor, which helps achieve uniform embedment of the aggregate. Then, allow the binder, aggregate, and slab assembly to cure for a specified duration at the recommended curing temperature (as per the manufacturer's guidelines).

5. After the sample has cured, rub the surface of each slab with a wooden board to dislodge loosely bound particles, Figure B.4.

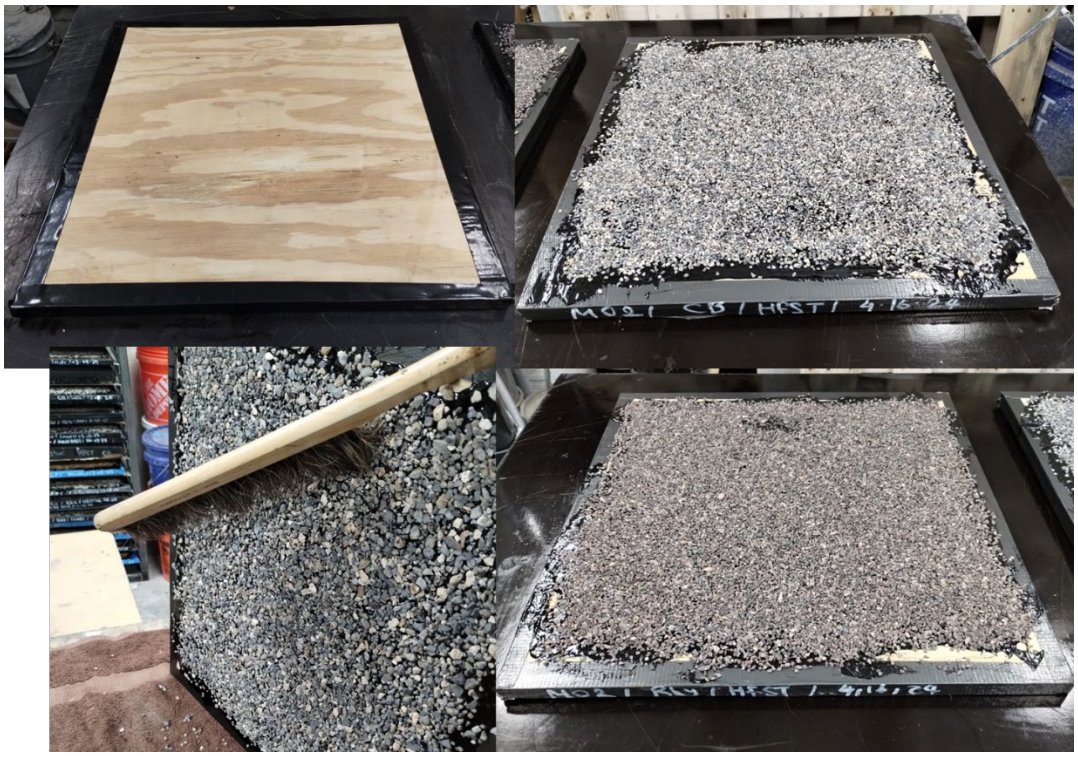

Figure B.4 Slab preparation with PG and modified asphalt binder

Slab Preparation with Emulsion:

1. Preheat the emulsion to 140 °F for 30 minutes and ensure that the temperature is consistent throughout the emulsion.

2. Apply the emulsion at standard rate onto the slab. Ensure that the desired coverage rate is achieved consistently across the entire surface (NJDOT, 424 Chip Seal HFCS).

3.Broadcast the high-friction aggregate immediately after applying the emulsion. Continue adding aggregate until reaching the point of rejection, which typically occurs when approximately 12-15 pounds of aggregate per square yard (12-15 lb/yd²) have been applied. During this process, ensure that the aggregate is evenly distributed and embedded into the binder.

4. Place the heavy plate and using manual compactor, which help in achieving uniform embedment of the aggregate. Then, allow the binder, aggregate, and slab assembly to cure for a specified duration at the recommended curing temperature (as per the manufacturer's guidelines). Due to premature failure and severe bleeding observed in some specimens after 30K polishing cycles, all emulsion slabs were kept at room temperature for over 15 days to ensure proper curing. This measure was taken to prevent insufficient curing time from affecting the test results.

5. After the sample cured, the surface of each slab was rubbed with a wooden board to dislodge loosely bound particles.

B.3.2.1 Procedure for Measuring Pavement Macrotexture Properties Using the Circular Track Meter

1.Place the CT Meter on a dry and clean slab surface for measurement.

2.Mark the location of the CT Meter so the DF Tester can be placed in the same spot.

3.Start and run the program on the notebook computer, select the option to compute the MPD, RMS, or both of the profiles, and initiate the measurement.

4.Record the test results or store the data for future analysis.

B.1.2.2 Procedure for Measuring Surface Frictional Properties Using the Dynamic Friction Tester

1.Place the DF tester on a clean, uncontaminated test slab surface.

2.Start the rotation of the disk and verify that the disk, with three rubber sliders, rotates without contacting the test surface.

3.The water flow will automatically start at 20 km/h (13 mph) prior to reaching a set target speed of 60 km/h (36 mph) or greater.

4.When the rotational speed reaches the target speed, lower the flywheel so the rubber sliders contact the test surface, initiating the friction measurement.

5.Record the test results or store the data for future analysis.

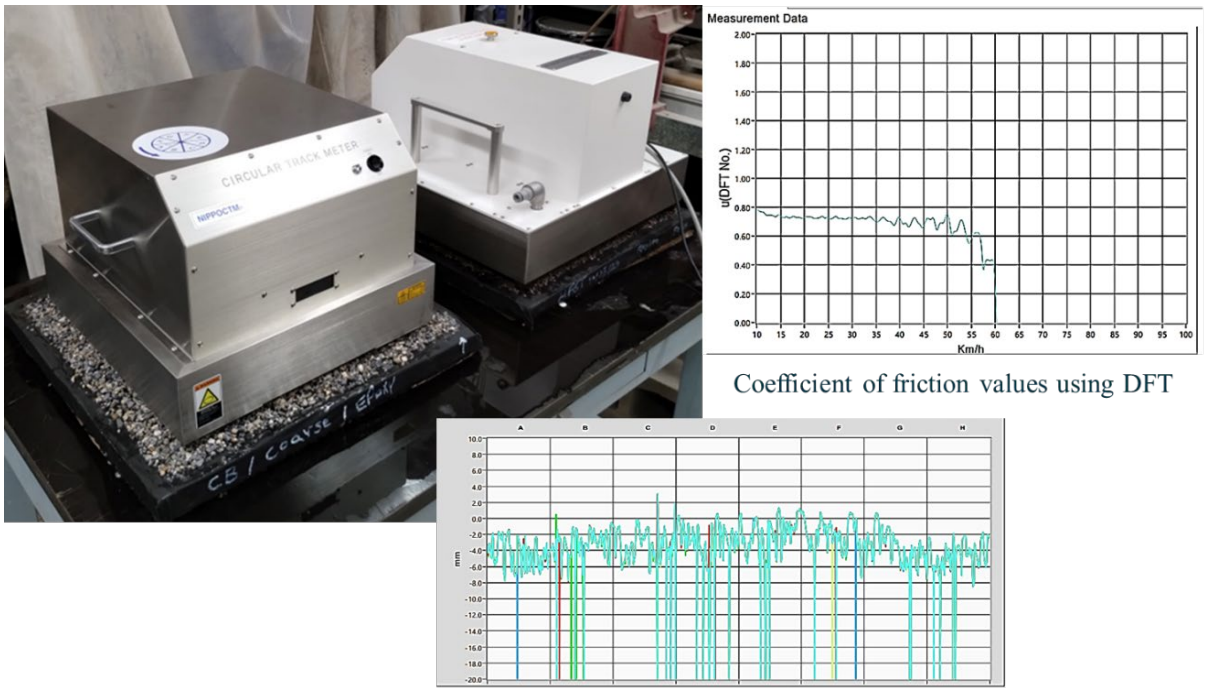

Figure B.5 Circular Track Meter and Dynamic Friction Tester

B.1.2.3 Procedure for polishing of samples using a three-wheel polishing device (TWPD)

1.Remove the slab from the DFT and slide it under the wheel assembly of the TWPD.

2.Gently lower the polishing tire carriage onto the sample.

3.Set the Automatic Counter to the desired number of revolutions (30K, 70K, 140K). Turn on the water flow and begin polishing. One revolution of the polishing carriage corresponds to one pass made by all three wheels.

Note: The tire size should be 2.80/2.50-4. Several tire manufacturers supply a 2.80/2.50-4 pneumatic tire, but the rubber compound chemistry and tread style are unique to each manufacturer. For consistent polishing of each test surface in this project, always replace the tires with the same tire from the same manufacturer.

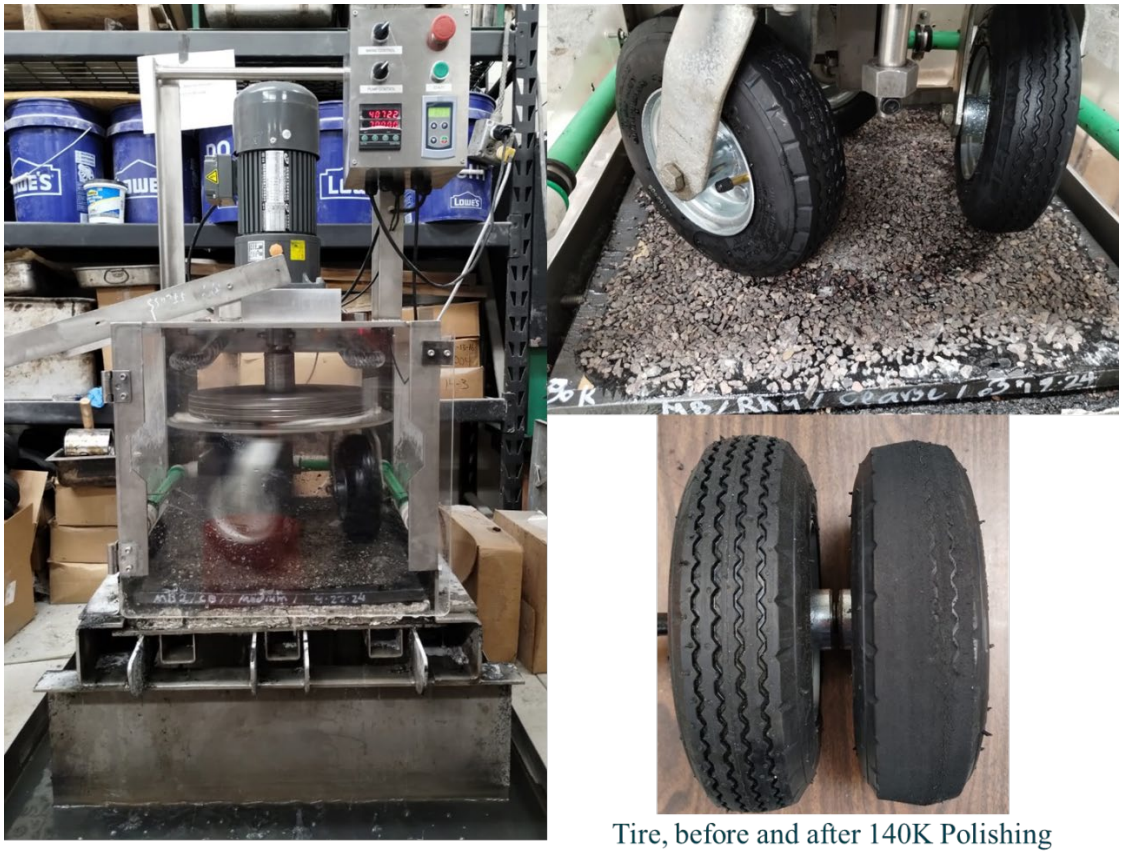

Figure B.6 Three-Wheel Polishing Device (TWPD)

B.2 General steps in Modified binders' preparation process

1.Pre-heat base asphalt binders (PG64-22 and PG76-22) to 135°C until they are liquid.

2.Pour an appropriate amount of liquid asphalt into the mixing container. Place the container in a mixing-environment mantle and heat it to 170°C. Continuously stir the asphalt until it reaches an equilibrium temperature.

3.For Modified Binder 1 (PG64-22), add 8% Kraton D0243KT, and for Modified Binder 2 (PG76-22), add 6% Kraton D0243KT. Shear the mixture using a high shear mixer at 170 ± 5 °C and 3000 RPM for 90 minutes. Then, add 0.1% sulfur by weight of bitumen as a cross-linker and continue high shear mixing for an additional 30 minutes.

4.To homogenize the mixture, reduce the mixing rate to 500 RPM and continue mixing the modified binders for 4 hours. This process allows for additional polymer swelling and networking before casting test samples, simulating asphalt plant conditions more accurately.

Modified binder preparation Shear Mixing and development

Figure B.7 Modified binders' preparation process

APPENDIX C: IMAGE OF THE TESTED HFST COUPONS AND SLABS OF DIFFERENT ASPHALT-BASED AGGREGATE COMBINATIONS

C.1 Coupons

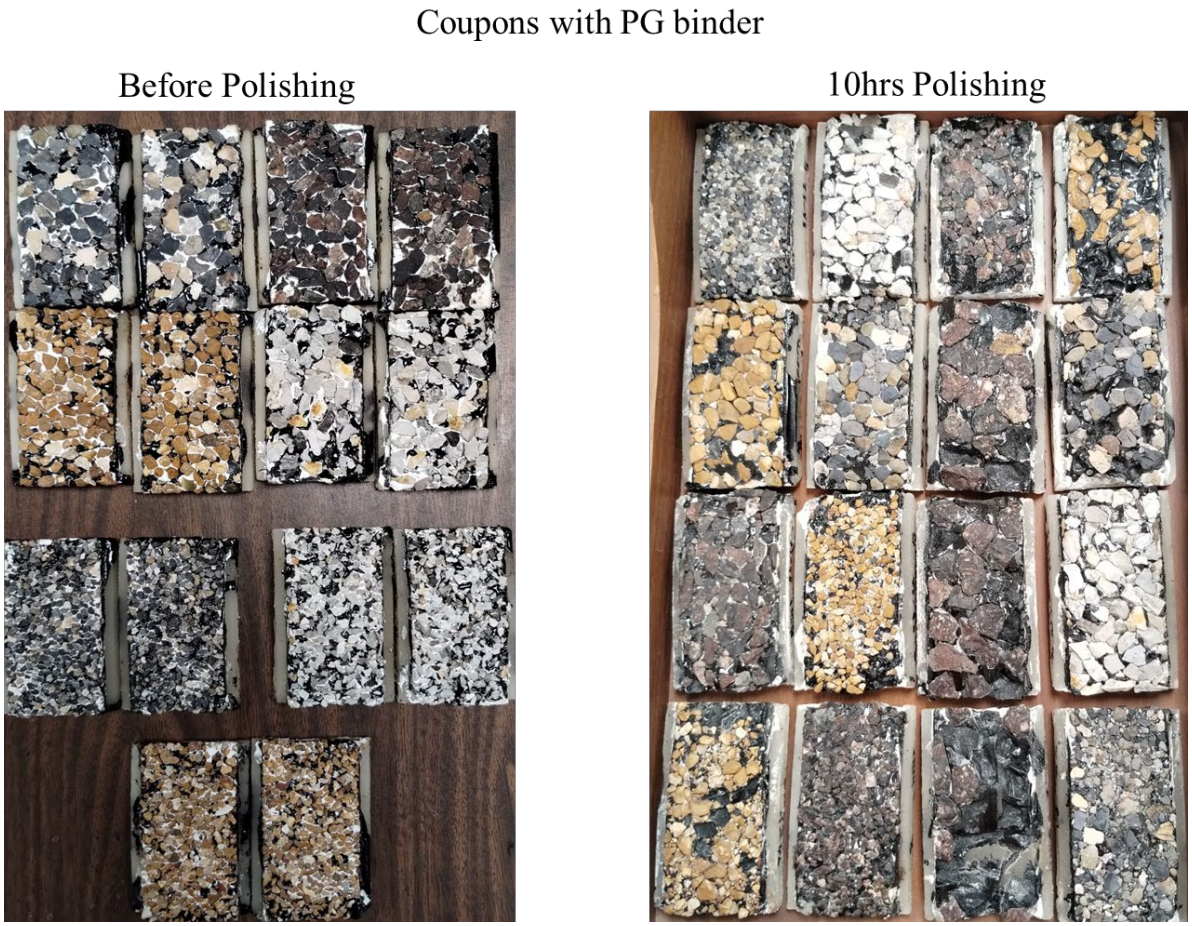

Figure C.1 Coupons with PG binders

Figure C.2 Coupons with PG binders before and after polishing

Coupons with Emulsion

Before Polishing

10hrs Polishing

Figure C.3 Coupons with Emulsion

Before Polishing

10hrs Polishing

Figure C.4 Coupons with CRS-2P Emulsion before and after polishing

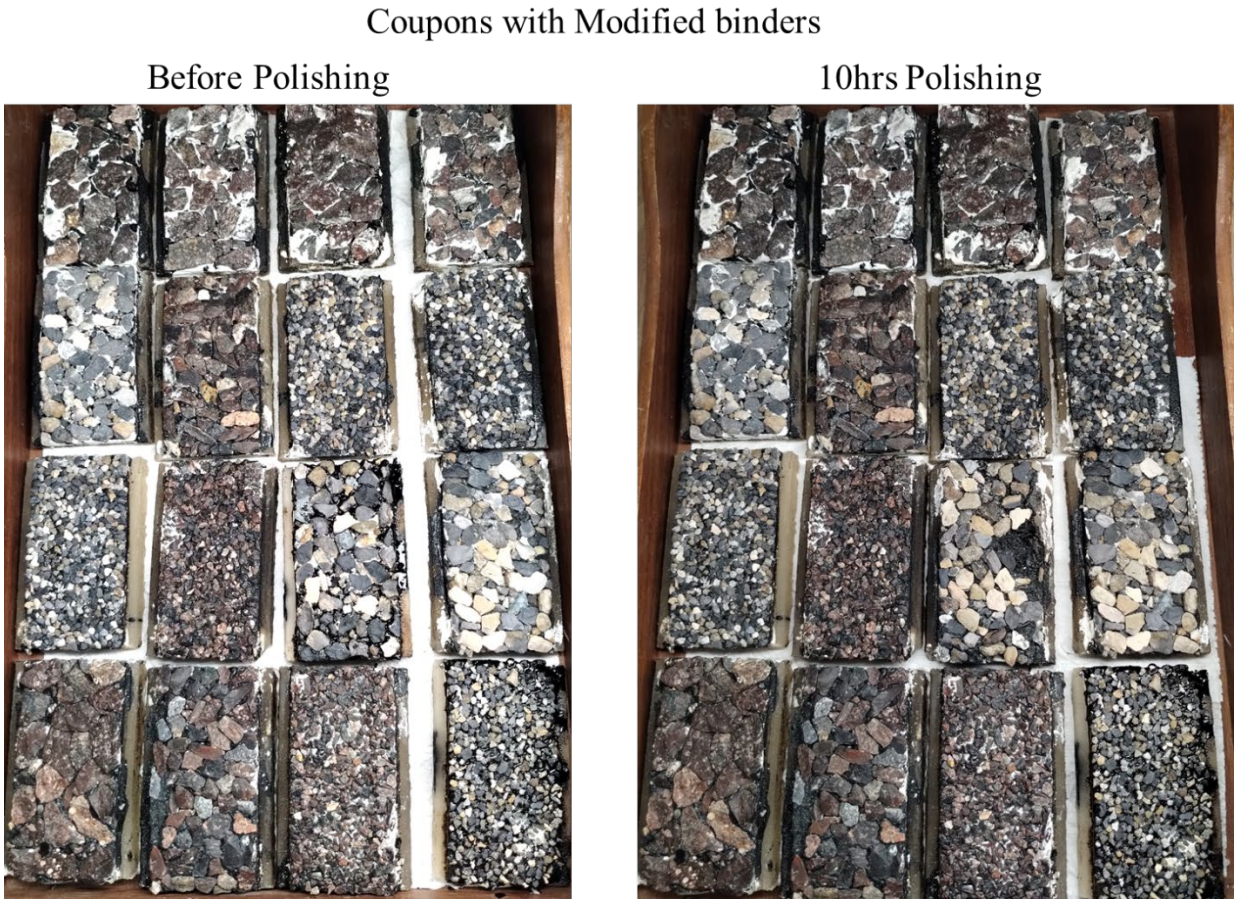

Figure C.5 Coupons with Modified binders

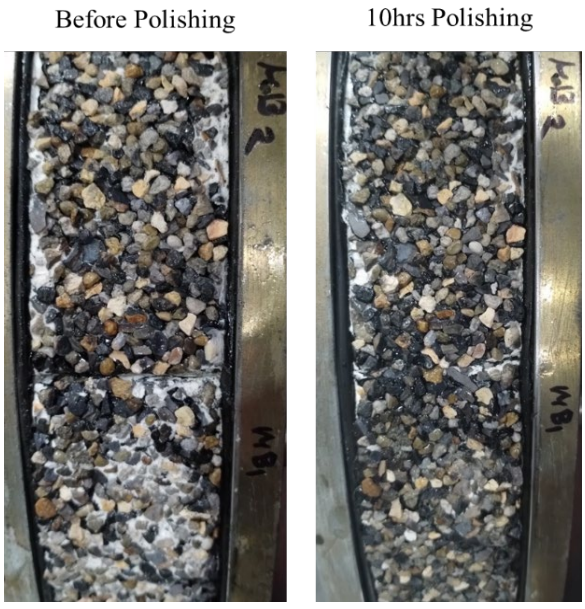

Figure C.6 Coupons with Modified binders before and after polishing

C.2 Slabs

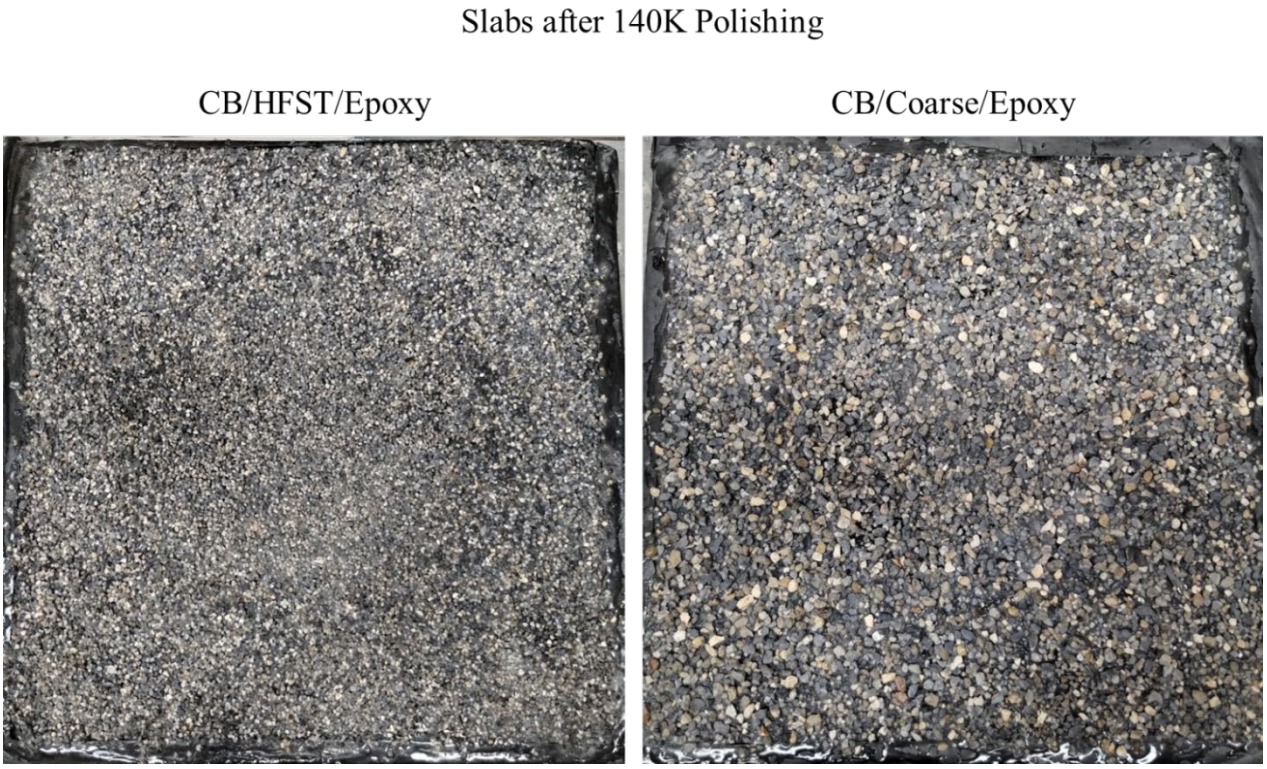

Figure C.7 Slabs with Epoxy resin (Left, CB/HFST. Right, CB/coarse)

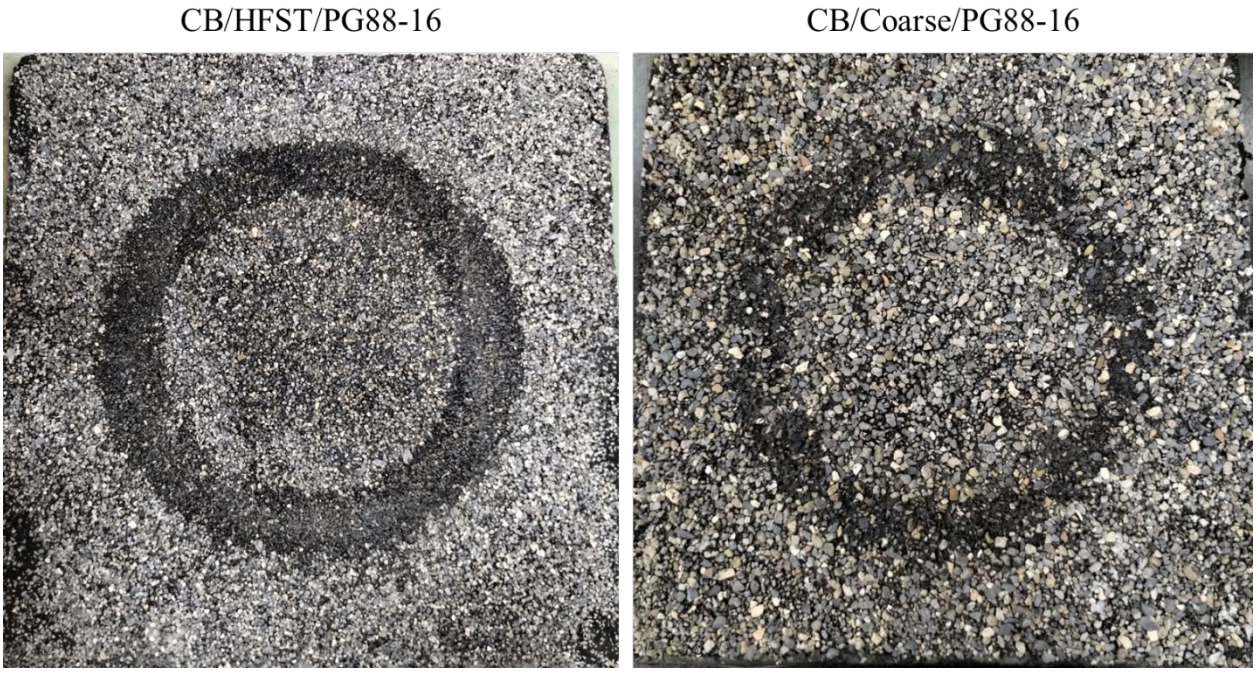

Figure C.8 Slabs with PG88-16 (Left, CB/HFST. Right, CB/coarse)

Slabs after 140K Polishing

CB/HFST/PG82-22(PM)

CB/Coarse/PG82-22(PM)

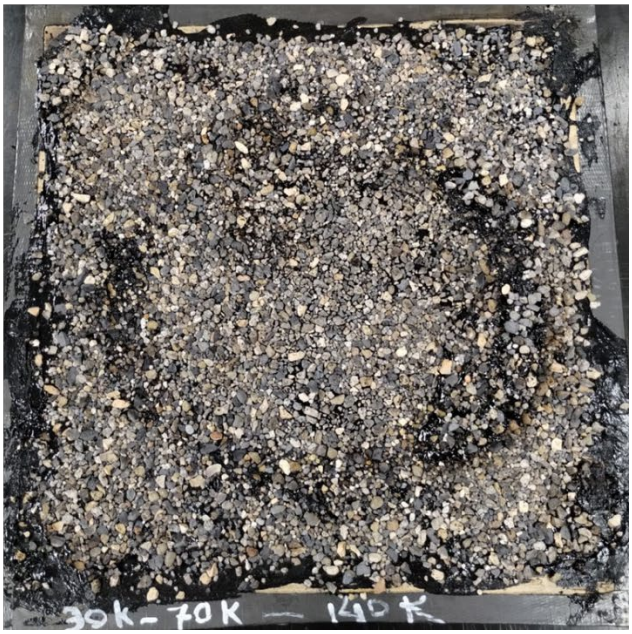

Figure C.9 Slabs with PG82-22(PM) (Left, CB/HFST. Right, CB/coarse)

CB/HFST/PG88-16(PM)

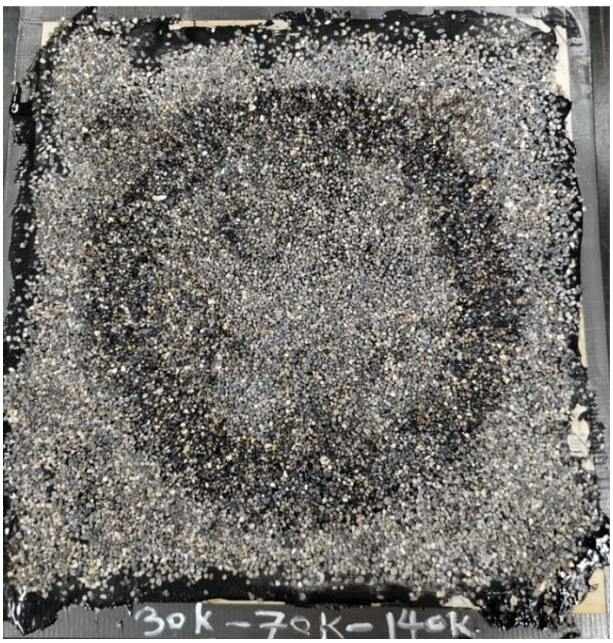

CB/Coarse/PG88-16(PM)

Figure C.10 Slabs with PG88-16(PM) (Left, CB/HFST. Right, CB/coarse)

Slabs after 140K Polishing

CB/Medium/PG82-22(PM)

CB/Medium/PG88-16(PM)

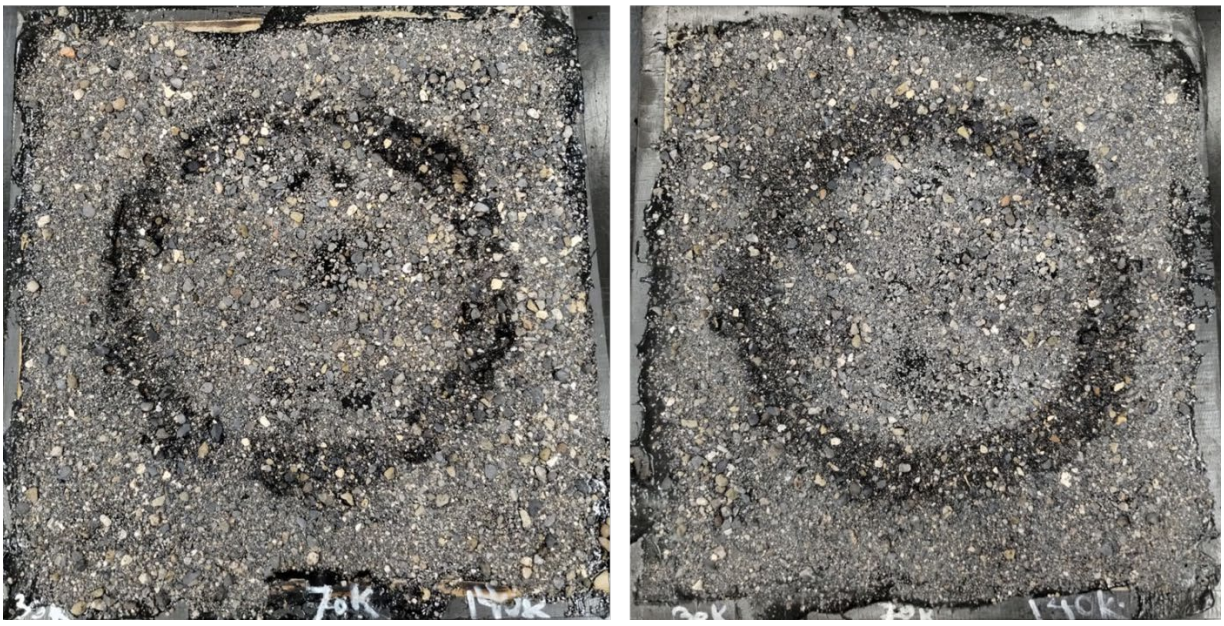

Figure C.11 Slabs with (Left, PG82-22(PM)/CB/medium. Right, PG88-16(PM)/CB/medium)

Slabs after 30K Polishing

CB/HFST/Emulsion CRS-2P

CB/Coarse/Emulsion CRS-2P

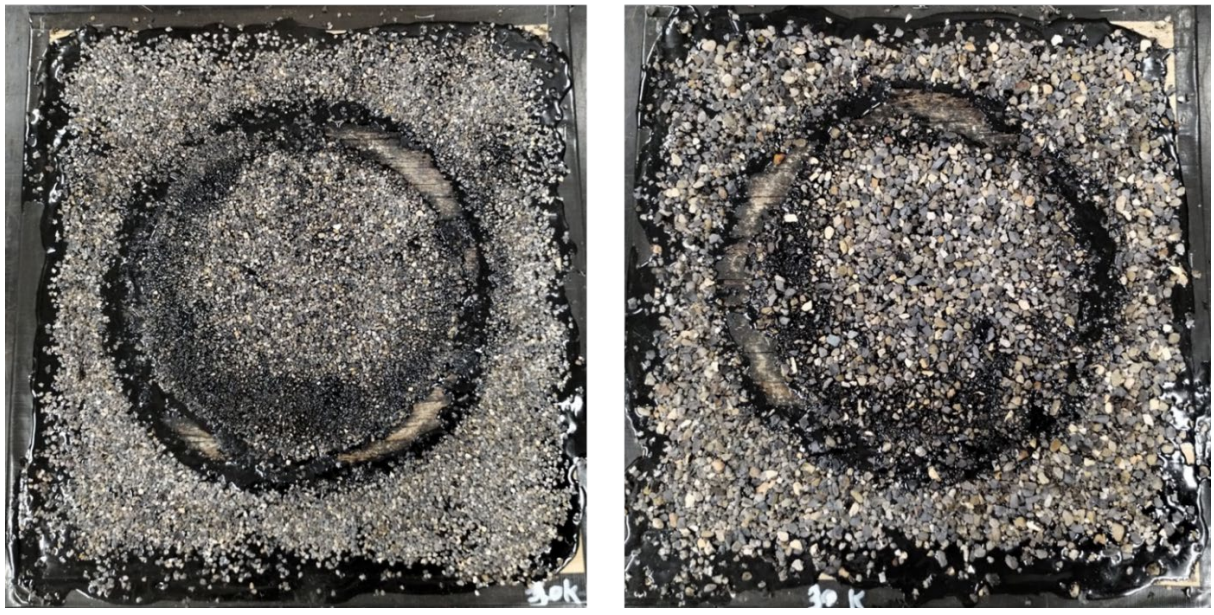

Figure C.12 Slabs with CRS-2P (Left, CB/HFST. Right, CB/coarse)

APPENDIX D: LIFE CYCLE COST ANALYSIS CALCULATION PROCESS

The researchers developed a simple Life Cycle Cost (LCC) program using Excel to conduct Life Cycle Cost Analysis (LCCA) for High Friction Surface Treatment (HFST) applications with different binders and aggregates. This program incorporated results from the British Pendulum Number (BPN), Dynamic Friction Tester (DFT), and Circular Track Meter (CT Meter). It predicted the Skid Number (SN) and the Net Present Value (NPV) for HFST applications. The major input data were categorized into material and project specifics, and the program's results included the SN and NPV. Further details about these data and results are explained in the following sections.

D.1 Input Data

The input data used in the LCC program were categorized into two categories: material specifics and project specifics.

D.1.1 Material Specifics

The material specifics depended on the HFST aggregates' results (BP, DFT and MPD) and other specifics as follows.

D.1.1.1 British Pendulum Test Results

The BP results came from the British Pendulum Number (BPN) values measured before and after 10 hours of polishing with the British wheel. The BPN was determined using the British Pendulum Tester.

D.1.1.2 Dynamic Friction Test Results

The DFT results were determined from the Coefficient of Friction (COF) values measured at 20 and 40 km/hr across four polishing cycles (0, 30K, 70K, and 140K cycles). The COF values at zero polishing cycles were considered initial values, while the COF values at 140K polishing cycles represented the terminal values.

D.1.1.3 Circular Track Meter Results

The Circular Texture Meter (CTM) is a relatively new macro-texture measuring device based on laser profiling, which measures the Mean Profile Depth (MPD) of the pavement surface. The CTM offers strengths over traditional volumetric techniques such as the sand patch method, which is cumbersome and has poor repeatability. The MPD values were recorded across four polishing cycles (0, 30K, 70K, and 140K cycles). The MPD values at zero polishing cycles were considered initial values, while the MPD values at 140K polishing cycles represented the terminal values.

D.1.1.4 Other Specifics

Aside from the material specifics, the following details were taken into consideration:

- Aggregate costs in $/ton
- Aggregate shipping costs in $/mile
- The distance in miles from the origin (aggregate source) to the destination (Columbia, MO, USA)
- Aggregate load size in tons per load (tons/load)
- Applied rate of aggregate in tons/yd^2
- Binders' costs in $/gallon
- Binder's shipping costs in $/gallon
- Binders applied rate in gallons/yd^2
- Construction, labor, equipment, etc. costs in $/yd^2

D.1.2 Project Specifics

The second data input category, project specifics, includes the following details:

- Average Annual Daily Traffic (AADT) per section in vehicles/day
- Percentage of trucks (%T)
- Highway classification (rural or urban) and whether the highway is divided or undivided.
- Number of lanes in each direction
- Lane width in feet
- HFST length in miles
- Cost of removing HFST in $/yd^2
- The recommended terminal Skid Number (SN) value
- Terminal Polishing Cycles(N)(Terms of 1000 cycles)
- Interest rate and inflation rate in %

D.2 Skid Performance Prediction Models

Performance prediction models were utilized to predict the Skid Number (SN) values. Subsequently, the rehabilitation decision was made based on the rehabilitation matrix.

D.2.1 Skid Number Prediction Model Based on British Pendulum Test Results

The British Pendulum (BP) test results, both before and after 10 hours of polishing using the British Wheel Device, were utilized to predict the Skid Number at 40 mi/hr (SN40R), as measured by a skid trailer with ribbed tires. The relationship between the British Pendulum Number (BPN) and the SN40R is described in Equation D.1 (John Jewett Henry and Wambold 1992):

$$SN40R = -10.5 + 0.83(BPN) \quad \text{Equation D.1}$$

D.2.2 Skid Number Prediction Model Based on COF values measured by Dynamic Friction at 40 km/hr (DFT40)

The COF values measured by the Dynamic Friction Tester at 40 km/hr (DFT40) during different polishing cycles were used to predict the Skid Number at 40 mi/hr (SN40R) as measured by a skid trailer with ribbed tires. The initial SN40R was calculated at zero polishing cycles, while the terminal SN40R was calculated at 140,000 polishing cycles. The prediction model, presented in Equation D.2 and developed by Heitzman et al. (2015), was used in this study to compare the different binders and aggregates used in High Friction Surface Treatment (HFST). This model is based on laboratory friction measurements using DFT40 and SN40R in the field. The friction limits vary by state, and Table D-1 presents the friction limits for states based on SN40R values (John J. Henry 2000). Equation D.2 explains the relationship between SN40R, and the COF measured by DFT40:

$$SN40R = 92.3 \times DFT40 - 13.9 \quad \text{Equation D.2}$$

where:

- SN40R is the predicted skid number measured in the field using a skid trailer with ribbed tires at 40 mi/hr
- DFT40 is the COF value measured by the Dynamic Friction Tester at 40 km/hr in the lab

Table D-1 Friction limits for states based on SN40R (John J. Henry 2000)

State	SN40R
Illinois	> 30
Kentucky	> 28
New York	> 32
SouthCarolina	> 41
Texas	> 30
Utah	> 30–35
Washington	> 30
Wyoming	> 35
Puerto Rico	> 40
Maine	> 35
Wisconsin	> 38

D.2.3 Skid Number Prediction Model Based on COF values measured by Dynamic Friction at 20 km/hr (DFT20) and MPD measured by CTMeter

In accordance with ASTM E1960, the COF values recorded by the DFT at 20 km/hr (DFT20) and Mean Profile Depth (MPD) measurements were employed to calculate the International Friction Index (IFI) values. The IFI was established during the Permanent International Association of Road Congresses (PIARC) International Experiment to Compare and Harmonize Texture and Skid Resistance Measurements. This index facilitates the standardization of friction measurements across various types of equipment to a unified calibrated index.

Based on the Skid Number (SN) obtained using a skid trailer with smooth tires according to ASTM E 274 and the International Friction Index (IFI) calculated following ASTM E 1960, the modified SN (50) values can be calculated in Equation D.3 (Masad et al, 2011).

$$SN(50) = 1.41 + 143.19 \times (IFI - 0.045) \times e^{(-20/S_p)} \quad \text{Equation D.3}$$

The Sp value in Equation D.3 is a function of mean profile depth (MPD) (see Equation D.4), which is obtained using the CTMeter device. The IFI is predicted based on COF values recorded by the DFT at 20 km/hr (DFT20) (see Equation D.5).

$$Sp = 14.2 + 89.7 \times MPD \quad \text{Equation D.4}$$

$$IFI = 0.081 + 0.732 DFT_{20} \times e^{(-40/S_P)} \quad \text{Equation D.5}$$

Masad et al. (2009) established a relationship between in-situ traffic loading and laboratory polishing cycles using Equations D.6 and D.7. This relationship allows for the correlation of laboratory polishing results with actual traffic conditions. In this formula, N represents the number of polishing cycles and TMF (traffic multiplication factor) is what is being calculated. (Lal Das, V. K 2011).

$$TMF = 35600/(1 + 15.96 \times e^{(-4.78x10\text{-}2N)}) \quad \text{Equation D.6}$$

$$TMF = AADT \times \text{Years in Service}/1000 \quad \text{Equation D.7}$$

D.3 Output Data

The output data of the Life-Cycle Cost (LCC) program were the Net Present Values (NPVs), as exemplified in Figures D.1 and D.2. The best High Friction Surface Treatment (HFST) application was selected based on the lowest NPV.

LCCA ANALYSIS FOR HFST APPLICATION

1- Information:

→ This sheet was designed to perform the LCCA for the HFST using the different binders and different aggregates

One Application

BPN (SN40R) | DFT (SN40R) | DFT/CTM (SN50)

Two Applications DFT/CTM(SN50)

								Application 1	Application 2
						Select type of Application		Epoxy Resin	PG binder
						Analysis Period(year)			
	2- Input Data:								
	a- Project Specifics:		**Calcined Bauxite**	**Rhyolite**	**Meramec**	**Flint**			
→	AADT per each section (veh/day),		5800	5800	5800	5800			
→	Percentage of trucks (%),		10	10	10	10			5- Instruction
→	Highway calssification (Rural or Urban),		Rural	Rural	Rural	Rural		→	Fill the yellow
→	Divided or Undivided highway,		Divided	Divided	Divided	Divided		→	Input the averag
→	Number of lanes per each direction,		2	2	2	2		→	Input the termin
→	Lane width (ft),		12	12	12	12		→	Input the recon
→	Length of HFST (mile),		1	1	1	1		→	Select the type
→	Cost of HFST removing ($/yd^2),		1	1	1	1		→	Input the Coeff
→	Terminal Polishing Cycles(N)(Terms of 1000 cycles)		140	140	140	140		→	Input the Mean
→	Recommended Terminal SN50,		30	30	30	30			
→	Interest rate (%), and		4	4	4	4			
→	Inflation rate (%).		3	3	3	3			
	b-Material Specifics (Costs)								
	Please Select type of binder	PG binder							
→	Aggregate Costs ($/ton),		575	19.5	300	395			
→	Distance from Aggregate Source to Columbia City (mile),		572	121	968	111			
→	Aggregate Applied Rate (ton/yd^2),		0.00675	0.00675	0.00675	0.00675			
→	Construction, Labor, ….etc. Costs ($/yd^2), and		5.41	5.41	5.41	5.41			
→	Shipping Costs ($/mile),		3	3	3	3			
→	Binder Costs ($/gallon),		2.50	2.50	2.50	2.50			
→	Binder Shipping Costs ($/gallon),		0.16	0.16	0.16	0.16			
→	Binder Applied Rate (gallon/yd^2),		0.40	0.40	0.40	0.40			
→	Aggregate tons per load,		26	26	26	26			
→	Total Shipping Costs ($ per load),		1716	650	2904	650			
→	Aggregate Shipping Costs ($/ton),		66	25	112	25			
→	Total Aggreagte Costs ($/ton),		641	45	412	420			
→	Total Aggregte Costs ($/yd^2),		4.33	0.30	2.78	2.84			
→	Total Binder Costs ($/gallon),		2.66	2.66	2.66	2.66			
→	Total Binder Costs ($/yard^2),		1.06	1.06	1.06	1.06			
→	Total Aggreagte & Binder Costs ($/yd^2),		5.39	1.36	3.84	3.90			
→	Cost of HFST application ($/yd^2).		11	7	9	9			

Figure D.1 LCC program input data based on DFT/CTM(SN50)

LCCA ANALYSIS FOR HFST USING DFT						
	c- Other Material Specifics:					
→						
	Dynamic Friction Tester (DFT20) Results	0-cycles (Initial)	0.88	0.59	0.45	0.61
		30K cycles	0.85	0.55	0.43	0.57
		70K cycles	0.76	0.46	0.41	0.48
		140K cycles(Terminal)	0.74	0.37	0.38	0.41
	Circular Track Meter (CTM) Results	0-cycles (Initial)	1.94	1.58	1.6	1.62
→		30K cycles	2.03	1.73	1.51	1.57
		70K cycles	1.83	1.69	1.48	1.5
		140K cycles(Terminal)	1.89	1.63	1.45	1.46
→						
→	3- Analysis:					
	Estimated traffic multiplication factor(TMF)		34908.69792	34908.69792	34908.69792	34908.69792
	Estimated years in service		16.5	16.5	16.5	16.5
	Predicted Skid Number Measured using a Skid Number measured at 50 mi/hr by a skid trailer (SN50)	0-cycles (Initial)	73.10500182	48.03247953	38.19288552	49.85057135
		30K cycles	71.69399019	46.44328233	36.10311605	46.51196775
		70K cycles	62.92087347	39.55370898	34.4777031	39.52778834
		140K cycles(Terminal)	61.98727999	32.64037337	32.17501042	34.32635216
	Loss in SN50(%)		15.21	32.05	15.76	31.14
→	Action		Do nothing	Do nothing	Do nothing	Do nothing
→	4- Outputs:					
→						
→						
→	Cost of action ($/yd^2)		0.00	0.00	0.00	0.00
→	Initial cost of HFST		11	7	9	9
→	Cost of action ($/mile/lane)		0.00	0.00	0.00	0.00
	Initial cost of HFST ($/mile/lane)		76,037.20	47,691.55	65,140.51	65,535.29
	Total cost ($/mile/lane)		76,037.20	47,691.55	65,140.51	65,535.29
	NPV ($)		76,037.20	47,691.55	65,140.51	65,535.29
	Best alternative.		**PG binder**			

Figure D.2 LCC program output data based on DFT(SN50)